ISSN : 2165-4069(Online)
ISSN : 2165-4050(Print)

IJARAI

International Journal of
Advanced Research in Artificial Intelligence

Volume 2 Issue 11

www.ijarai.thesai.org

A Publication of
The Science and Information Organization

INTERNATIONAL JOURNAL OF ADVANCED RESEARCH IN ARTIFICIAL INTELLIGENCE

THE SCIENCE AND INFORMATION ORGANIZATION

www.thesai.org | info@thesai.org












Editorial Preface

From the Desk of Managing Editor…

"The question of whether computers can think is like the question of whether submarines can swim." — Edsger W. Dijkstra, the quote explains the power of Artificial Intelligence in computers with the changing landscape. The renaissance stimulated by the field of Artificial Intelligence is generating multiple formats and channels of creativity and innovation.

This journal is a special track on Artificial Intelligence by The Science and Information Organization and aims to be a leading forum for engineers, researchers and practitioners throughout the world.

The journal reports results achieved; proposals for new ways of looking at AI problems and include demonstrations of effectiveness. Papers describing existing technologies or algorithms integrating multiple systems are welcomed. IJARAI also invites papers on real life applications, which should describe the current scenarios, proposed solution, emphasize its novelty, and present an in-depth evaluation of the AI techniques being exploited. IJARAI focusses on quality and relevance in its publications.

In addition, IJARAI recognizes the importance of international influences on Artificial Intelligence and seeks international input in all aspects of the journal, including content, authorship of papers, readership, paper reviewers, and Editorial Board membership.

The success of authors and the journal is interdependent. While the Journal is in its initial phase, it is not only the Editor whose work is crucial to producing the journal. The editorial board members , the peer reviewers, scholars around the world who assess submissions, students, and institutions who generously give their expertise in factors small and large— their constant encouragement has helped a lot in the progress of the journal and shall help in future to earn credibility amongst all the reader members.

I add a personal thanks to the whole team that has catalysed so much, and I wish everyone who has been connected with the Journal the very best for the future.

Thank you for Sharing Wisdom!

Managing Editor
IJARAI
Volume 2 Issue 11 November 2013
ISSN: 2165-4069(Online)
ISSN: 2165-4050(Print)

Editorial Board

Reviewer Board Members

CONTENTS

Case Study on Effectiveness Evaluation of Business Procedure Reengineering: BPR for Local Government in Saga Prefecture, Japan

Kohei Arai [1]
Graduate School of Science and Engineering
Saga University
Saga City, Japan

Youm Jong Sun[2]
President
e-Corporation
Tokyo, Japan

***Abstract*—Case study on validation of effeteness of Business Procedure Reengineering: BPR for local government in Saga prefecture, Japan is conducted. As the results, if it found that BPR is effective. The local government, environment established a government CIO room introduction of a number system was a long-cherished wish is determined in 2013, it is possible to promote e- government and e-municipality and the banner of great incredibly plan called "world-leading creative nation" is being put into place some. We would like you to realize the municipality a cloud can be enhanced administrative services to pour our best to take this opportunity, give the impression to the residents as possible; the operational efficiency of the civil service, the foundation is reduced large flower IT costs.**

Keywords—Business Procedure Reengineering; BPR; local govenment

I. INTRODUCTION

Business Procedure Reengineering: BPR is getting popular for federal and state governments as well as private company, obviously. One of the difficult things is method for evaluation of effectiveness of the BPR.

Nowadays, e-governments are getting popular and common to the local government. Standardized e-government is now populated. On the other hand, through trial and error processes, some of the e-government systems are getting much smart. In particular, information processes and services systems are improved remarkably together with cloud computing technologies. Meanwhile, Business Process Re-engineering: BPR [1] is advanced not so remarkably. Not so many business procedures are changed results in poor progress of the total system performance.

As Michael Hammer[2] said in his article of "Reengineering Work: Don't automate, Obliterate" in the Business Review 1990, a new business process reconstruction utilizing computer and network technologies has to take over the re-structuring with layoff which has been done in 1980s [1]. The old fashion of the business processes in 1980s are based on the design philosophy of the business processes are constructed with the business processes which can be divided into small pieces of tiny sub processes. He, however, proposed much more integrated business processes without division of business processes utilizing computer and network technologies. Namely, useless and/or overlapped business processes are removed together with re-design of business processes for creation of a new concept of the business processes. Thus required cost can be reduced while quality of services is improved with acceptable speed. Namely, it is totally better, cheaper, and faster system.

Local government business processes, on the other hand, are computerized in the early stage followed by e-government. The e-government is not extension of the computerized system at all. It is totally different from the old fashioned computerized system. Namely, all the required data for administrative processes are in a commonly useable database. Individual processes are integrated with interoperable system and data in the database (exchangeable data format, character code conversions, file conversions, etc.) [2].

In Saga Prefecture, after the establishment of Saga ICT Promotion Agency August 20, 2008, under the strong leadership of cities and towns and length Governor, joint procurement of information systems, Analysis of the current state of information systems, joint use of information systems it is where you are been working steadily to such [3].

The municipality cloud demonstration project in Saga which I have worked as an information planning audit, analyze the business processes that are carried out each cities and towns, improving to residents service, operational efficiency, and reduce IT costs drastic from the viewpoint, out leads to a new business process, developed a system for interoperable municipalities based on them, verify the effects, eventually, it was the contents for realizing to interoperate. In addition, it was visualized, such as "time required" to improve effectiveness compares the current business processes and (or less - current model), business processes of BPR after (below, next model) specifically.

As a way of BPR, as the current model to create a work flow analyzes, such as business and the amount of business process status quo, for the work that needs to be improved, and displayed over work flow on them make the best business improvement However, - by reflecting in system development pilots for the next model them to achieve a current model, and business execution time of the next model, it was decided to measure the results of the BPR.

[1] http://e-words.jp/w/BPR.html
[2] http://en.wikipedia.org/wiki/Michael_Hammer

II. PROPOSED MODEL

A. Evaluation Method for effectiveness of the BPR

Prior to the BPR, to check the room for improvement for the important business of the cities and towns, we conducted a questionnaire survey as for the person who of cities and towns, but the table above is the result. 0 points if there is no need of improvement, as 4 points if room for improvement is large, it was decided to get the results to say that over the business of many a result of the investigation, room for improvement is large, but the system of tax department in particular it can be seen that in the example leads to 3.2 points, it is necessary to improve the most: Room for improvement degree of critical business.

B. Current Status of the BPR

Current status of municipalities that participated in the municipality cloud demonstration of Saga Local government's description (March 31, 2009) 51,599 people: Takeo population,

- It is located in the western province, china, agriculture is the main industry. (March 31, 2009) 31,849 people: Kashima population
- It is located in the southern western, Yutoku Inari shrine of one of Japan's three major Inari worshipers of 2.8 million people a year visit is located (March 31, 2009) 29,153 people: Ureshino population
- It is located in the western part of the prefecture, Ureshino Onsen million tourists per year visit the main industry location, and tourism (March 31, 2009) 7,746 people: Omachi town population
- It is located in the center of the county, agriculture, animal husbandry has become a major industry. (March 31, 2009) 9,678 people: Jiangbei town population
- It is located in the center of the county, agriculture, animal husbandry has become a major industry. (March 31, 2009) 26,530 people: Shiraishi town population
- It is located in the southern part of the province, the main industry is agriculture and.

C. Evaluation Results on effectiveness of the BPR

Figure 1 shows Room for improvement degree of critical business (Source: Saga municipality cloud development demonstration project report).

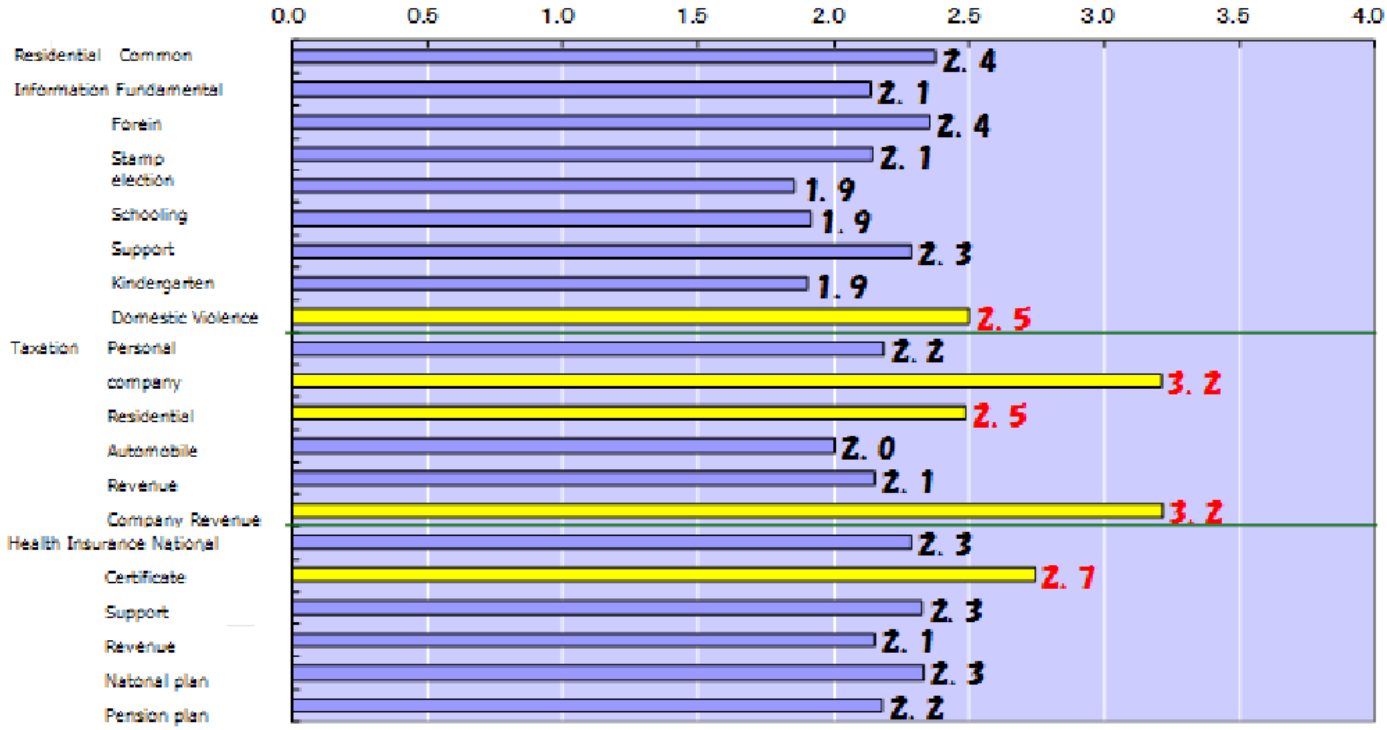

Fig. 1. Room for improvement degree of critical business Source: Saga municipality cloud development demonstration project report

The room for improvement degree survey results for each business Residents better service, operational efficiency in individual, measurement results of field trials of qualitative and quantitative effect is as follows:

Measurements of

① Residents service improvement (shortening the processing time)

Residents visited a government office, after certain procedures, description and delivery. Table 1 shows the results from measurements of the effect by experiment. Meanwhile, Table 2 shows measurement result of operational efficiency in the

case of the transition to next-generation model was BPR from the current model. As the results, it is confirmed that around 30 % of required processing time Business Procedure is reduced by BPR. In particular, systemized procedure from the manual base procedure is effective followed by media conversion from paper to electronics form, and personal information processing. On the other hand, it is also found that outsourcing is not so effective.

Meanwhile, resident information processing is the most cost effective by 41 % followed by national health insurance (32 %), and taxation business (28 %) processes.

TABLE I. MEASURED EFFECTIVENESS OF THE PROPOSED BPR

Business Lines	Name	City Name	Procedure	Reduction of processing time (1 per procedure) (minutes)				Remark
				Past	Current	Reduction		Annual count
Resident Information	Basic Resident Register	Ureshino	Transference accepting applications for grant-related documents	24.4	16.4	8.0	33%	695
			Moving out accepting applications - moving out certification issue	22.2	11.2	11.0	50%	785
	Seal Registration		Registration accepted - seal return	16.6	16.4	0.2	1%	1,100
			Certificate application forms check-receipt issue	3.7	3.7	0.0	0%	950
			Deregistration application forms check-notice distribution	4.5	4.5	0.0	0%	500
	DV・Stalker		Deregistration application forms check-notice distribution	11.0	9.0	2.0	18%	3
Taxation	Corporate inhabitant tax	Kashima	Contact reception - answer	43.0	18.0	25.0	58%	20
	Property tax		Certificate accepting applications-price receipt	3.5	3.5	0.0	0%	100
National Health Insurance	National Health Insurance levy	Takeo	Contact reception ~ levy tax calculations described	16.0	7.0	9.0	56%	1,500
	National Health Insurance Eligibility		Transference Social Insurance retention withdrawal reception - elderly claimant certification issued	2.5	2.5	0.0	0%	36
			Burden classification certificate accepting applications for grant-	8.0	6.0	2.0	25%	30
			Retirement insured qualification acquisition and loss delivered accepted - insurance card issued	5.5	5.5	0.0	0%	30
			specialized science-accepted insurance card issued	4.5	4.5	0.0	0%	20
			Qualification changes accepted - reissue imprint mark, issue	6.5	6.5	0.0	0%	50
			Insurance card reissue accepted - reissue imprint mark-issue	9.0	9.0	0.0	0%	600
			Issue short-term proof-acceptance issue	5.0	3.6	1.4	28%	300
	National Health Insurance Benefits		Request entry written request high-cost medical care accepting applications - appropriation (delinquent)	21.0	21.0	0.0	0%	1,000
			Specific disease medical treatment proof delivery acceptance-delivery	12.0	6.0	6.0	50%	12
			Standard burden reduction applied certificate issued reception-delivery	16.0	11.0	5.0	31%	108
			Total	234.9	165.3	69.6	30%	7,839

Colored row shows the process the effect of more than 30% is expected to shaded

TABLE II. MEASUREMENT RESULT OF OPERATIONAL EFFICIENCY IN THE CASE OF THE TRANSITION TO NEXT-GENERATION MODEL WAS BPR FROM THE CURRENT MODEL

Business lines	Business	Reduction of business management (hours / year)				Systemize of manual		Online personal information cooperation		Electronic data from paper storage		Outsourcing		Other	
		Past	Current	Reduced time	Effect	No.	Time	No.	Time	No.	Time	No.	Time	No.	Time
Residents information	Basic Resident Register	681	320	361	53%	0	0	4	188	3	19	0	0	7	107
	Seal	470	422	57	12%	0	0	2	43	1	4	0	0	0	0
	DV・Stoker	16	13	2	15%	5	2	2	0	1	0	0	0	1	0
	Election	228	181	47	21%	7	23	2	1	7	15	8	8	0	0
	School age book	101	20	80	80%	8	50	3	1	6	26	0	0	2	4
	School Aid	189	34	155	82%	7	55	2	10	2	28	0	0	6	46

	Sub-Total	1692	990	702	41%	23	129	15	244	20	91	8	8	16	158
Taxation	Individual inhabitant tax	10482	6661	3822	36%	15	1825	9	462	12	1317	217	217	11	12
	Corporate inhabitant tax	433	211	222	51%	12	194	0	0	4	13	0	0	2	5
	Corporation storage	276	120	156	56%	12	156	0	0	0	0	0	0	0	0
	Property tax	7127	6144	983	14%	20	250	11	617	2	11	105	105	3	0
	Sub-Total	18318	13136	5183	28%	59	2425	20	1080	18	1341	322	322	16	17
National Health Insurance	Levy	884	391	492	56%	15	289	19	82	0	0	110	110	1	11
	Eligibility	509	368	142	28%	11	35	1	0	4	8	98	98	3	0
	Benefit	662	637	24	4%	9	24	0	0	0	0	0	0	0	0
	Sub-Total	2054	1396	658	32%	35	497	20	82	4	8	207	207	4	12
Total		22065	15522	6543	30%	121	2903	55	1406	42	1441	537	537	36	185

Results of the measurement of the reduction rate of the operational procedure time for 19 processes to become such, it were reduced by 31% on average. In particular, answer inquiries and corporate inhabitant tax (58%), estimated tax imposition description of national health insurance levy, specific disease medical treatment proof issue of National Health Insurance benefits (50%) , moved out acceptance of Basic Resident Register is (50%) , residents reduction of latency was high.

D. Introduction of improvement case

Because when performing the move-out process at the counter, to perform the storage situation confirmation regardless of the delinquent existence, time-consuming, because of the business contact, improvement case traditional

① moving out notification had been spelled to come up with a paper, but the next model in the order to be able to query the system removal and check mark votes of non-payment, work spell in the job mark votes spelling check and to charge storage tissue is eliminated. I can be shortened to five minutes to process 3 per processing time and change in the next model for the 3/17 process per the processing time of the current model before and after performing the improvement of business processes in detail.

② school aid procedures In the past, against one per process processing time was 480 minutes from the fact that in order to make the school aid certification deliberation, it was asked in the paper collection of various types of information to obtain a Person consent of personal information collected in the next model Te, only the required information, staff there are authorizations to be identifiable.

Figure 2 and 3 shows before and after BPR of Basic Resident Register, respectively. Through BPR procedure, 17 minutes of processing time is reduced to just 5 minutes. Due to the fact that it takes 10 minutes for checking the payment status, it takes 17 minutes in total. Meanwhile, it takes just 5 minutes because it does not need to check the payment status because payment status is recorded every time of resident leave their residence.

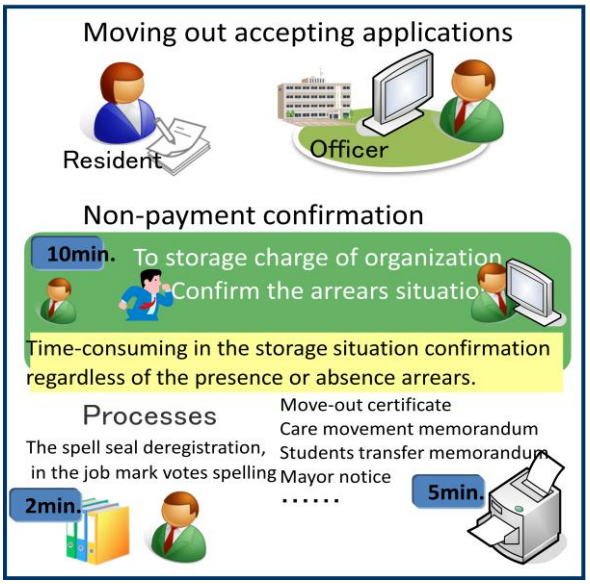

Fig. 2. Before BPR (Basic Resident Register)

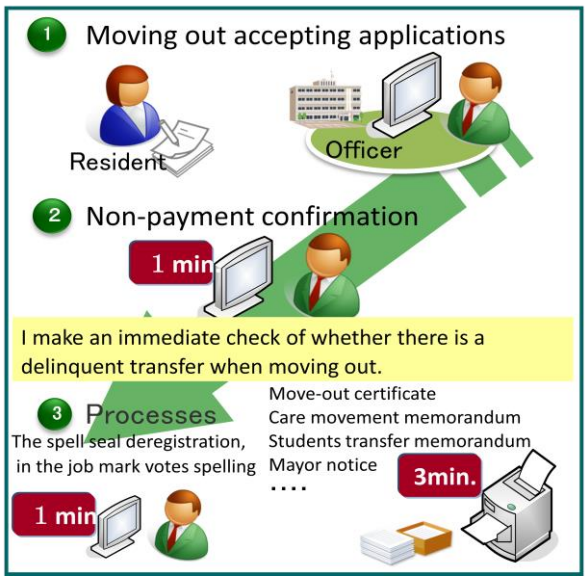

Fig. 3. After BPR (Basic Resident Register)

Can be reduced to 240 minutes per process processing time can be realized by MES "electronic data" from the "paper". Figure 4 and 5 shows before and after BPR of school aid (certificate). In the process of promoting the efficiency of business operations municipality, electronic systems for business use, which was developed as necessary. Hardware Internet and client-server format, use personal computer functions of high performance reduce the load of the main short-range computer networks and communication networks (LAN) technology,

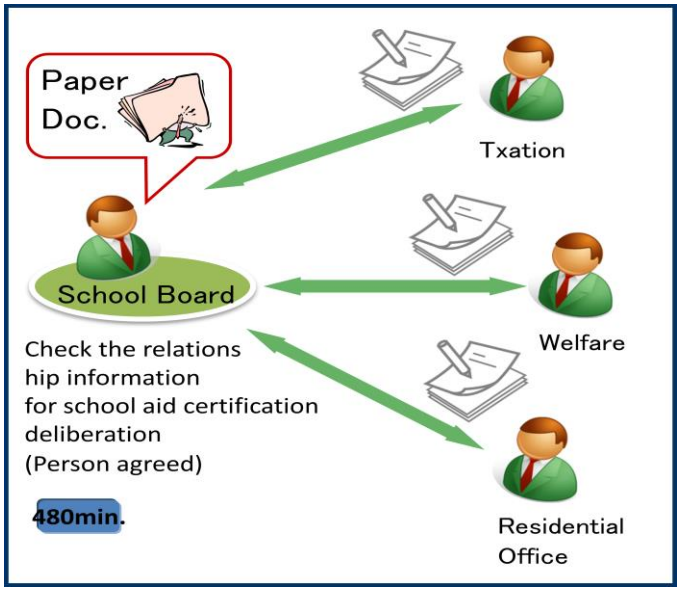

Fig. 4. Before BPR (School aid (Certification))

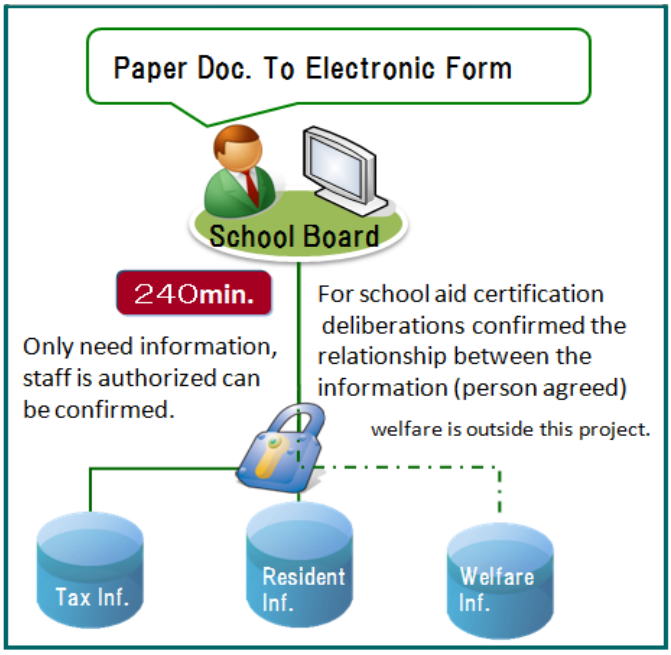

Fig. 5. After BPR (School aid (Certification))

Figure 6, 7 shows another example of BPR of Individual inhabitant tax payment process. Figure 6 shows the past business flow of the individual inhabitant tax payment process while Figure 7 shows the current process flow. Using bar code reader, the required time for individual inhabitant tax payment processes is reduced three minutes. The number of payment is so huge that effect of this BPR is quite large.

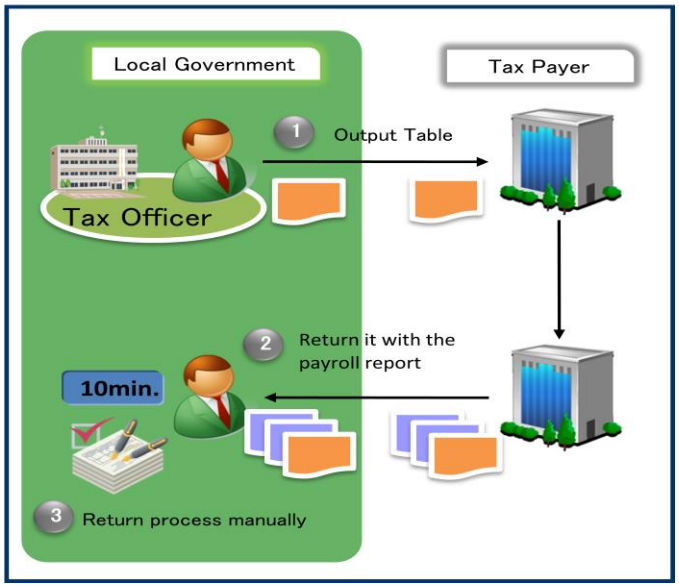

Fig. 6. Past business procedure for individual inhabitant tax payment process.

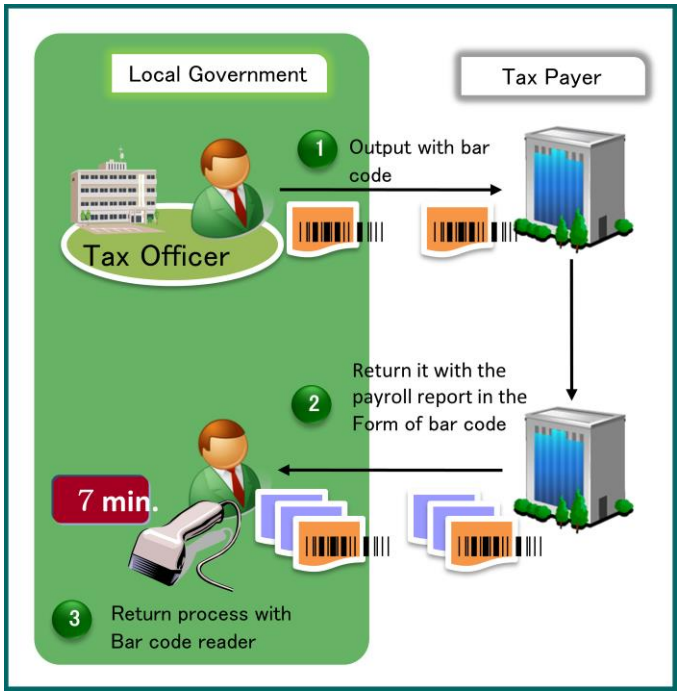

Fig. 7. Current business procedures for individual inhabitant tax payment process.

Another example for property tax payment processes can be shown with Figure 8, 9. In the past decades, property tax form is forwarded with paper form. Electronic form of property tax is available from law office to taxation office currently. Therefore, 1/3 of required process time can be reduced.

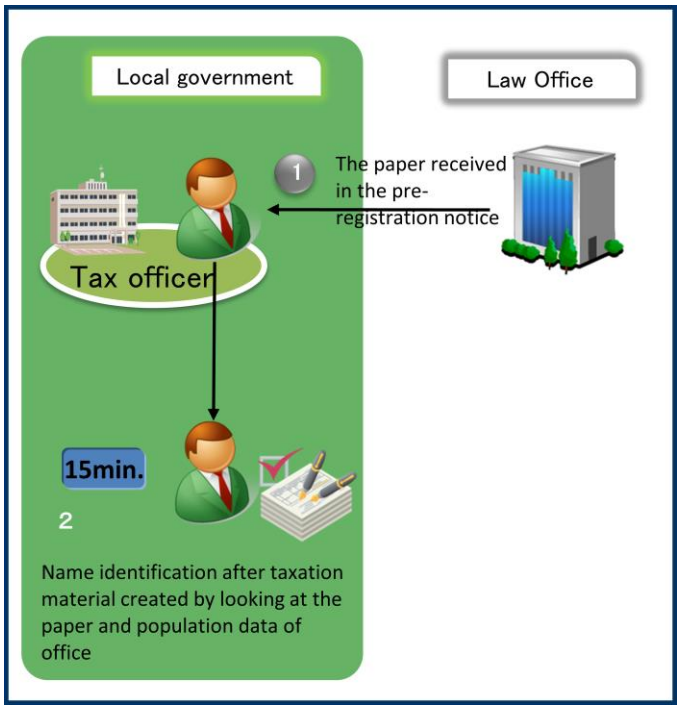

Fig. 8. Past business procedures for property tax payment process.

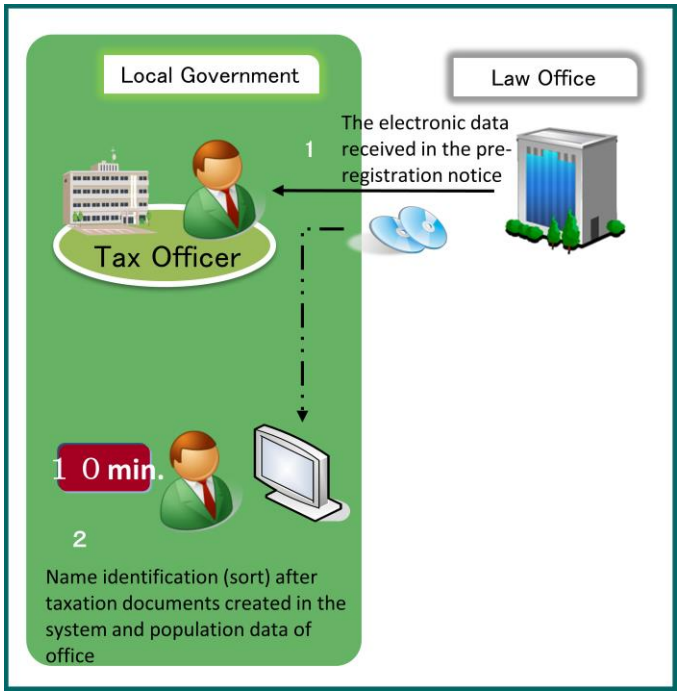

Fig. 9. Current business procedures for property tax payment process.

This is same thing for income tax payment process. As shown in Figure 10 and 11, the required time for income tax payment process is reduced 10.3 minutes by using electronic form of file transfer instead of paper from processing.

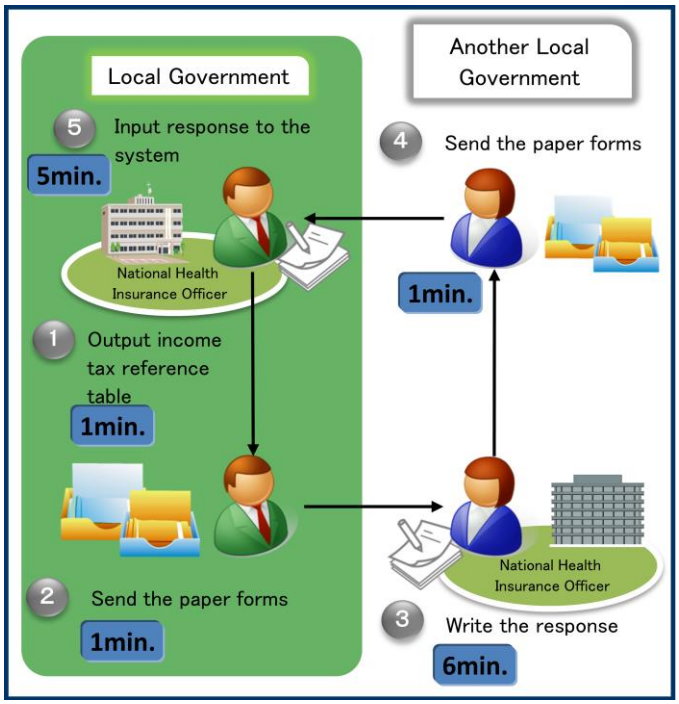

Fig. 10. Past business procedures for income tax payment process.

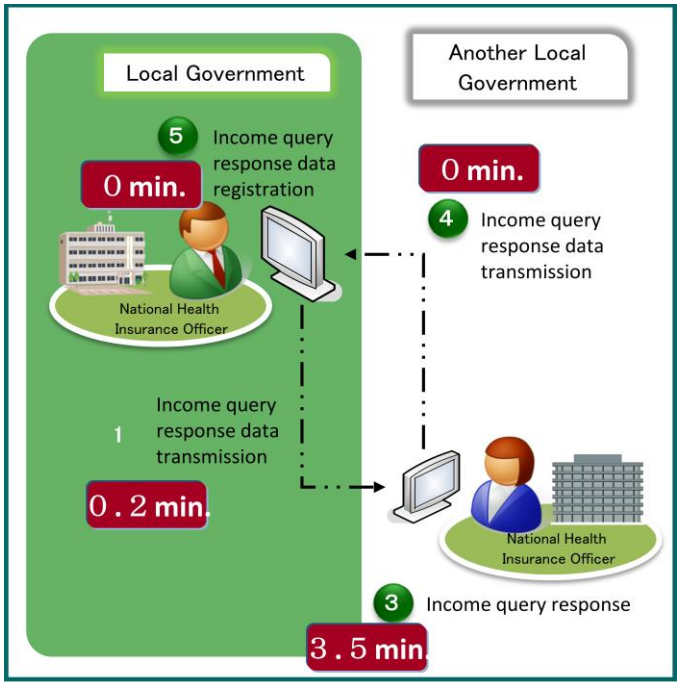

Fig. 11. Current business procedures for income tax payment process.

Another example is National Health Insurance levy (NHI tax calculations) process. As shown in Figure 12 and 13, the required time of National Health Insurance levy (NHI tax calculations) process in the past is 10 minutes while that in the current is just 1 minute. By using electronic form of National

Health Insurance levy (NHI tax calculations) file, the required process time becomes 1/10.

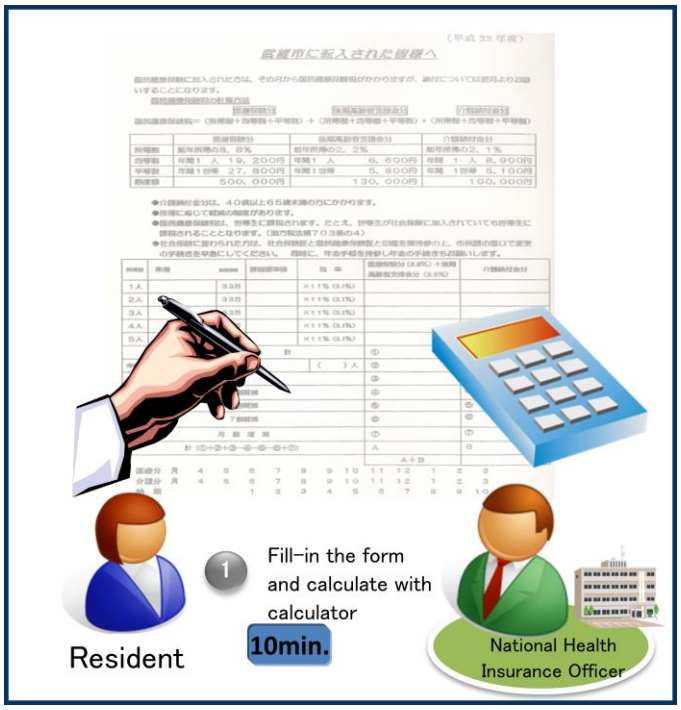

Fig. 12. Past business procedures for National Health Insurance levy (NHI tax calculations) process.

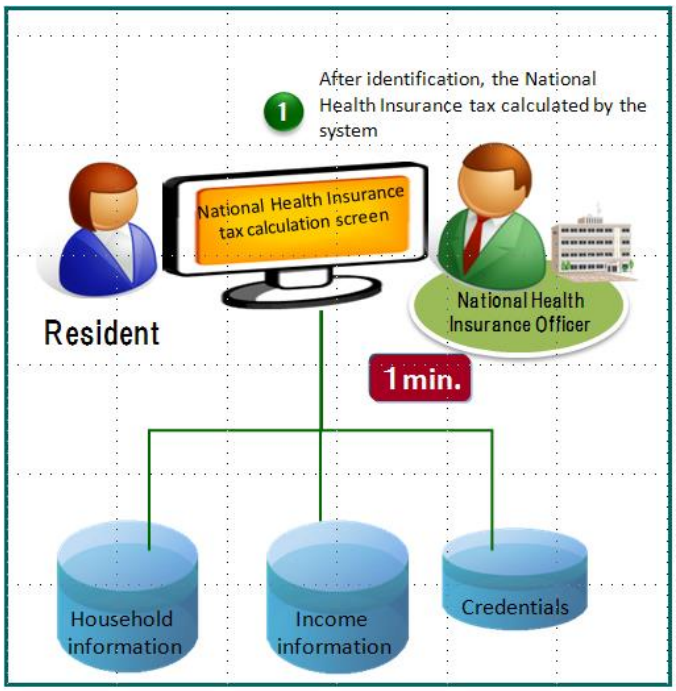

Fig. 13. Current business procedures for National Health Insurance levy (NHI tax calculations) process.

Also, the effectiveness of BPR for National Health Insurance Certificate (envelope stuffing outsourcing) process can be shown. As shown in Figure 14 and 15, the required time of the process is reduced by the factor of 1/10.

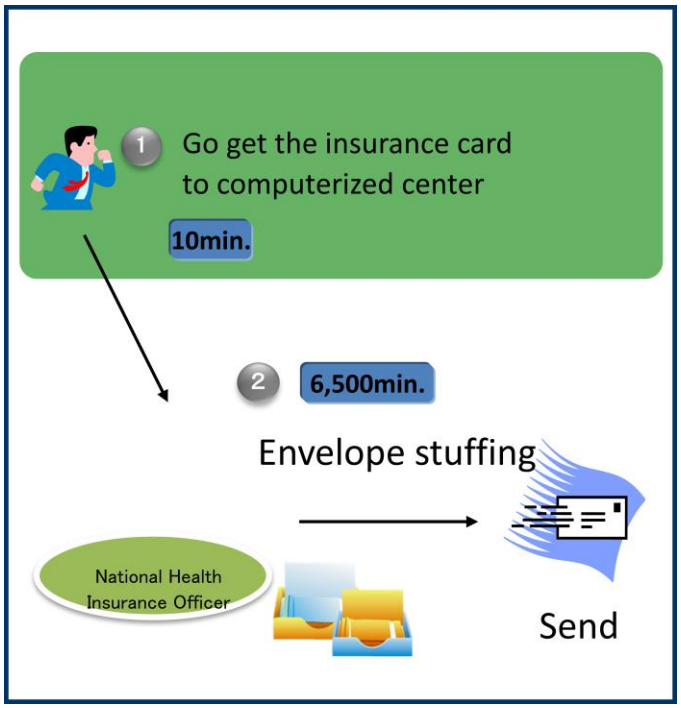

Fig. 14. Past business procedures for National Health Insurance Certificate (envelope stuffing outsourcing) process.

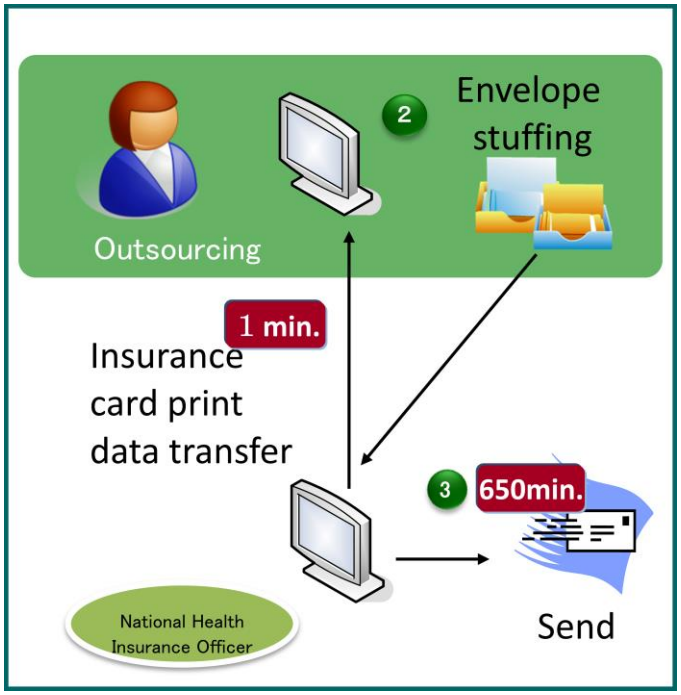

Fig. 15. Current business procedures for National Health Insurance Certificate (envelope stuffing outsourcing) process.

PC from birth to age from a general purpose computer, Office computer we used high-performance server and Web browser but is appearance, began from Netscape, the appearance of so-called Web system, combining the goodness of client-server and benefits of centralized processing of general-purpose machine format system by it . It is getting to the system development of Web-based era. Also in the

development language, or JAVA used for Web-based and 3GL language, is speak in such as Visual Basic from the COBOL language. It has evolved to the language of HTML5 such as NET languages or the like is used, to accommodate the tablet computer configuration and Smartphone in recent years. In addition, the storage technology of beta also developed, I have done the evolution to an RDBMS ISAM File format.

The private companies that take full advantage of the evolution of such technology, the benefits of them, at all, another world different there. A division cooperation through it. It is at present the system that was developed in COBOL language on a general-purpose machine -based system is still a lot of running. Unbelievable sight is accepted without any thing in local government as a private company.

In addition, the procurement system, in information technology knowledge of the civil service is the side you are using poor, mental state of civil servants want to avoid the trouble of the time of system installation also the apprenticeship, information system of local government, remains the oldest it is a reality has become.

Meanwhile, the vendor side have developed provide a system of local governments, a system utilizing the latest technology with the times the system outdated in a way that is enough for the special circumstances of the municipality such optimized than making the state-of-the-art technology of JAVA, and the like COBOL is mixed development language for some reason she fixes little by little the system was developed in the era of the past, hardware though it is a Web era, RDBMS is ISAM design database of thing to use is the present conditions have been created and will remain in the file, the system malformations, local governments without also have a choice of special for the products most vendors are similar , using the system of existing vendors it is placed in a situation where it is not forced to.

Moreover, no such copyright to the system in the past, database design document or design document that the system is in short supply, and help seeking data migration support to existing vendors when changing to other vendors from the vendor of the existing is not obtained, it is causing such case to be in trouble will be prompted to data migration cost a lot of money in many cases, a variety of problems in that case.

Under such circumstances, in order to save the information system cost municipal, and using the method to say municipalities cloud as a country, and is apparently trying a joint of the system of the municipality. Of course, we can expect the effect even moderate order to interoperate systems municipalities as talking at the beginning. But if you think about the information system of local government with much trouble, municipality of 1700 have much more to take advantage of the local government cloud vendors' systems, development and co-operation. There is also cautious to say information system development projects of local government if there are no, to give a serious blow to the IT industry in the part.

The joint-use integration and ultimate local government system of these, same sex cannot be denied a big blow to the IT vendors that can not only support the business model until now certainly. However , it can be said that also have a runaway to a specific industry the taxpayers on the other hand , and they will want to mass-produce IT vendors settle for work low level as a result, competitiveness falling international when IT companies it means that it away.

III. CONCLUSION

Case study on validation of effeteness of Business Procedure Reengineering: BPR for local government in Saga prefecture, Japan is conducted. As the results, if it found that BPR is effective.

In 2013, the government, environment established a government CIO room introduction of a number system was a long-cherished wish is determined, it is possible to promote e-government and e-municipality and the banner of great incredibly plan called "world-leading creative nation" is being put into place some. We would like you to realize the municipality a cloud can be enhanced administrative services to pour our best to take this opportunity, give the impression to the residents as possible; the operational efficiency of the civil service, the foundation is reduced large flower IT costs.

As the results, it is confirmed that around 30 % of required processing time Business Procedure is reduced by BPR. In particular, systemized procedure from the manual base procedure is effective followed by media conversion from paper to electronics form, and personal information processing. On the other hand, it is also found that outsourcing is not so effective.

Meanwhile, resident information processing is the most cost effective by 41 % followed by national health insurance (32 %), and taxation business (28 %) processes

ACKNOWLEDGMENT

The author would like to thank Saga prefectural local government officer for their efforts through experiments and simulations.

REFERENCES

[1] Michael Hammer, Reengineering Work: Don't automate, Obliterate, Harvard Business Review 1990

[2] Kohei Arai, Fundamental of Information Science and Engineering in ubiquitous era -ICT Technology for Business-, Gakujutsu-Tosho Publishing Co. Ltd., 2008.

[3] K.Arai, Y. J. Sun, Effects of business process re-engineering: BPR for local government Information Systems, International Journal of Research and Review on Computer Science, 3, 4, 1755-1760, 2012.

AUTHORS PROFILE

Kohei Arai, He received BS, MS and PhD degrees in 1972, 1974 and 1982, respectively. He was with The Institute for Industrial Science and Technology of the University of Tokyo from April 1974 to December 1978 also was with National Space Development Agency of Japan from January, 1979 to March, 1990. During from 1985 to 1987, he was with Canada Centre for Remote Sensing as a Post Doctoral Fellow of National Science and Engineering Research Council of Canada. He moved to Saga University as a Professor in Department of Information Science on April 1990. He was a councilor for the Aeronautics and Space related to the Technology Committee of the Ministry of Science and Technology during from 1998 to 2000. He was a councilor of Saga University for 2002 and 2003. He also was an executive councilor for the Remote Sensing Society of Japan for 2003 to 2005. He is an Adjunct Professor of University of Arizona, USA since 1998. He also is Vice Chairman of the Commission “A” of ICSU/COSPAR since 2008. He wrote 30 books and published 472 journal papers

Free Open Source Software: FOSS Based e-learning, Mobile Learning Systems Together with Blended Learning System

Kohei Arai [1]
[1] Graduate School of Science and Engineering
Saga University
Saga City, Japan

***Abstract*—Free Open Source Software: FOSS based e-learning system is proposed together with blended learning and mobile learning. Mashup search engine for e-learning contents search and content adaptation from e-learning to mobile learning content are also implemented. Through implementation of the proposed system, it is found that the system does work well for improvement of learning efficiency.**

Keywords—e-learning; blended learning; foree open source softeware; mushup; mobile learning

I. INTRODUCTION

Free Open Source Software: FOSS is getting popular now a day very much and is widely available for e-learning, blended learning and mobile-learning [1]-[12]. All the required components for creation of e-learning system can be created with FOSS software.

Comprehensive economy framework among ASEAN-Japan agreed in April 2003 emphasizes ICT related Human Resource. Concentrating realistic manner for creation of e-learning, m-learning contents, the tools, Moodle, apache, php, SQL, video streaming, Perl, blended learning, chat-bot, camera monitor, etc. are provided. Methods for contents creation for math., object oriented language, etc. subjects: Concentrate how to teach and learn, how to improve students' capability = FD. Content adaptation from e-learning to m-learning is also available together with Mashup contents search, AdHoc mesh network.

Japanese contribution on ICT technology to Asian countries, in terms of ICT infrastructure, ICT technology for higher education, Preparation of e-learning, m-learning content creations, Sharing contents are enhanced. Meanwhile, Web2.0 is getting popular and is widely used. In particular, Extensible Markup Language (XML), Simple Object Access Protocol (SOAP), Web Services Description Language (WSDL), Universal Description, Discovery, and Integration (UDDI), Social Networking Sites, Aggregators, Mashups are getting popular.

On the other hand, M-learning is widely used now a day. Because it is highly portable, available wherever the user needs to learn, individual, adapting to the learner's abilities, unobtrusive, the learner can capture situations and retrieve knowledge without the technology obtruding on the situation; available anywhere, to enable communication with teachers, experts and peers. Also it is adaptable, to the context of learning and the learner's evolving skills and knowledge; persistent, to manage learning throughout a lifetime, useful, suited to everyday needs for communication, reference, work and learning, easy to use, by people with no previous experience of the technology.

The system proposed here is FOSS based e-learning and mobile learning systems together with blended learning. It can be created with free open source software with PC which is getting much cheaper than before. Therefore, it requires a small amount of money while performance and capability is almost compatible to the conventional expensive system.

The following section describes the proposed system followed by some experiments on blended learning which shows an effectiveness of blended learning. Then conclusion is described together with some discussions,

II. PROPOSED SYSTEM

A. Free Open Sorce Software: FOSS

A variety of software is available as FOSS. The followings are just examples for FOSS. All the required modules for e-learning, blended learning and mobile learning systems can be created with FOSS

- Operating System: OS

Linux OS is freely available from the following site,

  - Linux: http://www.linux.org/

- Database: DB

Database handling and processing can be done with PostgreSQL, MySQL, etc. which are available from the following sites,

  - PostgreSQL: http://www.postgresql.org/
  - MySQL:

- Web design

e-learning, blended learning, mobile learning systems need web design and network control. Web design and networking

FOSS is available. For instance, JBOSS Tomcat of web design and networking FOSS is available from the following site,

- JBOSS Tomcat: http://openstandia.jp/services/jboss/jboss_basic_performance.html

Other than this, there is available JBOSS EAP and the other following functions of FOSS,

- Application Platform (JBoss EAP)
- Portal Platform
- SOA Platform
- Web Server
- Hibernate: DB mapping tool
- Seam: Web application
- jBPM: Workflow engine
- Rules: Execution

- Network Management

Network management of FOSS is also available. For instance, Hinemos can be downloading from the following site,

- Hinemos: http://sourceforge.jp/projects/hinemos/

The following functions are provided by the Hinemos,

- Efficient management and operation
- Log check
- Performance check
- Job execute
- Configuration management
- Batch processing
- Web server
- Network devices
- DB server
- AP server

- Programming

Ruby, Perl are typical programming languages and are downloaded from the following sites,

- Ruby: http://www.ruby-lang.org/en/
- Perl: http://www.perl.org/

- Office like application

Office like application FOSS is available from the following site,

- StarSuite: http://www.openoffice.org/

Word processing, table calculation, etc. Can be done with the StarSuite of FOSS.

- Web Browser

Web browsing can be done with FOSS of Mozilla FireFox which can be downloaded from the following site,

- Mozilla FireFox: http://www.mozilas.com/

- Specification, LMS

More important core software of Learning Management System of FOSS is available. As mentioned previously, SCORM standard is the key issues here in e-learning, blended learning, mobile learning systems. If the systems and created e-learning contents meet with all the required specifications of SCORM standard, then the systems can share the e-learning contents. One of SCORM standard of FOSS is Moodle followed by Attain. Moodle and Attain can be downloaded from the following sites,

- SCORM, Moodle, etc: http://satt.jp/product/attain3/download.htm
- http://moodle.org/downloads/

- Open Simulator for chatting (Second Life)

Chatting function can be created by using Open Simulator attractively. One of the examples of chatting capability included e-learning system is proposed already. Open Simulator can be downloaded from the following site,

http://opensimulator.org/wiki/Main_Page

By using the aforementioned FOSS software, all the components required for construction of e-learning system, blended learning, and mobile learning system can be created.

B. Conventional e-learning system

Conventional e-learning system is matched with SCORM1.2, SCORM2004 standard [1]. The followings are important for Learning Management System; LMS of the SCORM standard,

- reusability
- accessibility
- durability
- interoperability

Learnt information can be gathered through API adapter program. Content aggregation can be done with the followings,

- XML file with keywords, version, provider name, etc.
- XML+contents→ZIP
- Stored in LMS

Therefore, learnt information can be referred by all the students and the lecturers through Moodle.

C. Blended Learning System

Blended Learning is the way to teach and to learn through combination or 'blending' of multiple methods and learning styles together. Typical Blended Learning is based on the combination of online and face-to-face basis approaches for teach and learn. It is possible to provide flexible and alternative learning opportunities for students even if students are out the classroom and if after class.

[1] http://203.183.1.152/cgi-bin/csvmail/kigyou_scorm_download.html

To encourage learning, blended learning system can be used by students when students are out the classroom and when after school. In our face-to-face lecture, any e-learning system is used. Another example is a course which carries out alternately the face-to-face lecture and e-learning, m-learning.

Figure 1 shows a typical blended learning scheme. In a prior to start the class in concern, students can download the learning materials through e-learning system. After that, students have the class through face to face lectures with support from e-learning systems. Question and Answering system, chatting system, bulletin board system, and mobile learning system is used for students. After the class ends, students may learn about class subjects through e-learning and mobile learning systems.

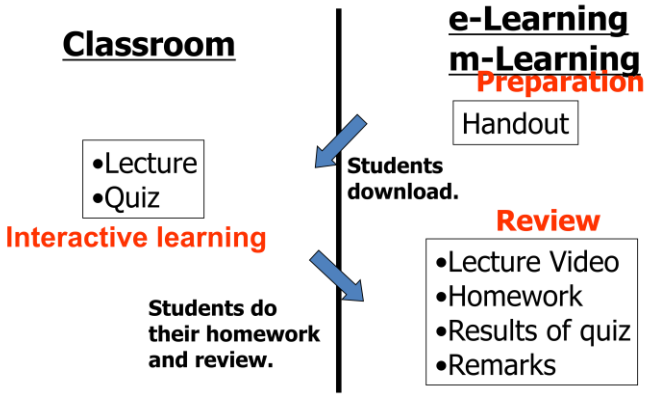

Fig. 1. Blended Learning Scheme

D. Moodle system

Moodle[2] is a widely used standard LMS of e-learning system. Example of my Moodle site in the Graduate School of Science and Engineering, Saga University is shown in Figure 2.

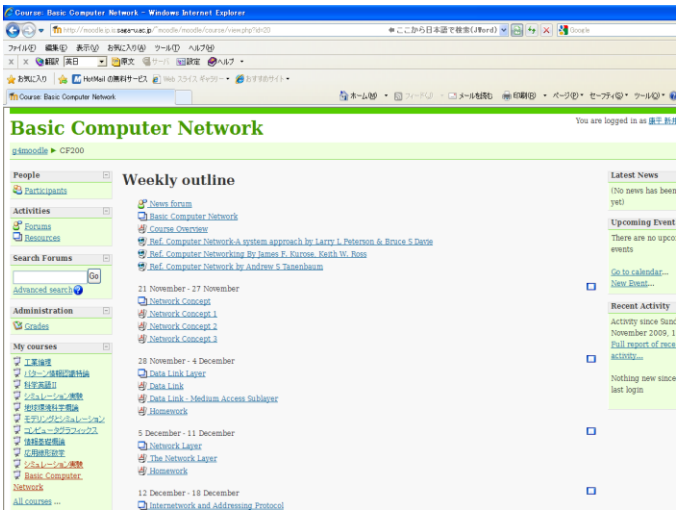

Fig. 2. Example of my Moodle site

[2] http://net.pd.saga-u.ac.jp/e-learning/

The URL for Saga University Moodle site is

http://net.pd.saga-u.ac.jp/e-learning/.

From the site, class related information, outline, schedule, contents, forum, Q/A, quiz, chat, achievement test are available. One month before class starts, this site has to be opened.

Contents resources archives are available from the following site, for example,

http://upo-net.code.u-air.ac.jp/about/

Open University in Japan creates ups of content database which allows download and retrieves Moodle contents.

E. Lecture scenario creation and edit

There are some software tools for lecture scenario creation and edit as follows,

- Basic HTML files
  - Pages for state explanation and instruction and links for selections
  - Free form
- Moodle's Lesson module: we can provide
  - Provides standard actions for the transition
- Captivate(Adobe)
  - Provides rich contents

Although the most recommendable software for scenario creation and editing is Captivate which is provided by Adobe, is can be done with basic html files and Moodle of FOSS. Captivate does cost.

Also lesson modules for Moodle are available as follows,

- Select "Lesson" from "Add an activity"
- Sample:

http://www.cs.is.saga-u.ac.jp/%7Emika/lecture/moodle/mod/lesson/view.php?id=24

- How to create it (SWF)

Small Web Format of files can be created easily. The following site provide a lesson learnt information,

http://www.cs.is.saga-u.ac.jp/%7Emika/lecture/moodle/mod/resource/view.php?id=26

Captivate has a project type for a scenario base material. Software and scenario simulations are available. Scenario simulation provides branching functionality.

- Capturing mode usage: Recording
- Editing mode usage: Editing
- Exporting into a flash file: Publishing
- Objects: Text Caption, Rollover Caption, Highlighting

Box, etc.

- Slides: Question Slide, Random Question Slide, Image Slide, etc.
- Timeline Editing
- Library Usage
- Branching

Scenario Simulation provides branching functionality as shown in Figure 3.

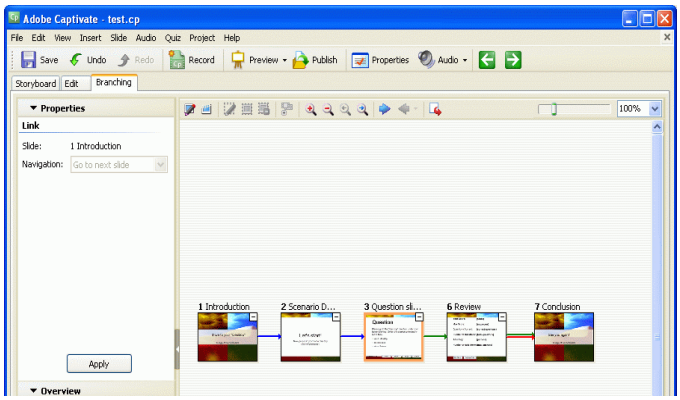

Fig. 3. branching function for scenario simulations

Scenario number can be rearranged by clinking the scenario block and drag and drop operation for replacing the scenario numbers easily.

F. Image manipulation

For creation of e-learning contents, image processing, capturing, processing, and output imagery data is needed. Green shot is an example of image manipulation software with the following functions.

- Simple screen shot tool for Windows
- Open Source (GPL)
- Current Version: Beta 6.0
  - Requires .Net framework 2.0
  - Still capture: region, window, full screen
  - Simple editor: rectangle, oval, text area
  - Several image formats: JPEG, GIF, PNG, BMP
  - Weak points: no timer, no undo,

It is also available for the following edit and save the files.

- The built in image editor popped up after capturing automatically
- Add objects: rectangle, oval, textbox
- Image file formats: JPEG, GIF, PNG, BMP
- Try them all using the “Save as …” menu

Irfan is the image manipulation software with the following functions,

You may convert from many kinds of still and moving picture formats to many kinds of formats

Figure 4 shows the available file formats which are supported by the Infan FOSS while Figure 4 shows the available image processing functions which are supported by Irfan FOSS software.

On the other hand, Irfan has many image processing capabilities as shown in Figure 5.

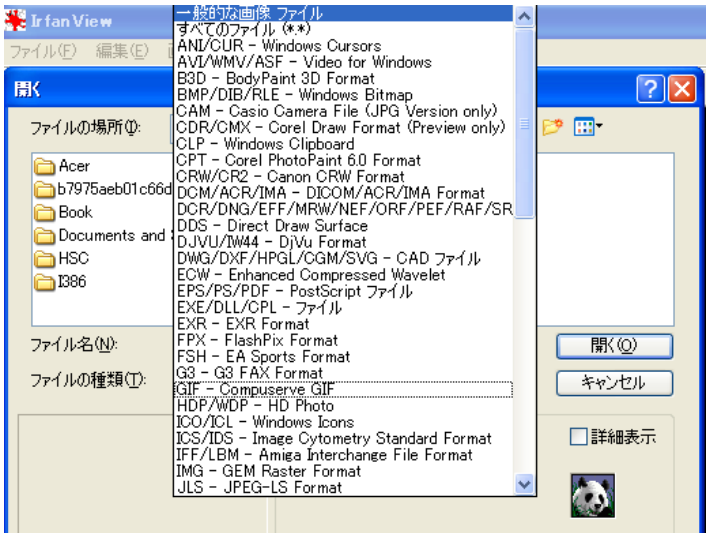

Fig. 4. Available file formats which is supported by Infan FOSS software

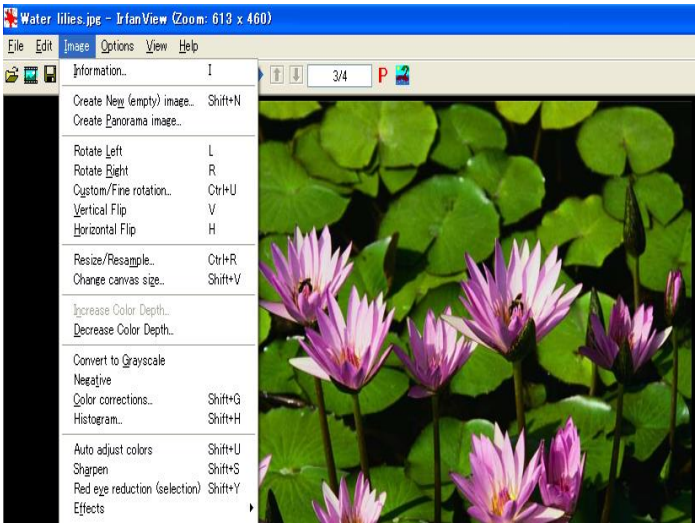

Fig. 5. Available functions which is supported by Irfan FOSS software.

G. Video capture and editing

Capture XP is the video capture and edits software with the following functions,

- Free but not open
- Japanese version only
- No built in viewer / editor
  - Requires external viewer / editor
- Timer function

Configuration of Capture XP has the following functions,

- Setup the external image viewer / editor
  - My recommendation: IrfanView
- http://www.irfanview.com/
- Supports a lot of image formats
- Provides basic edit functionalities
- Area selection, cut and past, resize, rotation, etc.

Camstudio is the another video capture software with the following features,

- Open Source (GPL)
- Capturing screen motion in the AVI format and the SWF format.
- Original codec (CamStudioCodec10) provided.

Camstudio can be work as follows,

- Run CamStudio
- Click Record button
- Set area on CamStudio
- After a while click Stop button
- Save the file into My Documents
- Toggle the mode to SWF
- Record again and save the file too
- SWFTOOLS

http://www.swftools.org/

- PDF2SWF, JPEG2SWF, AVI2SWF, etc.
- FLVTool2

http://rubyforge.org/projects/flvtool2/

- Setup to output images as files in a folder
- Capture region
  - Select menu or Print
  - Left-click and drag, then release to capture the area
- Capture window
  - Select menu or Alt + Print
  - Left-click the target window
- Capture full screen
  - Select menu or Ctrl + Print

Capture region has to be designated before the capturing moving picture obviously with the function provided by Camstudio which is shown in Figure 6.

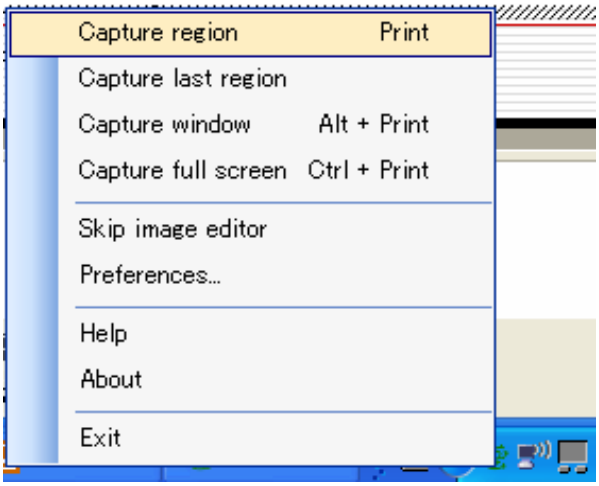

Fig. 6. Designation of capture regions

H. XML based contents

SCORM meta-tag and XML based database management is key.

http://wareseeker.com/free-scorm-metadata-generator/

- These tags are very important if you want your web pages to be crawled by search engines and play an important role in determining your web site ranking.
- Metadata Generator is the quickest and simplest way to create META tags for your web pages.
- This program guarantees to be the best one out there in its category - with inclusion of all the essential tags for your pages. And the best part is no knowledge of META tags is necessary to use Metadata Generator.
- Just key in the required information and voila, your metadata has been generated.

I. Mush-up web services

A web mashup is a new type of web application that uses data and services from one or more external sources (usually from the Internet) to build entirely new and different web applications

Mashup web services are not a web portal. Combining Web service technologies with fresh content, collaborative approaches (such as Web 2.0 technologies), and possibly Web data management and semantic technologies (RSS, RDF). Mashup architecture is shown in Figure 7.

There are some mushup editors as shown below,

- **Online**
  - Yahoo Pipes (http://pipes.yahoo.com/pipes/)
  - Microsoft Popfly (http://www.popfly.com/) died on Aug 24, 2009
  - Ubiquity (http://ubiquity.mozilla.com/)
- **Application**

- Jackbe (http://www.jackbe.com/)

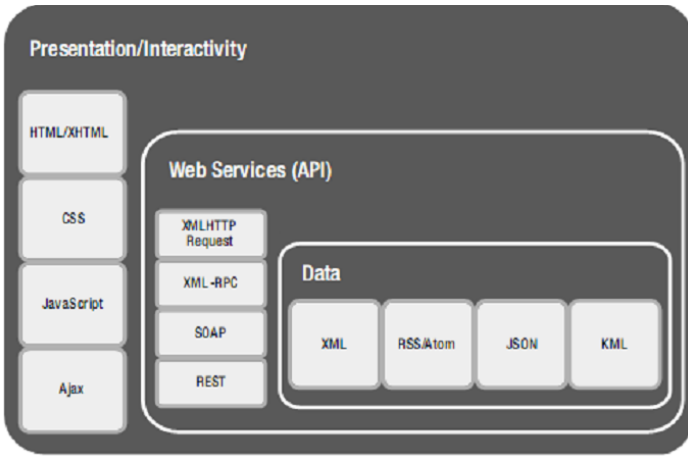

Fig. 7. Mush-up Architecture

Mashup API allows the functions as shown in Figure 8.

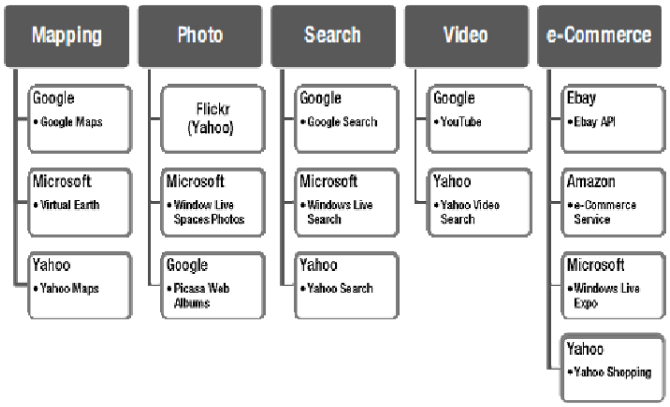

Fig. 8. Available functions for mashup API.

J. Mobile learning

XHTML MP and WCSS are examples of mashup for m-learning as shown below,

- Client open the application just using standard browser.
- XHTML Mobile Profile & WAP CSS (WCSS) for Mobile is new standard for develop web application for mobile client (proposed by W3C and OMA)
- Support W3C standard for Mobile Web

In accordance with WiKipedia, mobile learning, m-learning is defined as follows,

- Wikipedia: Learning that happens across locations, or that takes advantage of learning opportunities offered by portable technologies.
- In other words, mobile learning decreases limitation of learning location with the mobility of general portable devices.

· E-learning + mobile computing
  - PDA
  - Cell phones
  - Any small, autonomous and unobtrusive device

There are limitations for mobile devices as follows,

- Smaller Screen Size
- Limit of input key
- Lower memory
- Slower processor speed
- Slower bandwidth rates
- Short battery life

In order to overcome the limitations, the following treatments are required for the m-learning system,

- Format transcoding e.g. XML to XHTML
  - http://www.slideshare.net/ : automatic transcoding PowerPoint to Flash
- Scalable Vector Graphics - SVG to GIF
- Scaling (of images as well as video and audio streams),
- Media conversion (e.g. text-to-speech),
- Re-sampling,
- File size compression
- Document fragmentation
- Structure of the typical e-learning content based on XML
- Easily converted to m-learning contents based on the structure described with XML

Thus the contents conversion and display onto mobile devices can be done as shown in Figure 9.

Example of m-learning domain is illustrated in the Figure 10.

There are some content adaptation schemes as follows,

- Proxy based:
  - New Mobile Specific Browser
  - Opera Mobile, Skyfire
- Server based:
  - Server provide specific mobile access: Yahoo
  - Mobile, YouTube Mobile, Facebook Mobile, etc

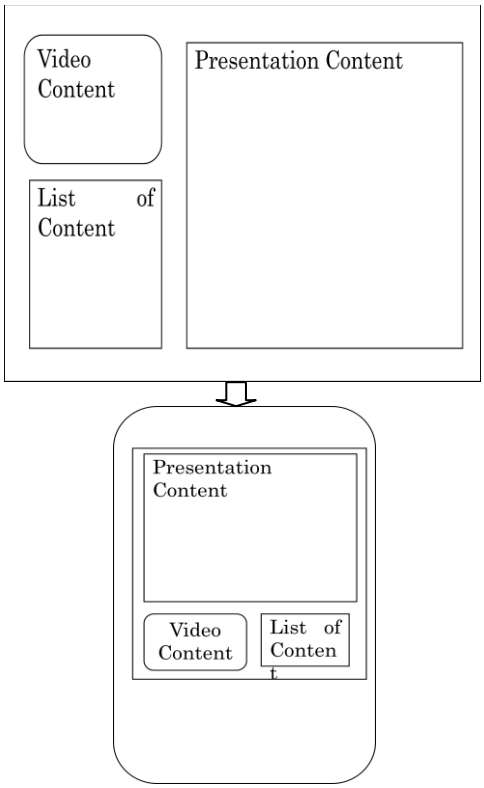

Fig. 9. Content conversion from e-learning to m-learning

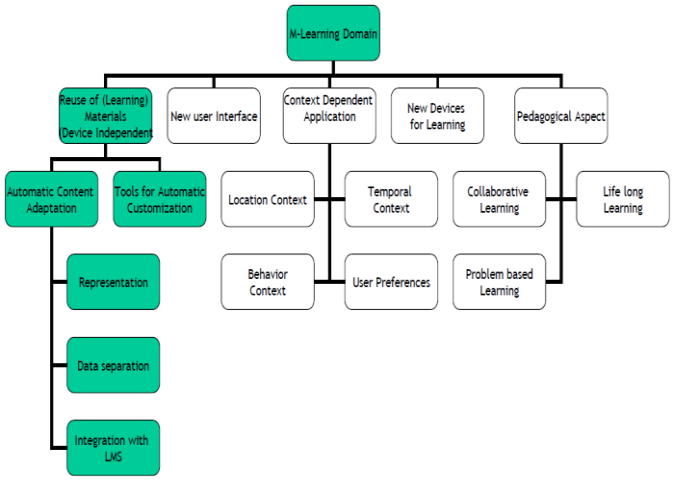

Fig. 10. m-learning domains

There are some W3C standards for m-learning web services as shown below,

- W3C-Deined Default Delivery Context
- Usable Screen Width: 120 pixels, minimum
- Markup Language Support: XHTML Basic 1.1 delivered with content type application/xhtml+xml
- Character Encoding: UTF-8
- Image Format Support: JPEG, GIF 89a
- Maximum Total Page Weight: 20 kilobytes
- Colors: 256 Colors minimum
- Style Sheet Support: CSS Level 1. In addition, CSS Level 2 @media rule together with the handheld and all media types
- HTTP: HTTP/1.0 or more recent HTTP 1.1
- Script: No support for client-side scripting

Example of XML tagging is shown in Figure 11.

Fig. 11. Example of XML tagging

In the Web 2.0, the followings are available,

- AJAX
- Tagging
- Blogs and blogging
  - A list of most “linked-to” blogs
- Really Simple Syndication (RSS)
- Wikis
  - Wikis used in business
- Podcasts and Videocasts

III. EXPERIMENTS

Implementation of the proposed e-learning, mobile learning system is successfully done. All the functions of the proposed system are confirmed perfectly. Also, it is confirmed the proposed content adaption for displaying e-learning contents on a relatively small size of display of the mobile devices. Mashup e-learning content search engine is validated with a limited web domain with tagging capability.

Figure 12 shows histogram of students’ score of achievement tests when before and after the blended learning is conducted. It shows more than 10 points of improvement can be done with the blended learning.

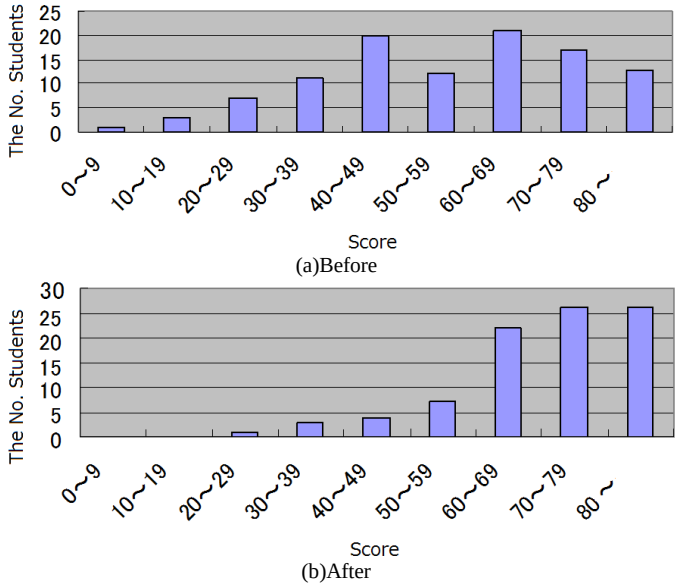

Fig. 12. effectiveness of the blended learning on the applied linear algebra class

IV. CONCLUSION

At the beginning of the course, readiness of the students has to be confirmed. Blended learning is very useful for that and for improvement their readiness. Through face-to-face lectures with interactive learning, they need to review the contents and exercise is required simultaneously with lecture. Blended learning is applicable for that. After the class, they can re-review the contents through e-learning and m-learning.

The followings are the recommendations for the e-learning and m-learning systems,

- Using SCORM meta-tag, DB management with XML
- Self Instructional Design
- Linkage with class time schedule is effective to the lectures
- Create contents database like the UPO in Japan
- Create portal for free open source software for e-learning and m-learning

Table 1 also shows summarized recommendations for creation of e-learning and m-learning contents using FOSS software..

TABLE I. SUMMARY OF THE ZRECOMMENDATIONS FOR E-LEARNING, BLENDED LEARNING AND MOBILE LEARNING SYSTEM

Environment	Development Tools	Database	Programming Language	Web Server
Java	Net Beans 6.1	MySQL, PostgreeSQL	Java	Sun Java Web Server
Ruby on Rails	Aptana Studio	MySQL	Ruby, Perl	Mongrel
Microsoft.net	Visual Studio 8.0	SQL Server	C♯, VB	IIS 7.0
PHP	Framework?	MySQL	PHP	Apache

Acknowledgment

The author would like to thank Dr. Teruya Minamoto and Dr. Mika Otsuki of Saga University as well as Dr. Herman Tolle of Brawijaya University, Indonesia for their efforts through implementation and experiments.

REFERENCES

[1] M.Oda, S.Oda, K.Arai, CAI system for pronunciation practice in particular for discrimination of |l| and |r| on WWW site utilizing mouth movements and voices, Journal of Educational System and Information Society of Japan, Vol.17, No.3, pp.162-173, (2000).

[2] Mariko Oda, Seio Oda and Kohei Arai, Effect of pronunciation practice system using capture the mouse movement, Journal of Educational Engineering Society of Japan, vol.26, No.2, 65-75, 2003

[3] K.Arai, Mayumi Inokuchi, Web based e-learning system allowing BBS, chatting with equation representation together with annotations, Report of Science and Engineering Faculty Saga University, 36、 1、1—8、 2007

[4] K.Arai, Hiroshi Yoshida, e-learning system with users' confidence level evaluations through voice input system, Report of Science and Engineering Faculty Saga University, 36、 1、39-44、2007

[5] Kohei Arai,Herman Tolle, Model based content adaptation of composite e-learning content for delivering to mobile learners, International Journal of Computer Theory and Engineering, 3, 3, 382-387, 2011

[6] K.Arai, T.Herman, E-learning document search method with supplemental keywords derived from keywords in meta-tag and descriptions which are included in the header of the first search result, International Journal of Advanced Computer Science and Applications, 3, 4, 99-104, 2012.

[7] K.Arai, Method for leaning efficiency improvements based on gaze location notifications on e-learning content screen display, International Journal of Advanced Research in Artificial Intelligence, 1, 3, 1-6, 2012.

[8] K.Arai, M.Oda, Effect of pronunciation practice system based on personalized CG animations of mouth movement model, International Journal of Advanced Computer Science and Applications, 3, 6, 125-130, 2012.

[9] K.Arai, E-learning system which allows students' confidence level evaluation with their voice when they answer to the questions during achievement tests, International Journal of Advanced Computer Science and Applications, 3, 9, 80-84, 2012.

[10] K.Arai, Free Open Source Software: FOSS based GIS for spatial retrievals of appropriate locations for ocean energy utilizing electric power generation plants, International Journal of Advanced Computer Science and Applications, 3, 9, 95-99, 2012.

[11] Kohei Arai, Anik Nur Handayani, Predicting quality of answer in collaborative Q/A community, International Journal of Advanced Research in Artificial Intelligence, 2, 3, 21-25, 2013.

[12] Kohei Arai, Anik Nur Handayani, E-learning system utilizing learners' characteristics recognized through learning process with Open Simulator, International Journal of Advanced Research in Artificial Intelligence, 2, 4, 8-12, 2013.

AUTHORS PROFILE

Kohei Arai, He received BS, MS and PhD degrees in 1972, 1974 and 1982, respectively. He was with The Institute for Industrial Science and Technology of the University of Tokyo from April 1974 to December 1978 also was with National Space Development Agency of Japan from January, 1979 to March, 1990. During from 1985 to 1987, he was with Canada Centre for Remote Sensing as a Post Doctoral Fellow of National Science and Engineering Research Council of Canada. He moved to Saga University as a Professor in Department of Information Science on April 1990. He was a councilor for the Aeronautics and Space related to the Technology Committee of the Ministry of Science and Technology during from 1998 to 2000. He was a councilor of Saga University for 2002 and 2003. He also was an executive councilor for the Remote Sensing Society of Japan for 2003 to 2005. He is an Adjunct Professor of University of Arizona, USA since 1998. He also is Vice Chairman of the Commission "A" of ICSU/COSPAR since 2008. He wrote 30 books and published 478 journal papers.

Method for Tealeaves Quality Estimation Through Measurements of Degree of Polarization, Leaf Area Index, Photosynthesis Available Radiance and Normalized Difference Vegetation Index for Characterization of Tealeaves

Kohei Arai [1]
[1] Graduate School of Science and Engineering
Saga University
Saga City, Japan

***Abstract*—Method for tealeaves quality estimation through measurements of Degree of Polarization: DP, Leaf Area Index: LAI, Photosynthesis Available Radiance: PAR and Normalized Difference Vegetation Index: NDVI for characterization of tealeaves is proposed. The method allows estimations of PAR, NDVI, Grow Index: GI by using measured Degree of Polarization: DP of tealeaves. Through experiments at the tea farm areas, it is found that the proposed method is validated. Also, the method is validated through Monte Carlo Ray Tracing: MCRT simulations for discrimination between prolate and oblate shapes of tealeaves. In accordance with growing tealeaves, prolate shape of tealeaves changes their shape to oblate shape. Therefore, growing stage can be estimated with DP measurements.**

Keywords—adjucency effect; nonlinear mixed pixel model; Monte Carlo method; Ray tracing method

I. INTRODUCTION

It is highly desired to monitor vitality of crops in agricultural areas automatically with appropriate measuring instruments in order to manage agricultural area in an efficient manner. It is also required to monitor not only quality but also quantity of vegetations in the farmlands. Vegetation monitoring is attempted with red and photographic cameras [1]. Grow rate monitoring is also attempted with spectral observation [2].

This paper deals with automatic monitoring of tealeaves quality with polarization films attached visible and near infrared cameras. Also,, this paper proposes a method that allows estimation of total nitrogen and fiber contents in tealeaves as an example. Furthermore, this paper describes a method and system for estimation of quantity of crop products by using not only Vegetation Cover: VC and Normalized Difference Vegetation Index: NDVI but also Bi-directional Reflectance Distribution Function: BRDF because the VC and NDVI represent vegetated area while BRDF represents vegetation mass, or layered leaves.

Total nitrogen content corresponds to amid acid which is highly correlated to Theanine: 2-Amino-4-(ethylcarbamoyl) butyric acid for tealeaves so that total nitrogen is highly correlated to tea taste. Meanwhile fiber content in tealeaves has a negative correlation to tea taste. Near Infrared: NIR camera data shows a good correlation to total nitrogen and fiber contents in tealeaves so that tealeaves quality can be monitored with network NIR cameras. It is also possible to estimate total nitrogen and fiber contents in leaves with the acquired camera data. Moreover, VC, NDVI, BRDF of tealeaves has a good correlation to grow index of tealeaves so that it is possible to monitor expected harvest amount and quality of tealeaves with network camera data. BRDF monitoring is well known as a method for vegetation growth [3],[4]. On the other hand, degree of polarization of vegetation is attempted to use for vegetation monitoring [5], in particular, Leaf Area Index: LAI together with new tealeaves growth monitoring with BRDF measurements [6].

Other index for representation of tealeaves quality is Photosynthesis Available Radiance: PAR. There is relation among indexes. The proposed method and system is to monitor tealeaves quality with polarization films covered visible and near infrared cameras. Relation between Degree of Polarization: DP and the other indexes, NDVI, LAI, PAR is clarified in this paper.

In particular, method for estimation of Grow Index: GI derived from DP is validated through Monte Carlo Ray Tracing: MCRT [7]-[16] simulations.

Tea estate monitoring system with network cameras, meteorological robots and the aforementioned cameras is proposed in the following section followed by proposed estimation methods for total nitrogen and fiber contents with network camera data. The proposed method is validated with some experimental results conducted at tea farm areas which are situated in Saga prefecture, Kyushu Japan. Finally, concluding remarks is followed with some discussions.

II. Proposed Method and System

A. Proposed System

Figure 1 shows the proposed system for monitoring of tealeaves quality with polarization films attached visible and Near Infrared: NIR cameras. The cameras are situated at 5-6 m above the ground surface. Visible and NIR network cameras are equipped on the pole in order to look down with 10-80 degrees of incident angle (these angles allow BRDF measurements). The pole is used for avoid frosty damage to the tealeaves using fan mounted on the pole (for convection of boundary layer air). With these network cameras, reflectance in the wavelength region of 550nm (red color) and 870nm (NIR) are measured together with BRDF assuming that vegetated areas are homogeneous and flat. BRDF is used for estimation of Grow Index (GI) and BRDF correction from the measured reflectance of the tealeaves.

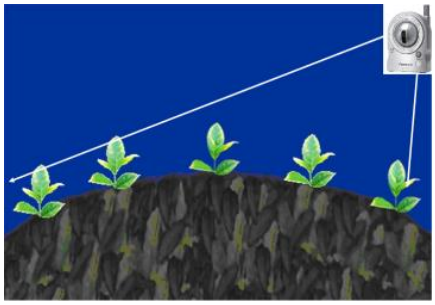

Fig. 1. Proposed system for monitoring of tealeaves quality with polarization films attached visible and Near Infrared: NIR cameras.

Figure 2 shows an example of acquired visible camera images of tea farm area which is situated in Ureshino city, Saga Prefecture, Kyushu, Japan. With these cameras, p and s polarized imagery data can be acquired. Using these polarized imagery data (p and s components of data, p and s), Degree of Polarization: DP can be estimated with Equation (1).

$$DP=(p - s)/(p + s) \quad (1)$$

B. Crop Quality (Nitrogen Contents)Mmonitoring from Space

Nitrogen content is one of representatives of crop quality. Nitrogen content is proportional to Theanine: 2-Amino-4-(ethylcarbamoyl) butyric acid. Because Theanine rich tealeaves taste good, nitrogen content in tealeaves is representative of tealeaves quality. Theanine: 2-Amino-4-(ethylcarbamoyl) butyric acid that is highly correlated to nitrogen contents in new tealeaves are changed to catechin [17],[18],[19] due to sun light. In accordance with sunlight, new tealeaves grow up so that there is a most appropriate time for harvest in order to maximize amount and taste of new tealeaves simultaneously.

Grow Index: GI is other representative for tealeaves growing. It can be measured with Green Meter: GM values of tealeaves. Leaf Area Index: LAI of tealeaves and Photosynthesis Available Radiance: PAR is another representative of harvesting amount and tealeaves quality. Through monitoring these GI, LAI, it is possible to find growing status while tealeaves quality can be found through GM and PAR monitoring.

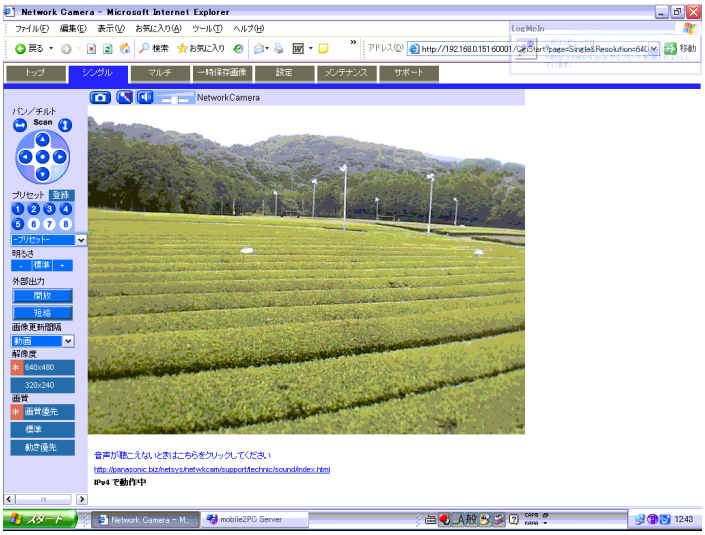

Fig. 2. Example of farmland monitored visible camera image.

C. Grow Stage Monitoring

Grow stage can be monitored by measuring shape of tealeaves. New tealeaves are borne from the matured tealeaves which are situated in Japan in the late of March or the begging of April. Tips of the new borne tealeaves are directed to the sky. Then tips of the tealeaves are directed to horizon in accordance with growing stage. Directions of tealeaves can be discriminated through DP measurements. Therefore, grow stage monitoring can be done with DP measurements.

III. Simulations

A. Monte Carlo Ray Tracing: MCRT Simulation Method

In order to validate the proposed method, MCRT simulation study and field experimental study is conducted. MCRT allows simulation of polarization characteristics of sea surface with designated parameters of the atmospheric conditions and sea surface and sea water conditions. Illustrative view of MCRT is shown in Figure 3.

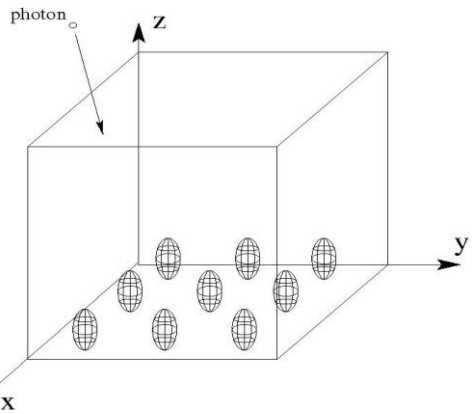

Fig. 3. Monte Carlo Ray Tracing: MCRT Simulation Cell

Photon from the sun is input from the top of the atmosphere (the top of the simulation cell). Travel length of the photon is calculated with optical depth of the atmospheric molecule and that of aerosol. There are two components in the

atmosphere; molecule and aerosol particles while three are also two components, water and particles; suspended solid and phytoplankton in the ocean. When the photon meets molecule or aerosol (the meeting probability with molecule and aerosol depends on their optical depth), then the photon scattered in accordance with scattering properties of molecule and aerosol.

The scattering property is characterized with phase function[1]. In the visible to near infrared wavelength region, the scattering by molecule is followed by Rayleigh scattering law [20] while that by aerosol is followed by Mie scattering law [20].

On the ground surface of MCRT model, there are 2D aligned tealeaves. The shape of these tealeaves is prolate or oblate shapes which are shown in Figure 4.

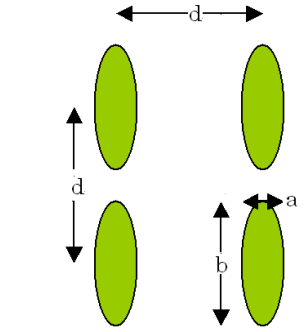

(a) Prolate shape of spheroid model of corn type of crops

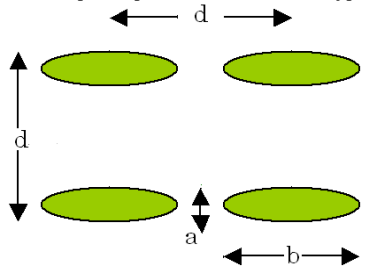

(b) Oblate shape of spheroid model of pea type of crops

Fig. 4. Illustrative view of computer simulation cell that consists of 50 km by 50km by 50km.

Oblate and prolate spheroid shapes of leaves are two dimensionally aligned on ground surface. Horizontal and vertical length of leaves is “a” and “b” while distance between leaves is “d”. The shape of new borne tealeaves from elderly tealeaves is prolate while that of grown-up tealeaves is oblate. Therefore, it is capable to discriminate between new and old tealeaves by using shape factor between prolate and oblate shapes of tealeaves of polarization characteristics. As shown in Figure 5, the shape of tealeaves is changed from prolate to oblate in accordance with their age.

Figure 6 shows DP of the surface consists of prolate and oblate shape of leaves for the solar zenith angle of 60 degree. Figure 6(a) shows DP for the leaves with the different reflectance (0.215 for p and 0.46 for s polarizations for prolate and 0.22 for p and 0.21 for s polarizations for oblate) from the surface, at wavelength of 730nm while Figure 6(b) shows DP for the same leaf reflectance of 0.22 for p and 0.21 for s polarizations for both. Prefatory note denotes long and short radius and (p) and (s) indicates p and s polarized radiance.

Fig. 5. Shapes of new borne tealeaves and old tealeaves

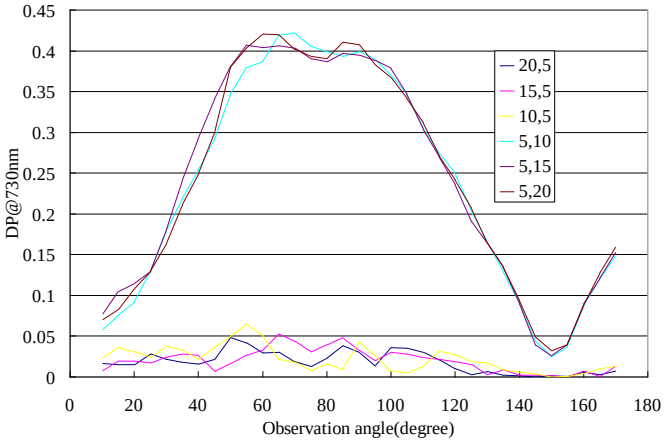

(a) DP for the different shape of spheroid with the different reflectance (0.215 for p and 0.46 for s polarizations for prolate and 0.22 for p and 0.21 for s polarization for oblate)

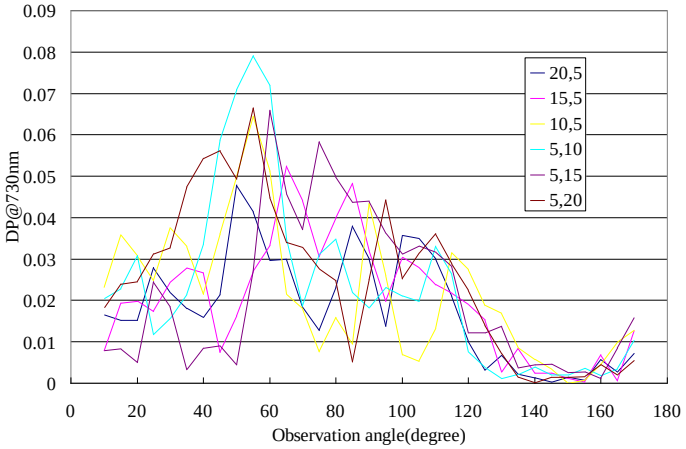

(b) DP for the different shape of spheroid with the same reflectance (0.22 for p and 0.21 for s polarizations for both)

Fig. 6. Degree of Polarization (DP) and the number of photons which correspond to p and s polarized radiance from the surface consists of prolate and oblate shape of leaves for the solar zenith angle of 60 degree. (a) and (b) shows the number of photons and DP for the leaves with the different reflectance (0.215 for p and 0.46 for s polarizations for prolate and 0.22 for p and 0.21 for s polarizations for oblate) from the surface, at wavelength of 730nm while (c) and (d) those for the same leaf reflectance of 0.22 for p and 0.21 for s polarizations for both. Prefatory note denotes long and short radius and (p) and (s) indicates p and s polarized radiance.

[1] http://ejje.weblio.jp/content/phase+function

Meanwhile, Figure 7 shows DP of the surface consists of prolate and oblate shape of leaves for the solar zenith angle of 60 degree. Figure 7(a) shows DP for the leaves with the different reflectance (0.1 for p and 0.5 for s polarizations for prolate and 0.08 for p and 0.21 for s polarizations for oblate) from the surface, at wavelength of 550nm while Figure 7(b) shows DP of the same leaf reflectance of 0.1 for p and 0.5 for s polarizations for both.

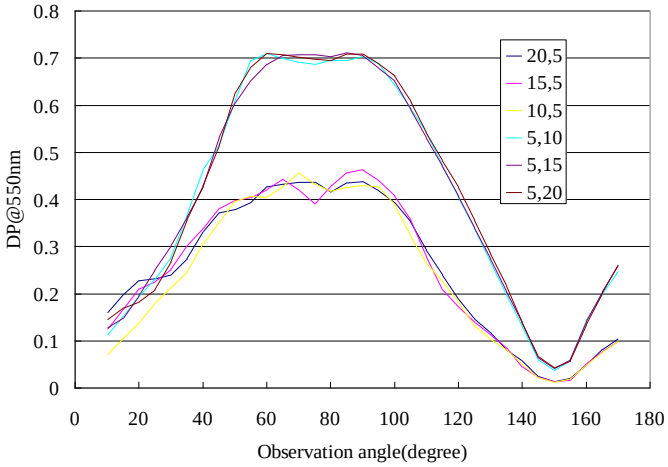

(a) DP for the different shape of spheroid with the different reflectance (0.1 for p and 0.5 for s polarizations for prolate and 0.08 for p and 0.21 for s polarization for oblate)

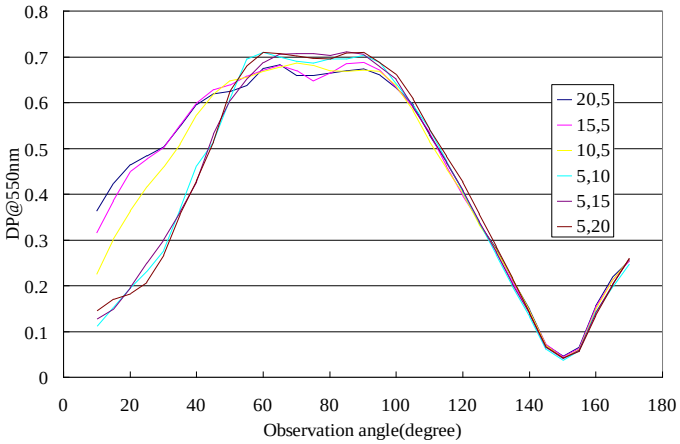

(b)DP for the different shape of spheroid with the same reflectance (0.1 for p and 0.5 for s polarizations for both)

Fig. 7. Degree of Polarization (DP) and the number of photons which correspond to p and s polarized radiance from the surface consists of prolate and oblate shape of leaves for the solar zenith angle of 60 degree. (a) and (b) shows the number of photons and DP for the leaves with the different reflectance (0.1 for p and 0.5 for s polarizations for prolate and 0.08 for p and 0.21 for s polarizations for oblate) from the surface, at wavelength of 550nm while (c) and (d) those for the same leaf reflectance of 0.1 for p and 0.5 for s polarizations for both. Prefatory note denotes long and short radius and (p) and (s) indicates p and s polarized radiance.

It is found that the difference between prolate and oblate shapes of tealeaves at 550nm (green band) is much clear than that of 730nm (near infrared band) through comparison between Figure 6 and 7. It is also found that the difference of DP for different reflectance for p and s polarized reflectance is much greater than that for same reflectance. DP difference between prolate and oblate shapes of tealeaves for both same and different reflectance at p and s polarization at around 30 degree of observation angle shows relatively clear than that for the other observation angle. Therefore, 30 degree of observation angle would be the best for DP observations.

IV. EXPERIMENTS

A. *Measuremeng Instruments*

Tracing Radiation and Canopy Architecture: TRAC of Leaf Area Index Measuring Instrument manufactured by The Third Wave Engineering, Canada is used for the experiment. Wavelength coverage ranges from 400 to 700 nm. Outlook of the TRAC is shown in Figure 8.

Fig. 8. Outlook of the TRAC for measurement of LAI

Meanwhile the outlook of the polarization film attached camera with fish eye lens is shown in Figure 9.

(a) Digital camera with fish eye lens

(b) Polarization film attached fish eye lens

Fig. 9. Camera for polarization measurements

Meanwhile, outlook of the measurement instrument for surface reflectance, PAR, NDVI is shown in Figure 10 while major specification of the measuring instrument is shown in Table 1.

Fig. 10. Measuring instrument for surface reflectance, PAR, and NDVI

TABLE I. MAJOR SPECIFICATION OF MS-720

Wavelength coverage	350～1,050nm
Wavelength interval	3.3nm
Wavelength resolution	10nm
Wavelength accuracy	Less than 0.3nm
Full aperture	180°
Stray light	Less than 0.15%
Temperature dependency	±5%
Output Unit	$W/m^2/\mu m$ or $\mu mol/m^2/s/\mu m$
Measurement time	0.005～5sec

Field experiments are conducted at the Saga Prefectural Tea Institute: SPTI situated at 33:07:03.9 N, 129:59:47.0 E on June 1 2008. The first harvesting is finished in the begging of May. After the harvesting of tealeaves, the top tea trees are used to be cut out. Then new tealeaves appear after that. June 1 is middle moment between the first and the second harvests. There are four tea farm areas which are situated North, East, South, and West sides of the SPTI main building as shown in Figure 11.

Figure 12 shows Proposed simple LAI monitoring method with cameras with p and s polarization films attached fish eye lens that allows calculation of Degree of Polarization: DP results in estimation of LAI together with examples of p and s polarized radiance images of new tealeaves acquired at Ureshino Saga Japan tea estate on June 1 2008.

Figure 13 shows typical new tealeaves grow process from the top view of tea estate. Typically, new tealeaves appear in the early April and are harvested in the late April or the early May.

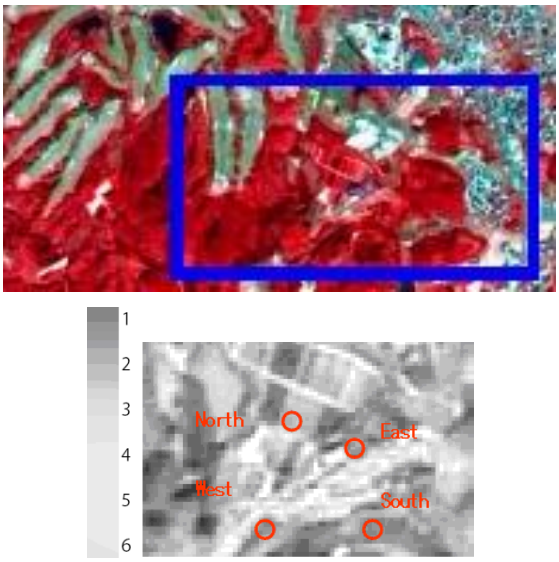

Fig. 11. Enlarged ASTER/VNIR image and total nitrogen contents in tealeaves at the tea estate (Red circles shows tea estates. Grayscale shows TN% of nitrogen contents in tealeaves derived from equation (1) of TN=22.474 Ref(Band#3)-10.177): Tea farm areas in concern situated at SPTI (33:07:03.9 N, 129:59:47.0 E)

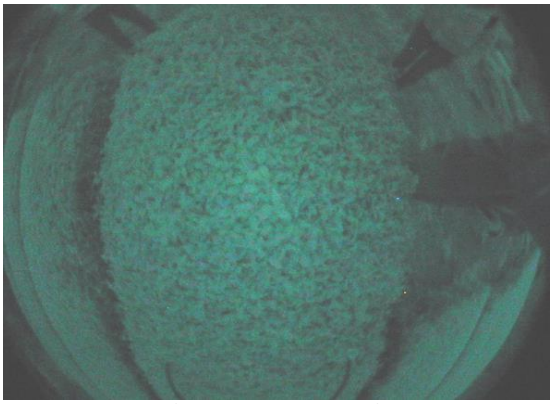

(a) Example of p polarized radiance of new tealeaves

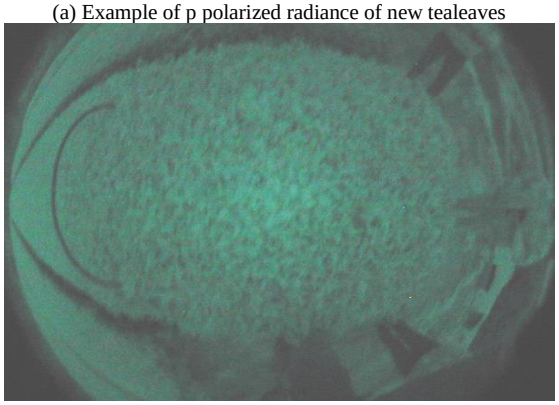

(b) Example of s polarized radiance of new tealeaves

Fig. 12. Proposed simple LAI monitoring method with cameras with p and s polarization films attached fish eye lens that allows calculation of Degree of Polarization: DP results in estimation of LAI together with examples of p and s polarized radiance images of new tealeaves acquired at Ureshino Saga Japan tea estate on June 1 2008.

Then new tealeaves grow up again in June and are harvested in July. After that new tealeaves grow up again and are harvested in September or October. After all, old tealeaves are cut a little bit for preparation of cold winter season. The idea proposed here is to evaluate vitality of the tea trees through evaluation of total nitrogen and fiber contents by using network cameras monitored in the winter season after harvesting new tealeaves. Such method that allows estimation of vitality of the tea trees is to use measured reflectance at 870nm acquired with NIR network cameras.

Reflectance at 550nm and 870nm together with GM: Green Meter value[2], Grow index, total nitrogen content, fiber content as well as water content are measured at the Prefectural tea research institute of Saga which is situated in Ureshino-city in April.

Through a comparison between measured total nitrogen and fiber content and estimated reflectance derived from the NIR camera data, Figure 14 of relationship is obtained. From this relation, the following equations are derived through linear regressive analysis,

$$TN=22.474Ref870 - 10.177 \quad (1)$$
$$F\text{-}NIR=-22.886Ref870 + 16.699 \quad (2)$$

where TN and F-NIR denote Total Nitrogen and Fiber content in tealeaves.

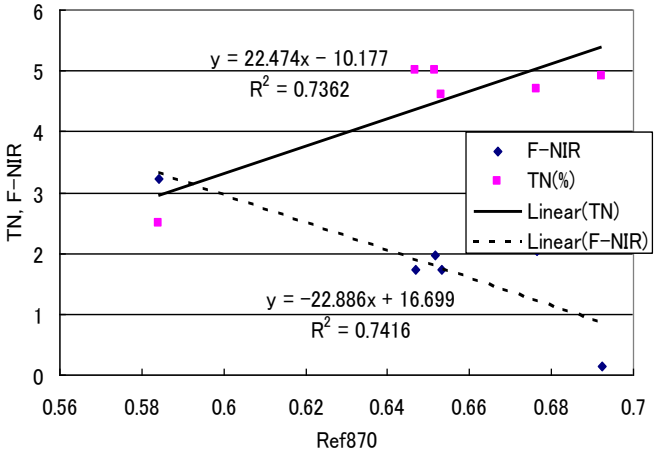

Fig. 13. Relation between total nitrogen and fiber contents in tealeaves and reflectance at 870nm measured with NIR camera.

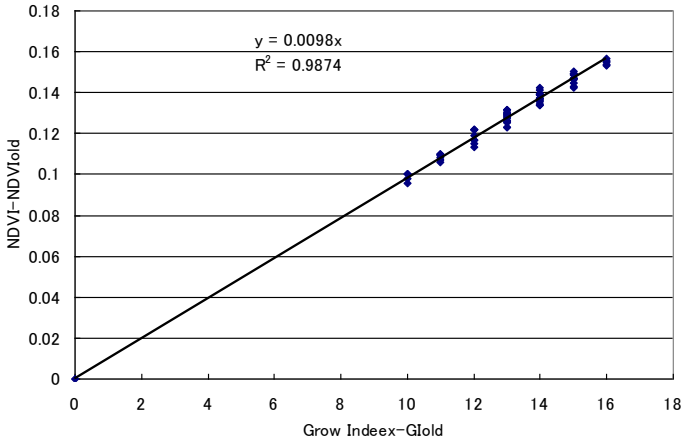

Fig. 14. Relation between Grow index and NDVI

R square value for TN is 0.736 while that for F-NIR is 0.742 so that it may say that TN and F-NIR can be estimated with reflectance at 870nm derived from NIR network camera.

On the other hand, grow index is also highly correlated to reflectance measured at 870nm. Grow index is defined as the ratio of the number of new tealeaves to the total number of tealeaves. In accordance with new tealeaves grow up, grow index is getting large. The grow index, essentially, highly correlated to NDVI,

$$NDVI=(Ref870-Ref550)/(Ref550+Ref870) \quad (3)$$

and GM. Figure 14 shows the relation between GI and NDVI where GIold=56 and Ref870=0.55518 as well as NDVI=0.562677.

In the figure, the horizontal axis shows GI-GIold while the vertical axis shows NDVI-NDVIold. Suffix of old denotes that the tea estate covers with old tealeaves only. In accordance with growing tealeaves, the number of new tealeaves is getting large results in increasing of GI as well as NDVI. Grow Index: GI is expressed with the equation (4) through a linear regressive analysis.

$$GI=102.041NDVI \quad (4)$$

Thus TN, F-NIR and GI can be estimated with Visible and NIR of network cameras data.

Measured DP, LAI, and NDVI are shown in Table 2.

[2] http://www.geocities.co.jp/nettaikaju/Observation4-04.html(Access on Jan.5 2009)

TABLE II. MEASURED DP, LAI, AND NDVI

DP@675nm	0.269	0.251	0.261	0.268	0.288	0.181	0.218	0.286	0.289
LAI	6.49	6.23	6.55	6.46	7.01	4.11	5.34	6.95	7.13
NDVI	0.498	0.497	0.497	0.498	0.494	0.438	0.485	0.495	0.498
PAR[W/m^2]	0.105	0.105	0.065	0.08	0.0138	0.02	0.0195	0.02	0.02

Through a regressive analysis, Figure 15 is obtained. Linear regressive equations for representations of LAI, NDVI and PAR are shown in the figure. Although R square value for PAR is not good enough, other LAI and NDVI can be estimated with measured DP data at 675 nm observed with 30 degree of observation angle.

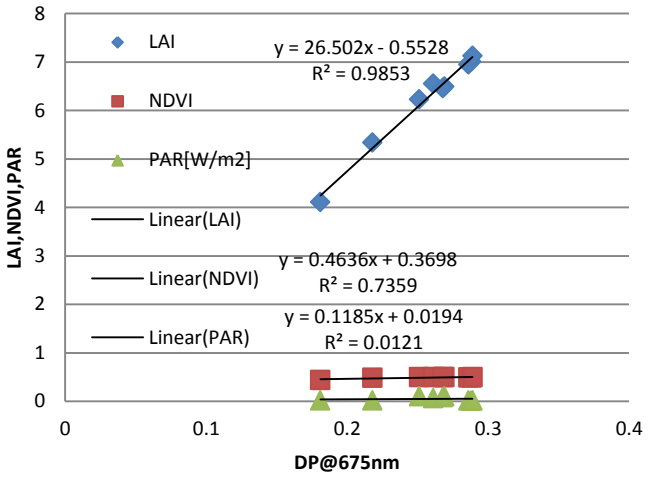

Fig. 15. Results from the regressive analysis between DP at 675 nm wavelength and LAI, NDVI, PAR.

V. CONCLUSION

Method for tealeaves quality estimation through measurements of Degree of Polarization: DP, Leaf Area Index: LAI, Photosynthesis Available Radiance: PAR and Normalized Difference Vegetation Index: NDVI for characterization of tealeaves is proposed. The method allows estimations of PAR, NDVI, Grow Index: GI by using measured Degree of Polarization: DP of tealeaves. Through experiments at the tea farm areas, it is found that the proposed method is validated. Also, the method is validated through Monte Carlo Ray Tracing: MCRT simulations for discrimination between prolate and oblate shapes of tealeaves. In accordance with growing tealeaves, prolate shape of tealeaves changes their shape to oblate shape. Therefore, growing stage can be estimated with DP measurements.

Through simulations and experiments, it is found that the difference between prolate and oblate shapes of tealeaves at 550nm (green band) is much clear than that of 730nm (near infrared band). It is also found that the difference of DP for different reflectance for p and s polarized reflectance is much greater than that for same reflectance.

DP difference between prolate and oblate shapes of tealeaves for both same and different reflectance at p and s polarization at around 30 degree of observation angle shows relatively clear than that for the other observation angle. Therefore, 30 degree of observation angle would be the best for DP observations.

Total nitrogen content in tealeaves can be expressed with measured DP together with fiber content in Near Infrared wavelength region. Also, grow index, leaf area index can be expressed with measured DP. Although R square value for PAR is not good enough, other LAI and NDVI can be estimated with measured DP data at 675 nm observed with 30 degree of observation angle.

ACKNOWLEDGMENT

The author would like to thank Mr. Yasunori Terayama for his efforts through experiments and simulations.

REFERENCES

[1] J.T.Compton, Red and photographic infrared linear combinations for monitoring vegetation, Journal of Remote Sensing of Environment, 8, 127-150, 1979.

[2] C.Wiegand, M.Shibayama, and Y.Yamagata, Spectral observation for estimating the growth and yield of rice, Journal of Crop Science, 58, 4, 673-683, 1989.

[3] S.Tsuchida, I.Sato, and S.Okada, BRDF measurement system for spatially unstable land surface-The measurement using spectro-radiometer and digital camera- Journal of Remote Sensing, 19, 4, 49-59, 1999.

[4] K.Arai, Lecture Note on Remote Sensing, Morikita-shuppan Co., Ltd., 2000.

[5] K.Arai and Y.Nishimura, Degree of polarization model for leaves and discrimination between pea and rice types of leaves for estimation of leaf area index, Abstract, COSPAR 2008, A3.10010-08#991, 2008.

[6] K.Arai and Long Lili, BRDF model for new tealeaves and new tealeaves monitoring through BRDF monitoring with web cameras, Abstract, COSPAR 2008, A3.10008-08#992, 2008.

[7] Kohei Arai, Y.Iisaka and X.Linag, Aerosol parameter estimation with changing observation angle of hround based polarization radiometer, Advances in Space Research, 39, 1, 28-31, 2007

[8] Ding Ya Liu, Kohei Arai, Forest parameter estimation based on radiative transfer model of Monte Carlo Simulation taking into account crown closer models, Journal of Japan Society of Remote Sensing, 27、2、141-152、2007

[9] Yaliu Ding, Kohei Arai, Forest parameter estimation, by means of Monte- Carlo simulations with experimental consideration of estimation of multiple reflections among trees depending on forest parameters, Advances in Space Research, 43, 3, 438-447, 2009.

[10] Kohei Arai and Yui Nishimura, Polarization model for discrimination of broad and needle shaped leaves and estimation of LAI using polarization measurements, Advances in Space Research, 44, 510-516, 2009.

[11] Kohei Arai, Method for estimation of grow index of tealeaves based on Bi- Directional reflectance function: BRDF measurements with ground based network cameras, International Journal of Applied Science, 2, 2, 52-62, 2011.

[12] Kohei Arai, Method for estimation of total nitrogen and fiber contents in tealeaves with ground based network cameras, International Journal of Applied Science, 2, 2, 21-30, 2011.

[13] K.Arai, Monte Carlo ray tracing simulation for bi-directional reflectance distribution function and grow index of tealeaves estimations, International Journal of Research and Review on Computer Science, 2, 6, 1313-1318, 2012.

[14] K.Arai, Fractal model based tea tree and tealeaves model for estimation of well opened tealeaf ratio which is useful to determine tealeaf harvesting timing, International Journal of Research and Review on Computer Science, 3, 3, 1628-1632, 2012.

[15] K.Arai, Y.Terayama, Monte Carlo ray tracing simulation of polarization characteristics of sea water which contains spherical and non-spherical

shapes of suspended solid and phytoplankton, International Journal of Advanced Computer Science and Applications, 3, 6, 85-89, 2012.

[16] Kohei Arai, Hideo Miyazaki, Masayuki Akaishi, Determination method for tealeaves harvesting with visible to near infrared cameras, Journal of Japanese Society for Remote Sensing and Photogrammetry 51, 1, 38-45, 2012

[17] Greivenkamp, John E., *Field Guide to Geometrical Optics*. SPIE Field Guides vol. FG01. SPIE. ISBN 0-8194-5294-7, 2004.

[18] Seto R H. Nakamura, F. Nanjo, Y. Hara, *Bioscience, Biotechnology, and Biochemistry*, Vol.61 issue9 1434-1439 1997.

[19] Sano M, Suzuki M ,Miyase T, Yoshino K, Maeda-Yamamoto, M.,J.Agric.Food Chem., 47 (5), 1906-1910 1999.

[20] Kohei Arai, Fundamental Theory for Remote Sensing, Gakujutu-Tosho-Shuppan Publishing Co. Ltd., 1998.

AUTHORS PROFILE

Kohei Arai, He received BS, MS and PhD degrees in 1972, 1974 and 1982, respectively. He was with The Institute for Industrial Science and Technology of the University of Tokyo from April 1974 to December 1978 also was with National Space Development Agency of Japan from January, 1979 to March, 1990. During from 1985 to 1987, he was with Canada Centre for Remote Sensing as a Post Doctoral Fellow of National Science and Engineering Research Council of Canada. He moved to Saga University as a Professor in Department of Information Science on April 1990. He was a councilor for the Aeronautics and Space related to the Technology Committee of the Ministry of Science and Technology during from 1998 to 2000. He was a councilor of Saga University for 2002 and 2003. He also was an executive councilor for the Remote Sensing Society of Japan for 2003 to 2005. He is an Adjunct Professor of University of Arizona, USA since 1998. He also is Vice Chairman of the Commission "A" of ICSU/COSPAR since 2008. He wrote 30 books and published 442 journal papers

Frequent Physical Health Monitoring as Vital Signs with Psychological Status Monitoring for Search and Rescue of Handicapped, Diseased and Eldery Persons

Kohei Arai [1]
Graduate School of Science and Engineering
Saga University
Saga City, Japan

***Abstract*—Method and system for frequent health monitoring as vital signs with psycholo9gical status monitoring for search and rescue of handicapped person is proposed. Heart beat pulse rate, body temperature, blood pressure, blesses and consciousness is well known vital signs. In particular for Alzheimer diseased persons, handicapped peoples, etc. it is very important to monitor vital signs in particular in the event of evacuation from disaster occurred areas together with location and attitude information. Then such persons who need help for evacuation can be survived. Through experiments wearing the proposed sensors with three normal persons including male and female, young and elder persons and one diseased person, it is found that the proposed system is useful. It is also found that the proposed system can be used for frequent health condition monitoring. Furthermore, physical health monitoring error due to psychological condition can be corrected with the proposed system.**

Keyword*—*vital sign; heart beat puls ratee; body temperature; blood pressure; blesses; consciousnes; seonsor network

I. INTRODUCTION

Handicapped, disabled, diseased, elderly persons as well as peoples who need help in their ordinary life are facing too dangerous situation in event of evacuation when disaster occurs. In order to mitigate victims, evacuation system has to be created. Authors proposed such evacuation system as a prototype system already [1]-[4]. The system needs information of victims' locations, physical and psychological status as well as their attitudes. Authors proposed sensor network system which consist GPS receiver, attitude sensor, physical health monitoring sensors which allows wearable body temperature, heart beat pulse rates; bless monitoring together with blood pressure monitoring [5]-[7]. Also the number of steps, calorie consumptions is available to monitor. Because it is difficult to monitor the blood pressure with wearable sensors, it is done by using the number of steps and body temperature. In addition to these, psychological status is highly required for vital sign monitoring (consciousness monitoring). By using eeg sensors, it is possible to monitor psychological status in the wearable sensor. These are components of the proposed physical health and psychological monitoring system.

Such the proposed system also allows frequent monitoring. Even for every minute, or every second, it may monitor all the required items. Therefore it is applicable to the patients in ICU. Also, it may find Alzheimer patients who used to walk away from their house and /or hospitals together with physical health and psychological status. Furthermore, it may reduce physical health monitoring error due to psychological status changes. Even for the healthy persons, it may occur such errors. For instance, heart beat pulse rate and blood pressure is used to be increased when medical doctor or nurse measures. By using eeg signal analyzed results, such errors may be corrected or at least it can be omitted from the monitored data. These are kinds of bi-products of the proposed system.

Section 2 describes the proposed system followed by experiment method and results. Then conclusion is described together with some discussions..

II. PROPOSED MOTHOD AND SYSTEM

A. System Configuration

Figure 1 shows the entire system configuration of the proposed physical and psychological health monitoring system.

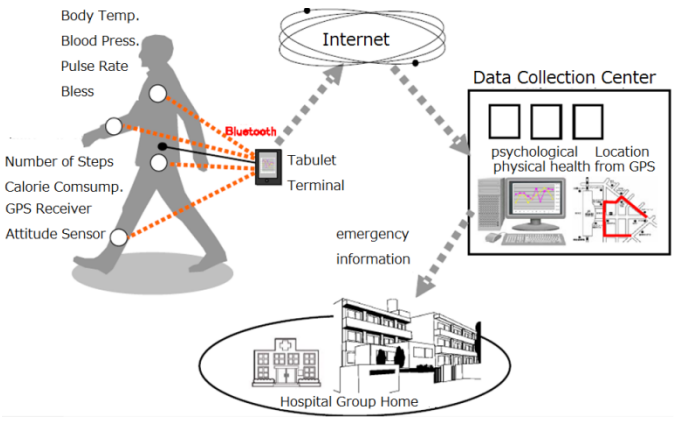

Fig. 1. Entire system configuration of the proposed wearable physical and psychological health monitoring system.

There are two types of stakeholders, patients (users) and volunteers who are responsible for evacuation, rescue, and help patients from disaster area as shown in Figure 2. Patients have physical and psychological health sensors and send the acquired data through Bluetooth and Internet to the Health Data Collection Center: HDCC server. On the other hand, volunteers receive health data of the previously designated

several patients together with traffic flow information and appropriate route information. When something wrong occurs on the designated patients, HDCC provides information which required for rescue to the designated volunteers then the volunteers rescue patients in an efficient and an effective manner.

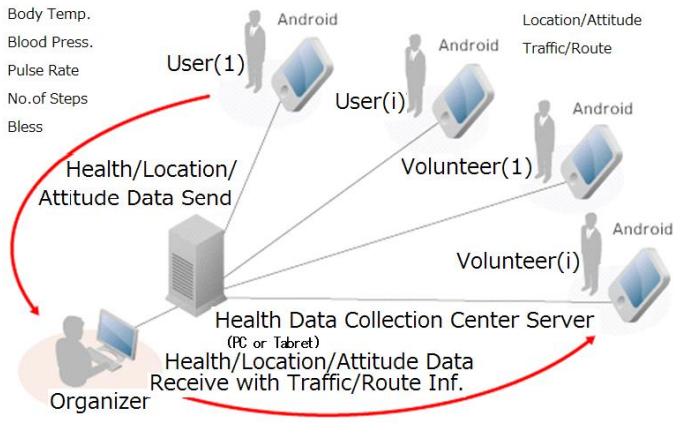

Fig. 2. Major components of the Proposed System

B. Sensor and Communication Ssystem

In order for evacuation and rescue, victims' location and attitude is important. Therefore, GPS receiver and accelerometer are added to the aforementioned measuring sensors for body temperature pulse rate, blood pressure, bless, and eeg, emg. All sensors should be wearable and can be attached to ones' tall forehead. Acquired data can be transmitted to mobile devices in ones' pockets. Through WiFi network or wireless LAN connection, acquired data can be collected in the designated information collection center. Then acquired data can be refereed from the designated volunteers who are responsible to help victims for evacuation and rescue.

III. Experiments

A. Experimental Method

1) Patients

Four patients are participated to the experiments. The difference due to gender can be discussed through a comparison between patients A and C while the difference due to age can be discussed through a comparison between patients B and C. Meanwhile, the difference due to the degree of Alzheimer can be discussed through a comparison between patients B and D as shown in Table 1.

Experiments are conducted for eight hours a day for almost every working day (Monday to Friday) for six months starting from May 2012. Measuring time intervals are different by the measuring items. GPS location can be measured every two seconds while accelerometer data can be obtained every 10 seconds. Meanwhile, body temperature, pulse rate can be measured every one minutes while blood pressure is measured every one hour together with eeg and emg signals. The number of steps is measured when the walking event happened.

At the end of day, four patients evaluate their physical and psychological conditions which are listed in Table 2.

TABLE I. Four Patients

Patient	Male/Female	Age	Remarks
A	Male	37	Good in Health
B	Female	47	Good in Health
C	Female	39	Good in Health
D	Female	91	Weak Alzheimer

TABLE II. Self Evaluation Items

A1	Feel fever
B1	Loosing thinking capability
A2	Feel tiredness
B2	Could not sleep well
A3	Get tired after exercise
B3	Feel bad
A4	Muscle hurt
B4	Unconfident about health
A5	Feel depression
B5	Do not want to work
A6	Limper hurt
B6	Cannot remember something
A7	Head ach
B7	Loosing balance
A8	Cannot recover after sleep
B8	Cannot think deeply
A9	Throat hurt
B9	Loosing concentration
A10	Joint hurt
B10	Sleep for too long time

2) Subjective Evaluation of Physical and Psychological Health Conditions

The 20 items listed in the Table 2 are questionnaires for four patients. In the Table, Ai is questionnaire for physical health while Bi is questionnaire for psychological health. The patients respond to the questionnaire above with five levels range from 0 to 4 grades. Total Score is defined as sum of the aforementioned self evaluation of 20 items including physical and psychological health items.

B. Experimental Results

1) Traced Route

Example of traced route measured with GPS receiver on GIS map is shown in Figure 3. Figure 3 (a) is traced route when patient walks on foot while Figure 3 (b) shows the traced route when patient moves by car, respectively.

Figure 4 shows the traced route locations data in the database of the HDCC. A couple of meters of the estimated location error are observed. Also Figure 5 shows an example of measured attitude data in directions of x, y, and z. It is not so easy to estimate the patients' situations (sit, stand up, walking, lay down, etc) from the attitude data derived from the single accelerometer data. As mentioned later, it is much easier to estimate the situations using eeg and emg sensor data.

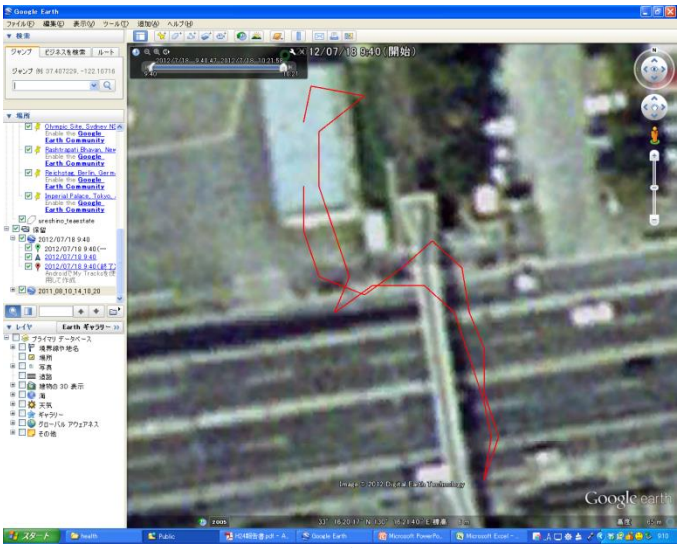

(a)On foot

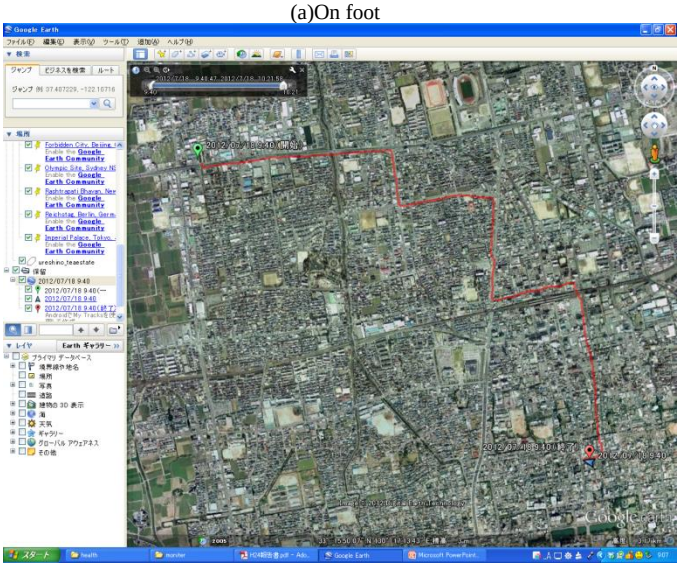

(b)With car

Fig. 3. Example of traced route measured with GPS receiver on GIS map

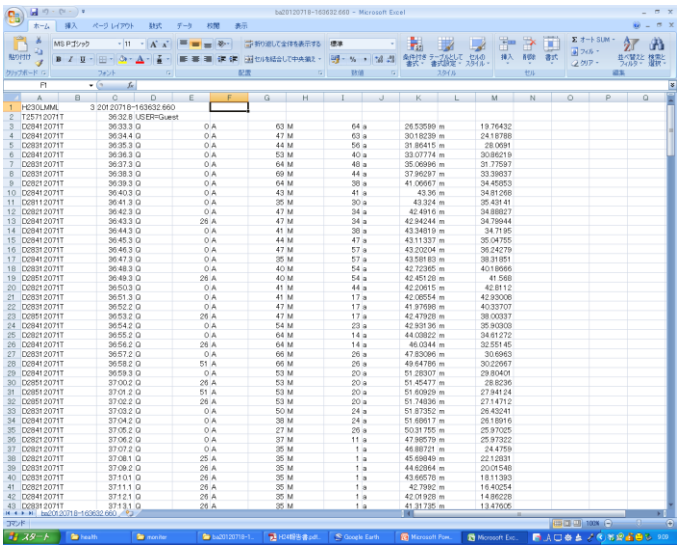

Fig. 4. Traced location in the database of the HDCC

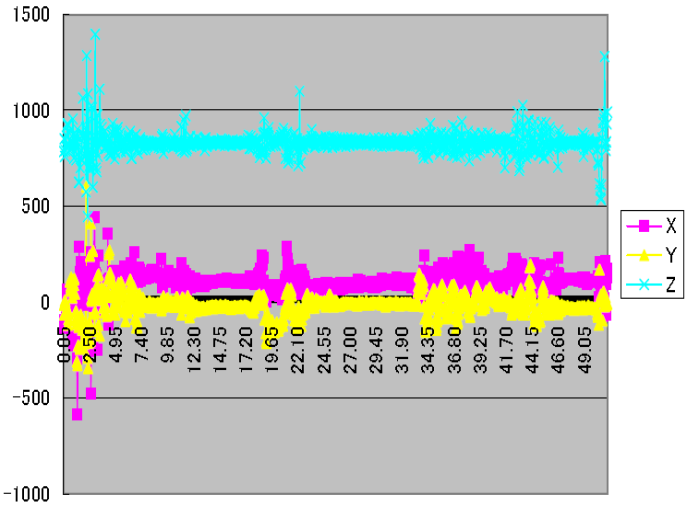

Fig. 5. Example of attitude data (x, y, and z axis movement)

2) Measured Physical Health Conditions

Relation between the measured physical health condition and the self evaluation of physical and psychological health conditions (Total Score) for the patient of weak Alzheimer is plotted in the Figure 6. Total Score denotes sum of the scores of the self evaluation items which are listed in Table 2.

Figure 7 (a) and (b) shows physical health data of the weak Alzheimer of patient at the minimum and maximum total scores, 5 and 8, respectively.

For both minimum and maximum total score cases, the weak Alzheimer patient walks for 10 minutes (one unit time equals to one hour) for five times every one and half hours. High total score implies high physical and psychological damages. Although blood pressure and pulse rate are increased in accordance with increasing of the number of steps for the minimum total score case, these are not so increased for the maximum total score case.

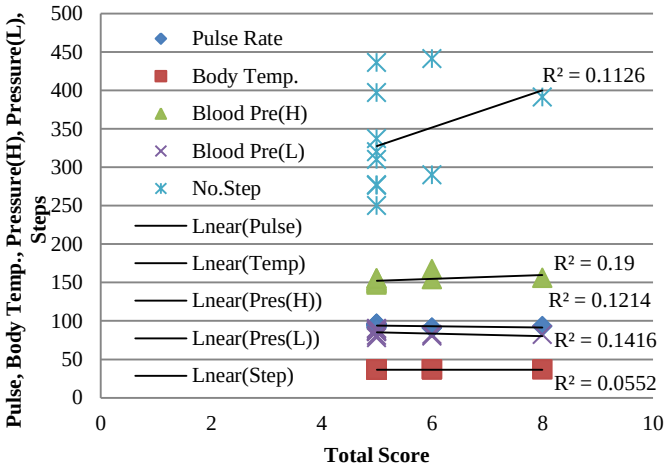

Fig. 6. Relation between the measured physical health condition and the self evaluation of physical and psychological health conditions (Total Score) for the patient of weak Alzheimer

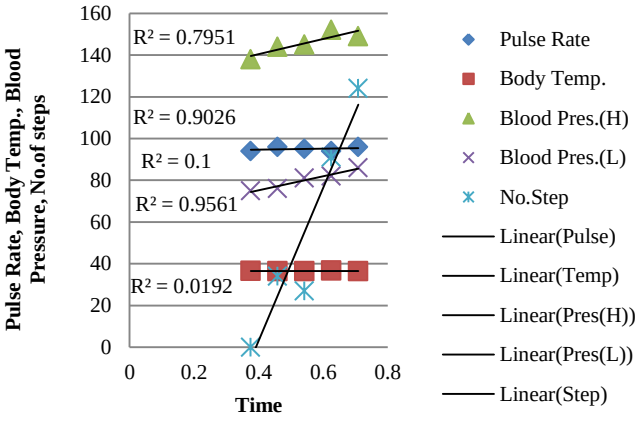

(a)Minimum total score of 5

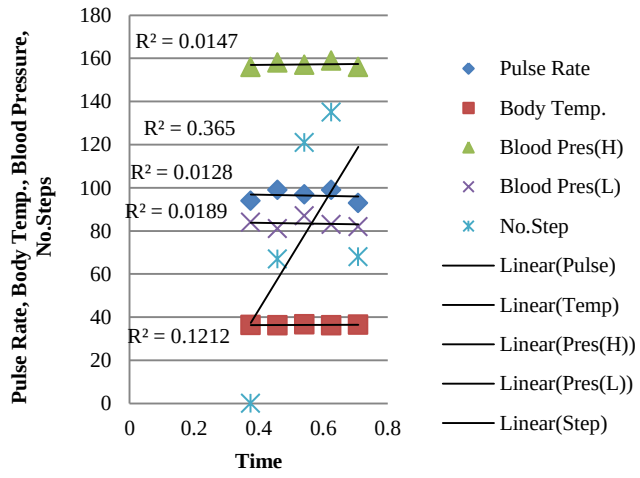

(b)Maximum total score

Fig. 7. Physical health data of the weak Alzheimer of patient at the minimum and maximum total scores, 5 and 8, respectively.

On the other hand, Figure 8 (a) and (b) shows physical health data of the patient who is good in health at the minimum and maximum total scores, 5 and 8, respectively. For both minimum and maximum total score cases, the patient who is good in health walks for 10 minutes (one unit time equals to one hour) for five times every one and half hours. Although blood pressure and pulse rate are quite stable in accordance with increasing of the number of steps for the minimum total score case, these are decreased for the maximum total score case.

As the results, the followings are concluded,

- Body temperature is relatively stable for a day
- In accordance with increasing of the number of steps, blood pressure (High and Low) is increased
- Even if the number of steps is increased and when blood pressure is stable, then physical and psychological health condition is good in health

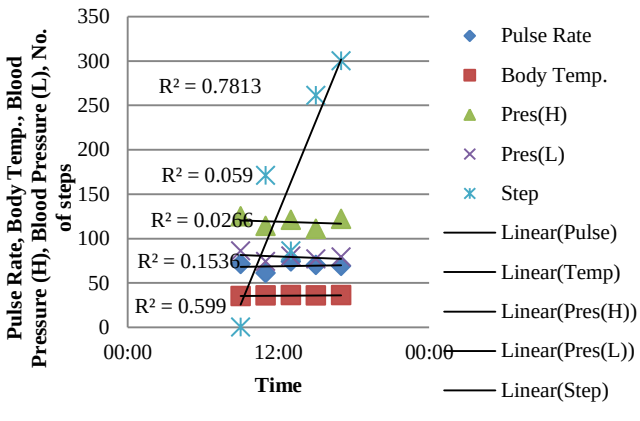

(b)Minimum total score

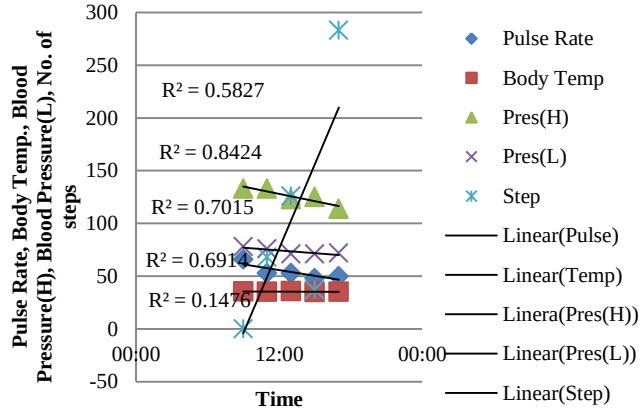

(b)Maximum total score

Fig. 8. Physical health data of the patient who is good in health at the minimum and maximum total scores, 7 and 11, respectively.

- Even if the number of steps is increased and when blood pressure is decreases, then physical and psychological health condition is excellent in health
- There is a correlation between blood pressure (High and Low) and a combination of pulse rate and body temperature

3) Relation Between Blood Pressure and the OtherMeasured Physical Health Conditions

Using all measured physical health data, linear regressive analysis is conducted. Table 3 shows correlation matrix among physical and psychological health conditions. There is relatively large correlation between blood pressure and body temperature and pulse rate.

Therefore, the coefficient body temperature and pulse rate multiplied by their correlation coefficients is proposed for regressive analysis. The result from the regressive analysis is shown in Figure 9. Although it is not so easy to measure blood pressure with small size of sensors, it can be estimated with measured body temperature and pulse rate.

TABLE III. CORRELATION MATRIX AMONG PHYSICAL AND PSYCHOLOGICAL HEALTH CONDITIONS

Body Temp.	Blood Pres.(H)	Blood Pres.(L)	Heart Beet	No.Steps	TotalA	TotalB
-0.0104	0.463	-0.245	0.133	-0.348	-0.171	0.809
	0.122	-0.166	-0.231	0.0321	0.0237	0.440
		-0.504	-0.0562	0.502	-0.482	-0.186
			0.161	0.198	-0.282	-0.420
				-0.387	-0.149	0.0421
					0.340	-0.0180
						0.0784

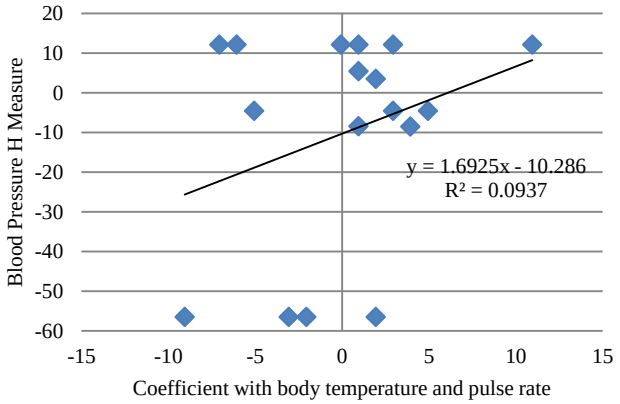

Fig. 9. Results from the regressive analysis between blood pressure high and the coefficient composed with body temperature and pulse rate

4) Measured Psychological Health Conditions

By using EEG analyzer tools, we analyze the fatigue effect between the condition when user is looking at one point and condition when user is looking at four points. In order to analyze fatigue effect, we use Peak Alpha Frequency: PAF [8]-[11] It is possible to measure psychological status by using PAF derived from EEG signal.

Psychological health condition is measured with Bio Switch MCTOS of Brain Wave Measuring instrument (BM-Set1) manufactured by Technos Japan Co. Ltd. every one hour. Figure 10 shows an example of the measured data of relax indicator, NB value which is derived from eeg and emg signals. Figure 11 (a) shows the NB value for the patient's action, sit down quickly and then stand up rapidly while Figure 11 (b) shows that for the patient's action of lay down slowly and the stand up normally. Meanwhile, Figure 11 (c) shows NB value for the patient's action, stand up, lay down slowly, stand up and then sit down slowly.

NB values change for the every event of the patient's action. It is found that the NB value changes for slow action are smaller than those for quick action. It is also found that the NB value changes for standup action is much greater than those for lay down and sit down actions as shown in Figure 12. These NB value change characteristics are almost same for patients A, B, and C. There are the different characteristics between A, B, C, and D as shown in Figure 13. Figure 13 (a) shows NB value changes for the patient A while Figure 13 (b) shows those for the patient D.

Fig. 10. Example of the measured data of relax indicator, NB value which is derived from eeg and emg signals.

(a)Case #1

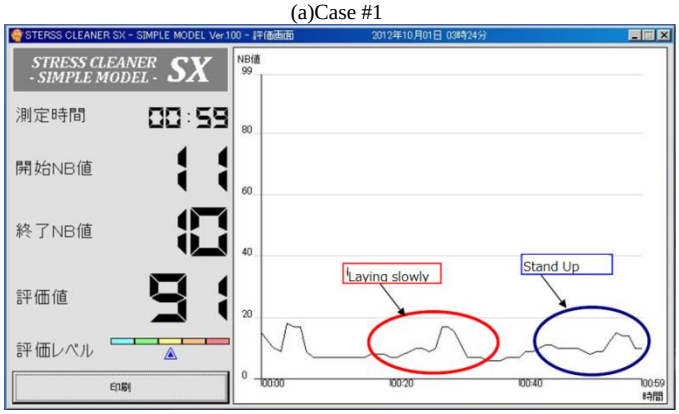

(b)Case #2

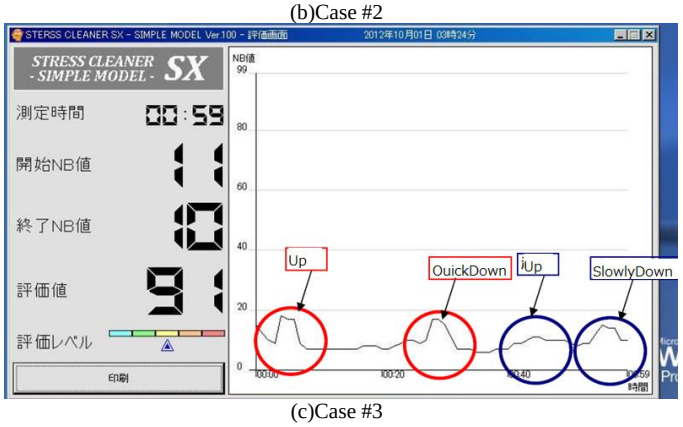

(c)Case #3

Fig. 11. NB values for the different patient's actions.

Fig. 12. Example of NB value changes for the patient action, sit down quickly, standup, slowly sit down and then standup.

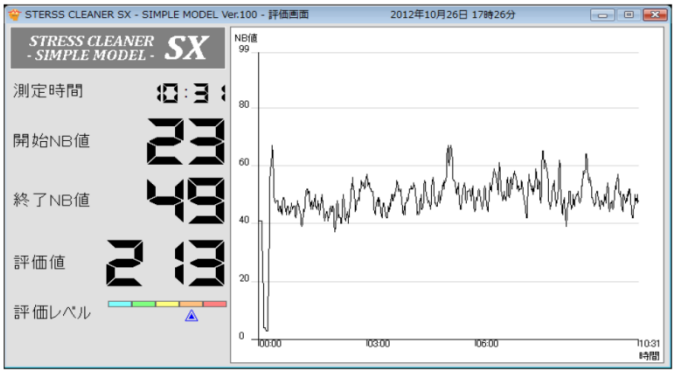

(a)Patient with normal healthy condition

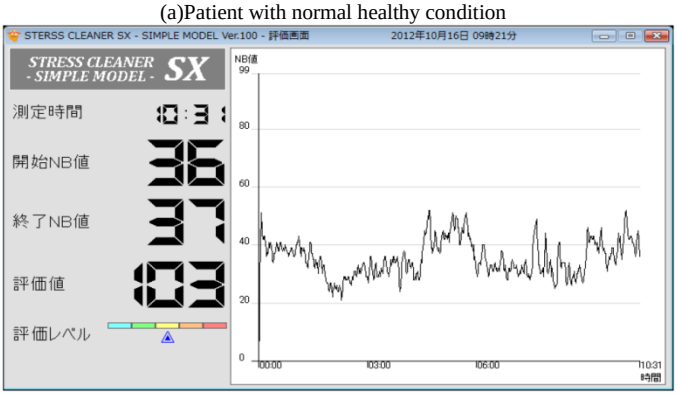

(b)Patient with weak Alzheimer

Fig. 13. NB value changes for the patients

It is concluded that the patient with weak Alzheimer feels much stress due to the actions rather than the patient in normal healthy condition. It also is found that there is no difference of psychological health condition due to age. There is no psychological health condition difference due to gender.

Example of raw eeg signal is shown in Figure 14. Figure 14 (a) shows the locations of electrodes and Figure 14 (b) shows the examples for the different two locations of eeg.

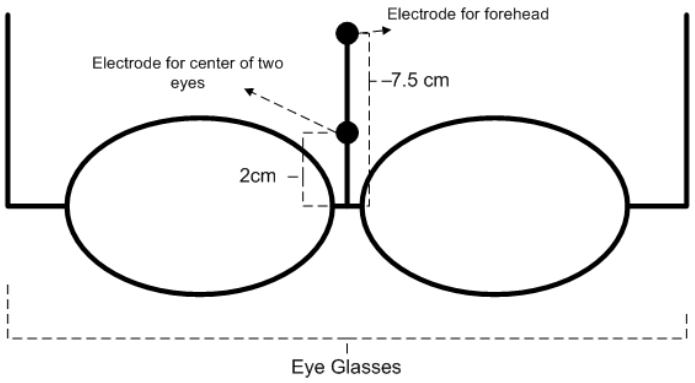

(a)Locations of electrodes

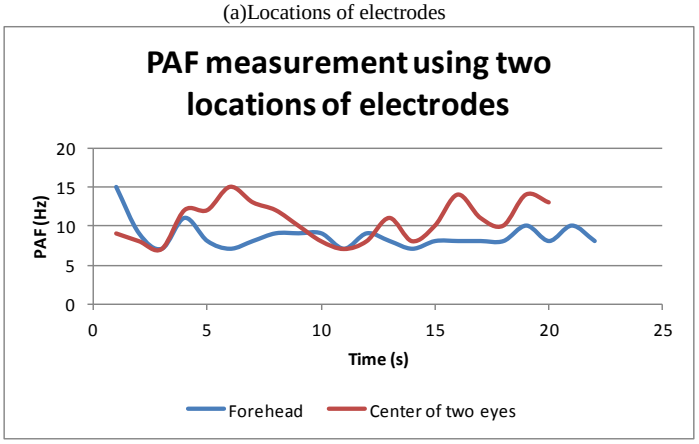

(b)Examples of eeg signals

Fig. 14. Locations of electrodes and examples for the different two locations of eeg

Obviously, eeg signals detected at the forehead is much greater than that from the center of two eyes. It is confirmed that it may reduce physical health monitoring error due to psychological status changes. Even for the healthy persons, it may occur such errors. For instance, heart beat pulse rate and blood pressure is used to be increased when medical doctor or nurse measures. By using eeg signal analyzed results, such errors may be corrected or at least it can be omitted from the monitored data.

IV. Conclusion

Method and system for frequent health monitoring as vital signs with psycholo9gical status monitoring for search and rescue of handicapped person is proposed. Heart beat pulse rate, body temperature, blood pressure, blesses and consciousness is well known vital signs. In particular for Alzheimer diseased persons, handicapped peoples, etc. it is very important to monitor vital signs in particular in the event of evacuation from disaster occurred areas together with location and attitude information. Then such persons who need help for evacuation can be survived. Through experiments wearing the proposed sensors with three normal persons including male and female, young and elder persons and one diseased person, it is found that the proposed system is useful.

It is also found that the proposed system can be used for frequent health condition monitoring. Furthermore, physical health monitoring error due to psychological condition can be corrected with the proposed system.

Wearable physical and psychological health monitoring system is proposed. All the sensors which allows monitoring blood pressure, body temperature, pulse rate, measuring sensor for the number of steps, calorie consumption, eeg, GPS receiver, WiFi or Wireless LAN receiver for location estimation, accelerometer are attached to the human body.

Measured data are transferred to the mobile devices through Bluetooth. Mobile devices are connected with Internet terminals through WiFi, or Wireless LAN. Thus these physical and psychological health data are collected in the Information Collection Center. Thus those who are wearing the sensors can get a help from the designated volunteer when evacuation from disaster areas.

From the experimental results, the followings are concluded,

- Body temperature is relatively stable for a day
- In accordance with increasing of the number of steps, blood pressure (High and Low) is increased
- Even if the number of steps is increased and when blood pressure is stable, then physical and psychological health condition is good in health
- Even if the number of steps is increased and when blood pressure is decreases, then physical and psychological health condition is excellent in health
- There is a correlation between blood pressure (High and Low) and a combination of pulse rate and body temperature
- It is concluded that the patient with weak Alzheimer feels much stress due to the actions rather than the patient in normal healthy condition. It also is found that there is no difference of psychological health condition due to age. There is no psychological health condition difference due to gender.

ACKNOWLEDGMENT

The author would like to thank all the patients who are contributed to the experiments conducted. The author also would like to thank Professor Dr. Takao Hotokebuchi, President of Saga University for his support this research works.

REFERENCES

[1] Kohei Arai, Tran Xuan Sang, Decision making and emergency communication system in rescue simulation for people with disabilities, International Journal of Advanced Research in Artificial Intelligence, 2, 3, 77-85, 2013.

[2] K.Arai, T.X.Sang, N.T.Uyen, Task allocation model for rescue disable persons in disaster area with help of volunteers, International Journal of Advanced Computer Science and Applications, 3, 7, 96-101, 2012.

[3] K.Arai, T.X.Sang, Emergency rescue simulation for disabled persons with help from volunteers, International Journal of Research and Review on Computer Science, 3, 2, 1543-1547, 2012.

[4] K. Arai, and T. X. Sang, "Fuzzy Genetic Algorithm for Prioritization Determination with Technique for Order Preference by Similarity to Ideal Solution", International Journal of Computer Science and Network Security, vol.11, no.5, 229-235, May 2011.

[5] Arai K., R. Mardiyanto, Evaluation of Students' Impact for Using the Proposed Eye Based HCI with Moving and Fixed Keyboard by Using EEG Signals, International Journal of Review and Research on Computer Science(IJRRCS), 2, 6, 1228-1234, 2011

[6] K.Arai, Wearable healthy monitoring sensor network and its application to evacuation and rescue information server system for disabled and elderly person, International Journal of Research and Review on Computer Science, 3, 3, 1633-1639, 2012.

[7] K.Arai, Wearable Physical and Psychological Health Monitoring System, Proceedings of the *Science and Information Conference 2013 October 7-9, 2013 | London, UK*

[8] Torsten Felzer , Rainer Nordmann, "Alternative text entry using different input methods", Proceedings of the 8th international ACM SIGACCESS conference on Computers and accessibility, pp 10-17, (2006)

[9] Majaranta, P., Ahola, U., and Špakov, O, "Fast gaze typing with an adjustable dwell time", In Proceedings of the 27th international Conference on Human Factors in Computing Systems, pp 357-360, (2009)

[10] Siew Cheok Ng and P. Raveendran, "EEG Peak Alpha Frequency as an Indicator for Physical Fatigue", In Proceedings of 11th Mediterranean Conference on Medical and Biomedical Engineering and Computing 2007, pp 517-520, (2007)

[11] Klimesch W, "EEG alpha and theta oscillations reflect cognitive and memory performance: A review and analysis", Brain Research Reviews, Rev 29 (2-3), pp. 169-195., (1999)

AUTHORS PROFILE

Kohei Arai, He received BS, MS and PhD degrees in 1972, 1974 and 1982, respectively. He was with The Institute for Industrial Science and Technology of the University of Tokyo from April 1974 to December 1978 also was with National Space Development Agency of Japan from January, 1979 to March, 1990. During from 1985 to 1987, he was with Canada Centre for Remote Sensing as a Post Doctoral Fellow of National Science and Engineering Research Council of Canada. He moved to Saga University as a Professor in Department of Information Science on April 1990. He was a councilor for the Aeronautics and Space related to the Technology Committee of the Ministry of Science and Technology during from 1998 to 2000. He was a councilor of Saga University for 2002 and 2003. He also was an executive councilor for the Remote Sensing Society of Japan for 2003 to 2005. He is an Adjunct Professor of University of Arizona, USA since 1998. He also is Vice Chairman of the Commission "A" of ICSU/COSPAR since 2008. He wrote 30 books and published 442 journal papers

Fisher Distance Based GA Clustering Taking Into Account Overlapped Space Among Probability Density Functions of Clusters in Feature Space

Kohei Arai [1]
Graduate School of Science and Engineering
Saga University
Saga City, Japan

***Abstract*—Fisher distance based Genetic Algorithm: GA clustering method which takes into account overlapped space among probability density functions of clusters in feature space is proposed. Through experiments with simulation data of 2D and 3D feature space generated by random number generator, it is found that clustering performance depends on overlapped space among probability density function of clusters. Also it is found relation between cluster performance and the GA parameters, crossover and mutation probability as well as the number of features and the number of clusters.**

Keywords—GA clustering; Fisher distance; crossover; mutation; overlapped space among probability density functions of clusters

I. INTRODUCTION

Genetic Algorithm: GA clustering is widely used for image clustering. It allows relatively good clustering performance with marginal computer resources. In particular, Fisher distance based GA clustering is well known [1]. It uses Fisher distance as fitness function of GA. It, however, is not clear the characteristics of Fisher distance based GA clustering. For instance, relation between clustering performance and overlapped space among probability density function of clusters. Also, relation between cluster performance and the GA parameters, crossover and mutation probability as well as the number of features and the number of clusters are unclear [2].

The paper describes the aforementioned characteristics through simulation studies with random number generator derived simulation data with the different parameters. Also, the results from GA based clustering are compared to the Simulated Annealing based clustering [3].

The following section describes fundamental theoretical background of the Fisher distance based GA clustering method followed by some experimental results with simulation data. Then finally, conclusion and remarks are described together with some discussions.

II. PROPOSED MODEL

A. Fisher distance based GA clustering

Fisher distance between two probability density functions of two features is defined as equation (1)

$$f = \frac{(\mu_{y_1} - \mu_{y_2})^2}{\sigma_{y_1}^2 + \sigma_{y_2}^2} \quad (1)$$

where μ_{y_1}, μ_{y_2}, $\sigma_{y_2}^2$, $\sigma_{y_1}^2$ denotes mean and variance of two features. The most appropriate linear discrimination function for multi-dimensional feature space is expressed as equation (2).

$$\mathrm{y} = \mathrm{H}^{\mathrm{t}}\mathrm{x} + \mathrm{w}_0 \quad (2)$$

Discrimination function is illustrated in Fig.1. The line with arrow (linear discrimination border) in the Fig.1 in the orthogonal coordinate is discrimination function between two classes (two clusters). The slant coordinate of probability density functions for two classes implies cross section of the one dimensional probability functions for two classes.

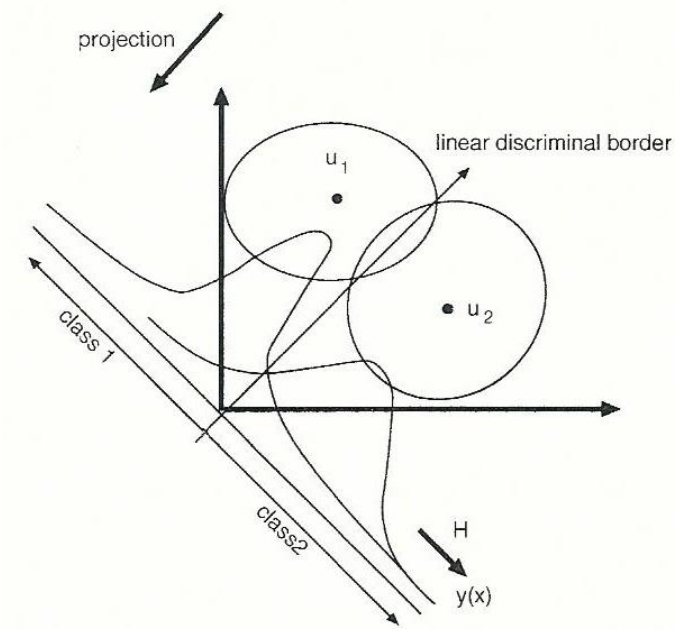

Fig. 1. Illustrative view of discrimination function in two dimensional feature space for two clusters

Therefore, fitness function as a function of H is expressed as equation (3) for two clusters case.

$$f(\mathbf{H}) = \frac{\mathbf{H^t}(\mu_1 - \mu_2)(\mu_1 - \mu_2)^{\mathbf{t}}\mathbf{H}}{\mathbf{H^t}(\mathbf{\Sigma_1} + \mathbf{\Sigma_2})\mathbf{H}} \quad (3)$$

If the following fitness function is set for GA, it allows finding of the most appropriate clustering results in the sense of minimizing Fisher distance.

$$Fitness = \frac{\Sigma_W}{\Sigma_B} \quad (4)$$

where

$$\Sigma_B = (\mu_1 - \mu_2)(\mu_1 - \mu 2)^t$$
$$\Sigma_W = \frac{\Sigma_1 + \Sigma_2}{2} \quad (5)$$

These are called between cluster variance and within cluster variance, respectively. Fisher distance based GA clustering is finding *f*(*H*) as to minimizing *Fitness* of equation (4).

B. Problem definition on GA clustering

Most of problems would occur when the probability density functions are overlapped in the feature space as shown in Fig.2. In this case, three clusters' probability density functions are overlapped.

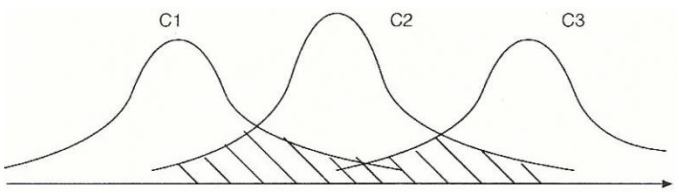

Fig. 2. Problem situations in GA clustering due to overlapping of probability density functions of clusters in feature space

If the following criterion equation is optimized, then *c* (crossover probability), *m* (mutation probability) would be optimized accordingly.

$$f(V_p) = \begin{cases} f_o(c, m, V_p) \rightarrow minimum \\ f_p(c, m, V_p) \rightarrow maximum \end{cases} \quad (6)$$

where

$$V_p = \int_{\mathbf{x}} P(\mathbf{x}) d\mathbf{x} \quad (7)$$

(the overlapped space volume in the feature space) and

$$P = \cup_{i,j}(p_i \cup p_j) \quad (8)$$

(overlapped space volume between two different probability density functions of two different cluster) as well as f_o and f_p denotes the functions which represent required computer resources and clustering performance, respectively. Through calculation of V_p' and $f(V_p')$, f_o and f_p are optimized. Thus optimum parameters of GA clustering (crossover and mutation probabilities) can be determined.

III. Experiments

A. Data Used

Using Merssene Twister of random number generator, Gaussian distributed image datasets are generated for simulation studies. Fig.3 shows just one example of generated simulation data set for three cluster and two features (band 0 and 1) with 16 by 16 pixels of imagery data. The data is assumed the variables which range from zero to one (normalized data). Quantization level is 256.

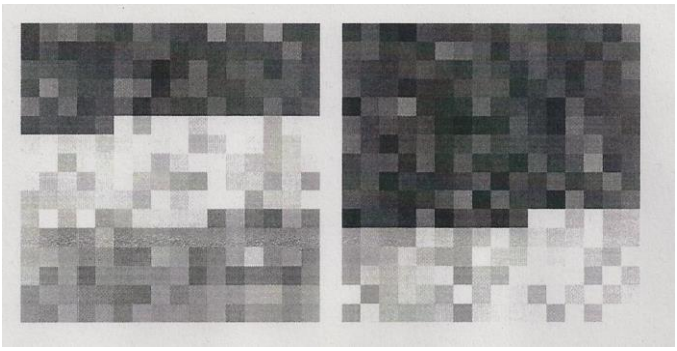

(a) band 0 (b) band 1

Fig. 3. An example of generated simulation data set for three cluster and two features (band 0 and 1) with 16 by 16 pixels of imagery data.

Two datasets are generated for simulation studies, two cluster cases and three cluster cases. In the two cluster cases, mean vector is set as follows,

(1)Case 1: $M_1=(0.25,0.25)^t$, $M_2=(0.75,0.75)^t$
(2)Case 2: $M_1=(0.3,0.3)^t$, $M_2=(0.75,0.75)^t$
(3)Case 3: $M_1=(0.35,0.35)^t$, $M_2=(0.75,0.75)^t$
(4)Case 4: $M_1=(0.4,0.4)^t$, $M_2=(0.75,0.75)^t$
(5)Case 5: $M_1=(0.45,0.45)^t$, $M_2=(0.75,0.75)^t$
(6)Case 6: $M_1=(0.5,0.5)^t$, $M_2=(0.75,0.75)^t$
(7)Case 7: $M_1=(0.55,0.55)^t$, $M_2=(0.75,0.75)^t$
(8)Case 8: $M_1=(0.6,0.6)^t$, $M_2=(0.75,0.75)^t$

Meanwhile, variance and covariance matrices for these 8 cases are set as same as follows,

$$C_x = \begin{vmatrix} 0.01 & 0.0 \\ 0.0 & 0.01 \end{vmatrix} \quad (7)$$

Simulation dataset of two class cases for the cases of 1 and 8 are distributed as shown in Fig.4 (a) and (b), respectively. Obviously, case 1 is easy to classify (best clustering performance) while case 8 is difficult to classify (worst

clustering performance) due to their overlapping situations of data distributions between two clusters.

On the other hand, mean vectors are set for the following 8 cases of three cluster case,

(1)Case 1: $M_1=(0.26,0.25)^t$, $M_2=(0.74,0.25)^t$, $M_3=(0.5,0.73)^t$
(2)Case 2: $M_1=(0.28,0.28)^t$, $M_2=(0.72,0.26)^t$, $M_3=(0.5,0.69)^t$
(3)Case 3: $M_1=(0.29,0.26)^t$, $M_2=(0.71,0.26)^t$, $M_3=(0.5,0.68)^t$
(4)Case 4: $M_1=(0.29,0.26)^t$, $M_2=(0.711,0.26)^t$, $M_3=(0.5,0.68)^t$
(5)Case 5: $M_1=(0.29,0.27)^t$, $M_2=(0.711,0.27)^t$, $M_3=(0.5,0.68)^t$
(6)Case 6: $M_1=(0.29,0.27)^t$, $M_2=(0.709,0.27)^t$, $M_3=(0.5,0.68)^t$
(7)Case 7: $M_1=(0.292,0.28)^t$, $M_2=(0.7,0.28)^t$, $M_3=(0.5,0.66)^t$
(8)Case 8: $M_1=(0.295,0.287)^t$, $M_2=(0.69,0.28)^t$, $M_3=(0.5,0.66)^t$

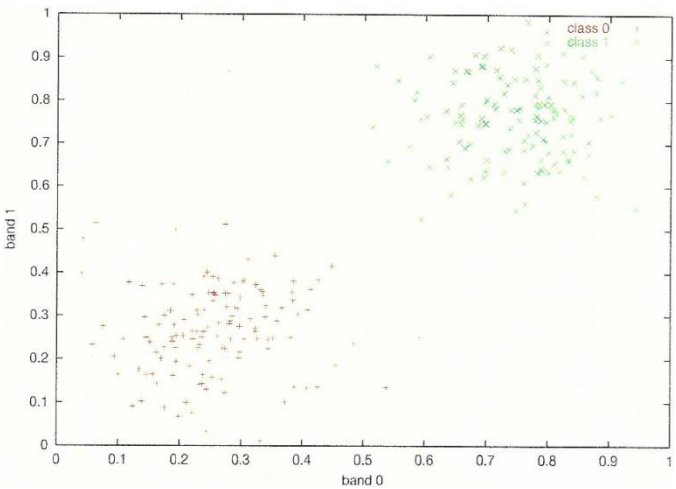

(a)Case1 (the most far case)

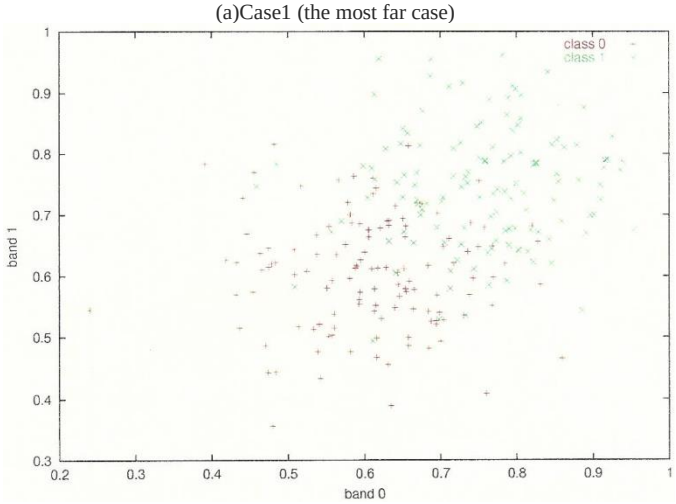

(b)Case 2 (the closest case)

Fig. 4. Data distribution of the simulation dataset in the feature plane for two class cases

Meanwhile, variance covariance matrices are set as follows for the 8cases of three cluster case,

(1)Case 1:
C_1=|0.008 0.0 | C_2=|0.008 0.0 | C_3=|0.008 0.0 |
|0.0 0.008| |0.0 0.008| |0.0 0.008|

(2)Case 2:
C_1=|0.008 0.0 | C_2=|0.008 0.0 | C_3=|0.008 0.0 |
|0.0 0.008| |0.0 0.008| |0.0 0.008|

(3)Case 3:
C_1=|0.01 0.0 | C_2=|0.009 0.0 | C_3=|0.009 0.0 |
|0.0 0.01| |0.0 0.009| |0.0 0.009|

(4)Case 4:
C_1=|0.01 0.0 | C_2=|0.011 0.0 | C_3=|0.011 0.0 |
|0.0 0.011| |0.0 0.012| |0.0 0.01|

(5)Case 5:
C_1=|0.012 0.0 | C_2=|0.013 0.0 | C_3=|0.011 0.0 |
|0.0 0.012| |0.0 0.013| |0.0 0.01|

(6)Case 6:
C_1=|0.013 0.0 | C_2=|0.015 0.0 | C_3=|0.011 0.0 |
|0.0 0.013| |0.0 0.016| |0.0 0.01|

(7)Case 7:
C_1=|0.013 0.0 | C_2=|0.015 0.0 | C_3=|0.012 0.0 |
|0.0 0.013| |0.0 0.016| |0.0 0.0125|

(8)Case 8:
C_1=|0.013 0.0 | C_2=|0.015 0.0 | C_3=|0.013 0.0 |
|0.0 0.013| |0.0 0.016| |0.0 0.014|

Simulation dataset of three class cases for the cases of 1 and 8 are distributed as shown in Fig.5 (a) and (b), respectively. Obviously, case 1 is easy to classify (best clustering performance) while case 8 is difficult to classify (worst clustering performance) due to their overlapping situations of data distributions among three clusters.

B. Cluster performance evaluations

Clustering performance is evaluated with the aforementioned simulation dataset together with the number of iteration for convergence. Convergence condition is set at 5% of residual error.

Fig.6 (a) and (b) shows the number of processing unit time as functions of crossover and mutation probabilities and Percent Correct Clustering: PCC as functions of crossover and mutation probabilities for the most far two data distributions of two cluster cases while Fig.7 (a) and (b) shows those for the closest two data distribution of two cluster cases.

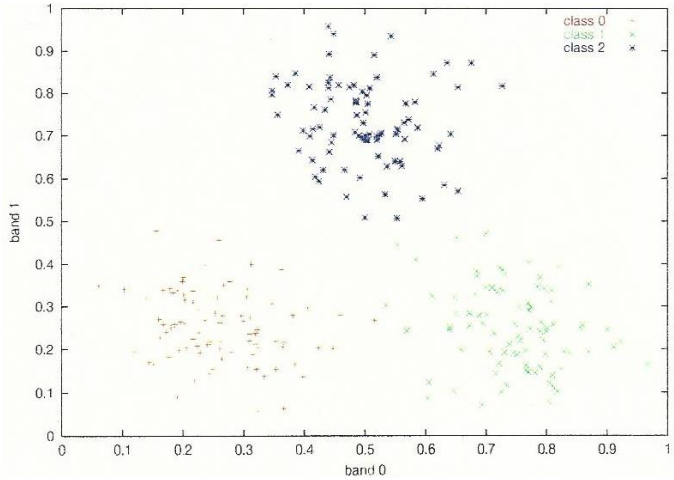

(a)Case1 (the most far case)

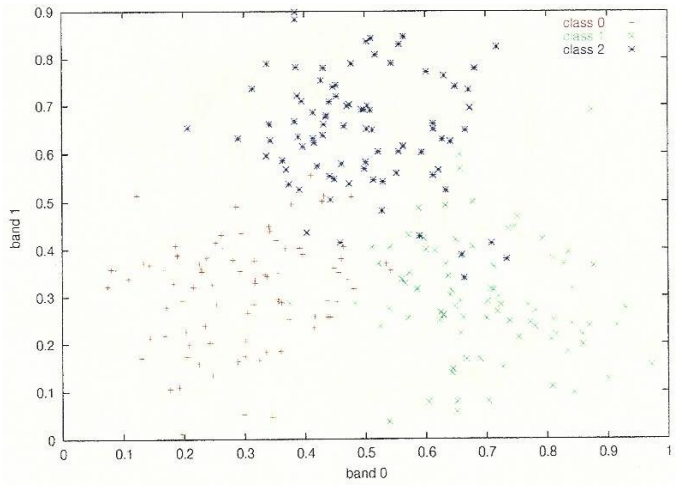

(b)Case 2 (the closest case)

Fig. 5. Data distribution of the simulation dataset in the feature plane for two class cases

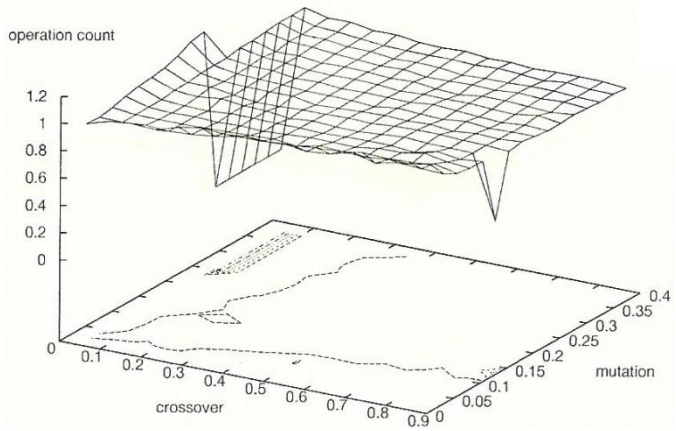

(a)Number of processing unit time

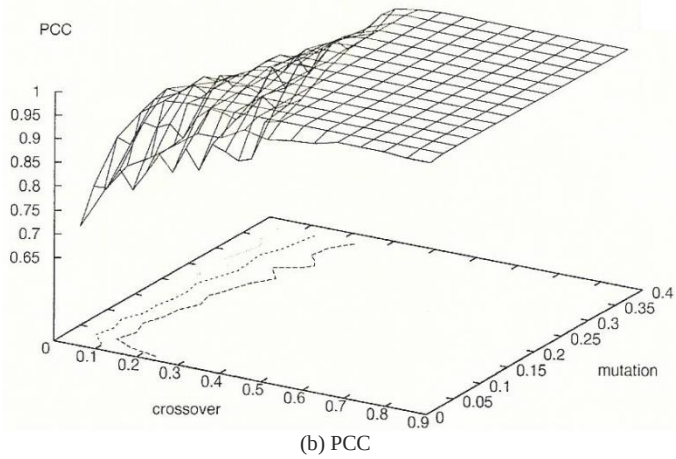

(b) PCC

Fig. 6. PCC and the number of processing unit time for the far data distribution of two cluster case of the simulation dataset.

As shown in Fig.6 and Fig.7, the most appropriate crossover and mutation probabilities depend on the overlapped space in the feature space which is expressed in equation (7). The relation between overlapped space volume and crossover and mutation probabilities is shown in Fig.8.

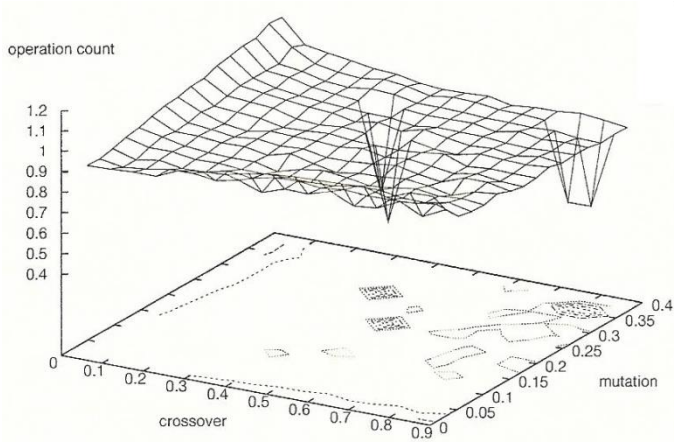

(a)Number of processing unit time

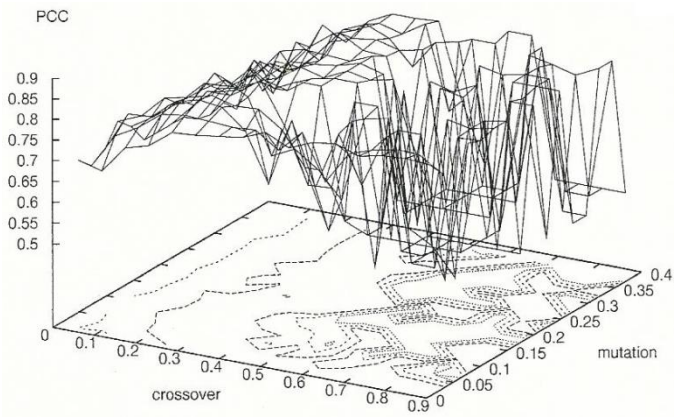

(b) PCC

Fig. 7. PCC and the number of processing unit time for the closest data distribution of two cluster case of the simulation dataset.

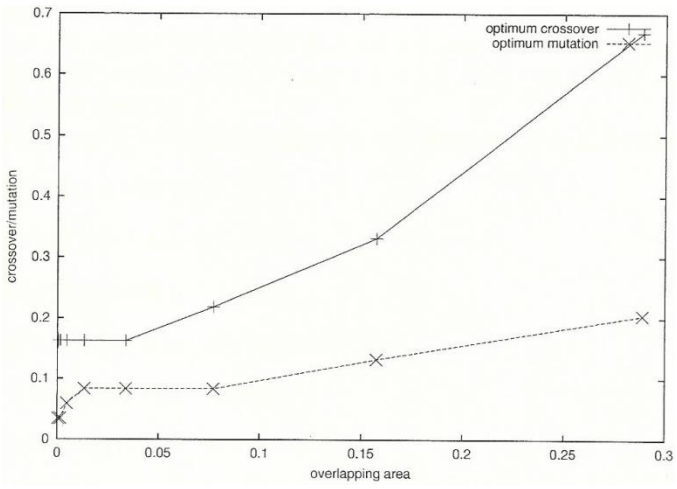

Fig. 8. Relation between overlapped space volume and crossover and mutation probabilities for two cluster datasets

Fig.9 (a) and (b) shows the number of processing unit time as functions of crossover and mutation probabilities and PCC as functions of crossover and mutation probabilities for the most far three data distributions of three cluster cases while

Fig.10 (a) and (b) shows those for the closest three data distribution of three cluster cases.

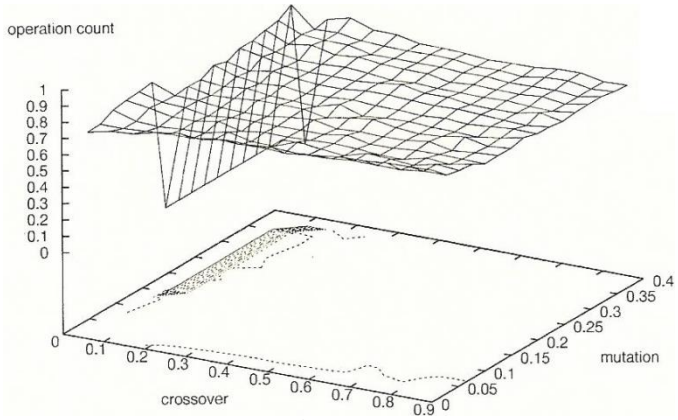

(a)Number of processing unit time

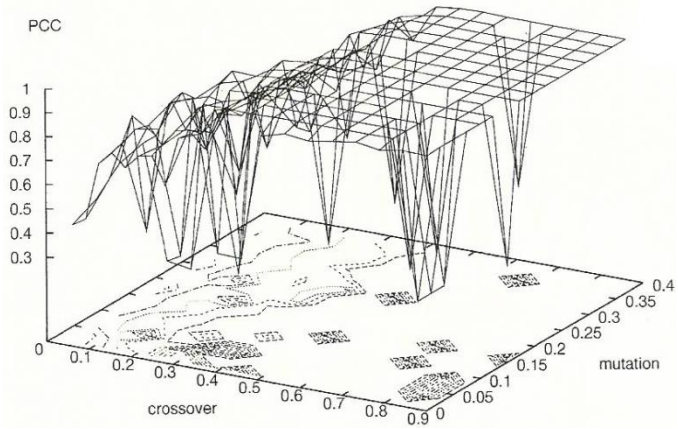

(b) PCC

Fig. 9. PCC and the number of processing unit time for the far data distribution of three cluster case of the simulation dataset.

As shown in Fig.9 and Fig.10, the most appropriate crossover and mutation probabilities depend on the overlapped space in the feature space which is expressed in equation (7). The relation between overlapped space volume and crossover and mutation probabilities is shown in Fig.11.

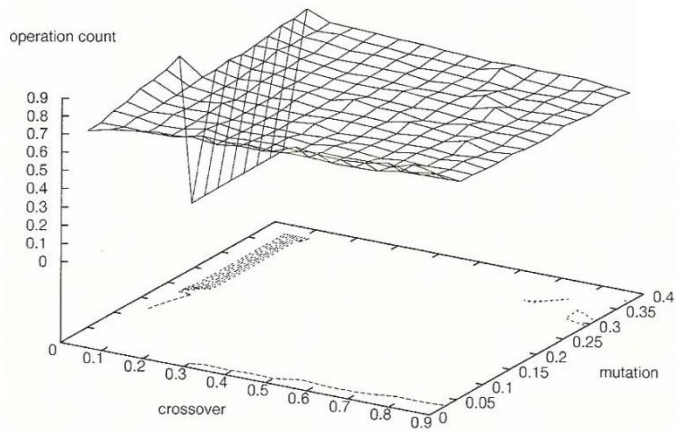

(a)Number of processing unit time

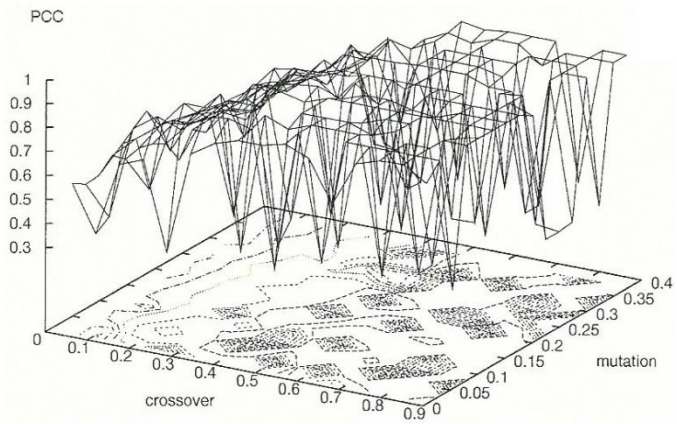

(b) PCC

Fig. 10. PCC and the number of processing unit time for the closest data distribution of two cluster case of the simulation dataset.

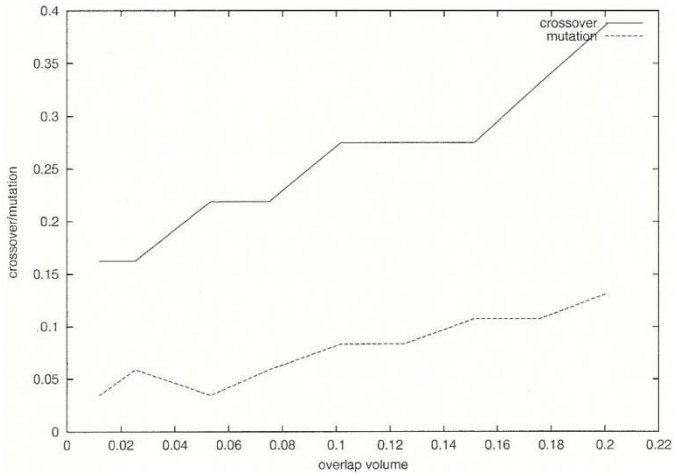

Fig. 11. Relation between overlapped space volume and crossover and mutation probabilities for three cluster datasets

Table 1 shows comparisons among GA clustering performance for three cluster case with the different parameters of crossover and mutation probabilities. It also shows a comparison between GA clustering and Simulated Annealing method.

TABLE I. COMPARISONS AMONG GA CLUSTERING PERFORMANCE FOR THREE CLUSTER CASE WITH THE DIFFERENT PARAMETERS OF CROSSOVER AND MUTATION PROBABILITIES AS WELL AS SIMULATED ANNEALING METHOD

CROSSOVER	MUTATION	CLUSTER PERFORMANCE	NUMBER OF ITERATION
0.1	0.05	0.85	88359
0.2(OPTIMUM)	0.08(OPTIMUM)	0.95	164670
0.8	0.4	0.97	707698
SIMULATED ANNEALING		0.98	8783578

Crossover and mutation probabilities are optimized empirically. As the results, 0.2 and 0.08 of crossover and mutation probabilities are optimum parameters ofr GA cluatering for this three cluster cases. Simulated Annealing SA allows global optimum. Therefore cluster performance for SA based clustering should be 100 % accurate. Due to tha fact that allowable residual error is set at 5% as convergence condition, cluster performance of the SA based clustering is 98% . On the other ahnd, the number of iterations for SA based clustering is 8783578 while that for GA based clustering is 164670 at the optimum GA parameters. Therefore, computation resources of SA based clustering requires 53 times longer than that of GA based clustering. The difference of clustering performance between SA based clustering and GA based clustering is just 3%. Therefore, GA based clustering allows much faster clustering than SA based clustering with acceptable clustering performance.

III. CONCLUSION

Fisher distance based Genetic Algorithm: GA clustering method which takes into account overlapped space among probability density functions of clusters in feature space is proposed. Through experiments with simulation data of 2D and 3D feature space generated by random number generator, it is found that clustering performance depends on overlapped space among probability density function of clusters. Also it is found relation between cluster performance and the GA parameters, crossover and mutation probability as well as the number of features and the number of clusters. From the experimental results with three cluster case, it is found that 0.2 and 0.08 of crossover and mutation probabilities are optimum parameters ofr GA cluatering. Although Simulated Annealing SA based clustering should be 100 % accurate, cluster performance of the SA based clustering is 98%.due to tha fact that allowable residual error is set at 5% as convergence condition, .

On the other ahnd, the number of iterations for SA based clustering is 8783578 while that for GA based clustering is 164670 at the optimum GA parameters.

Therefore, computation resources of SA based clustering requires 53 times longer than that of GA based clustering. The difference of clustering performance between SA based clustering and GA based clustering is just 3%. Therefore, GA based clustering allows much faster clustering than SA based clustering with acceptable clustering performance.

ACKNOWLEDGMENT

The author would like to thank Mr. Mitsuki Nakamura for his efforts through experiments and simulations.

REFERENCES

[1] Arai, K., Lecture note for image processing, Gakujutsu-Tosho-Shuppan publicing Co. Ltd., 1999.

[2] Arai, K., Remote Sensing Satellite image processing methods with Java programing language, Morikita Shuppan publicing Co. Ltd., 2001.

[3] Arai, K., Fundamental theory for pattern recognition, Gakujutsu Tosho Shuppan, Publicing Co. Ltd., 1999.

AUTHORS PROFILE

Kohei Arai, He received BS, MS and PhD degrees in 1972, 1974 and 1982, respectively. He was with The Institute for Industrial Science and Technology of the University of Tokyo from April 1974 to December 1978 also was with National Space Development Agency of Japan from January, 1979 to March, 1990. During from 1985 to 1987, he was with Canada Centre for Remote Sensing as a Post Doctoral Fellow of National Science and Engineering Research Council of Canada. He moved to Saga University as a Professor in Department of Information Science on April 1990. He was a councilor for the Aeronautics and Space related to the Technology Committee of the Ministry of Science and Technology during from 1998 to 2000. He was a councilor of Saga University for 2002 and 2003. He also was an executive councilor for the Remote Sensing Society of Japan for 2003 to 2005. He is an Adjunct Professor of University of Arizona, USA since 1998. He also is Vice Chairman of the Commission "A" of ICSU/COSPAR since 2008. He wrote 30 books and published 322 journal papers

Sub-goal based Robot Visual Navigation through Sensorial Space Tesselation

George Palamas
Faculty of Computing, Engineering and Science
University of South Wales
Wales, United Kingdom

J. Andrew Ware
Faculty of Computing, Engineering and Science
University of South Wales
Wales, United Kingdom

***Abstract*—In this paper, we propose an evolutionary cognitive architecture to enable a mobile robot to cope with the task of visual navigation. Initially a graph based world representation is used to build a map, prior to navigation, through an appearance based scheme using only features associated with color information. During the next step, a genetic algorithm evolves a navigation controller that the robot uses for visual servoing, driving through a set of nodes on the topological map. Experiments in simulation show that an evolved robot, adapted to both exteroceptive and proprioceptive data, is able to successfully drive through a list of sub-goals minimizing the problem of local minima in which evolutionary process can sometimes get trapped. We also show that this approach is more expressive for defining a simplistic fitness formula yet descriptive enough for targeting specific goals.**

Keywords—Self Organization; Growing Neural Gas; Genetic Algorithm; Robot Map Building; Visual Servoing; Recurrent Neural Network

I. INTRODUCTION

With respect of vision based robot navigation, most research work is focused on four major areas: map building and interpretation; self-localization; path planning; and obstacle-avoidance. Of these four major research areas, self-localization is of key importance. The recognition of the initial position, the target position, and the current position occupied by the robot while wandering around are all bound to a self-localization process. The main two approaches used for robot localization are landmark based and appearance based techniques. In this paper, we describe a combination of a developmental method for autonomous map building and an evolutionary strategy to verify the results of the map interpretation in terms of navigation usability.

Our strategy involves two discrete phases: map building and navigation phase. In the first phase an agent freely explores a pre-determined simulated terrain, collecting visual signatures corresponding to positions in the environment. After the exploration, a self-organizing algorithm builds a graph representation of the environment with nodes corresponding to known places and edges to known pathways.

During the second phase, a population of robot controllers is evolved to evaluate map usability. Robots evolve to autonomously navigate from an initial position to a goal position. In order to facilitate successful translation, a shortest path algorithm is employed to extract the best path for the robot to follow. This algorithm also reveals all those intermediate positions that the robot needs to traverse in order to reach the goal position. These intermediate positions act also as sub-goals for the evolution process.

II. SENSING THE ENVIRONMENT

To be fully autonomous, a robot must rely on its own perceptions to localize. Perception of the world generates representation concepts, topological or geometrical, within a mental framework relating new concepts to pre-existing ones [3]. The space of possible perceptions available to the robot for carrying out this task may be divided into two categories: Internal perception (proprioception) or perceptions of its own interactions with the world, associate changes of primitive actuator behavior like motor states; external or sensory perception (exteroception) is sensing things of the outside world. A robot's exteroceptors include all kinds of sensors such as proximity detectors and video cameras. Our system uses only visual information for map building and navigation.

III. ROBOT NAVIGATION

Landmark-based localization methods rely on the assumption that landmarks can be detected and accurately interpreted from raw sensor readings [2], [5]. However interpretation from sensor readings to accurate geometric representation is complex and error prone. On the contrary, an appearance-based representation of an environment is not encoded as a set of geometrical visual features, but as an appearance map that includes a collection of sensor readings obtained at known positions [1]. The advantage of this representation is that the raw sensor readings generate a qualitative estimate of position. The currently perceived image can be directly matched with past experiences stored in the appearance-based topological representation [6]. This method of using sensor readings does not rely on precise metric measurements as with traditional geometrical based maps.

In the field of computer vision the use of appearance based techniques has become widespread. A comparison between the two families of vision based localization methods can be found in [4], showing that appearance-based methods are more robust to noise, occlusions and changes in illumination, when compared to landmark based-methods. The source of inspiration for such techniques comes from the animal kingdom. Small animals, such as insects, navigate through natural environments seemingly with little effort. For example, despite their relatively simple nervous system (and hence limited memory capacity), bees and desert ants are able to

retrace their movements. Such a level of efficiency indicates flexible representations of the surroundings based on visual cues taken from target locations such as home and food sources [7]. These representations seem to have an appearance based flavor rather than a Cartesian arrangement of landmarks. To visit target locations after prior exploration, insects traverse in a way that reduce discrepancies between the stored snapshot and their current retinal image [8].

As stated already the main drawback of appearance-based methods is that localization is only possible in previously mapped areas. Several successful applications have shown promising results [9],[10]. Like landmark based mechanisms, appearance based navigation systems suffer from the problem of perceptual aliasing [11], the situation that different locations produce identical sensory perceptions. A possible solution could be the incorporation of temporal or odometry information to resolve any conflicts. Another possible solution is to divide the goal into a set of sub goals of smaller tasks easier to fulfill. Such an approach, even if perceptual aliasing is present, is more efficient since subtasks are easier to manage and achieve.

IV. Environment Representation

The most natural representation of a robot's environment is a map. In addition to representing places in an environment, a map may include other information, such as properties of objects, regions that are unsafe or difficult to traverse, together with information of prior experience. An internal representation of space can be used by a robot to pre-plan and pre-execute tasks that may be performed later.

A. Geometric Representation

Geometric maps are quantitative representations made up of discrete geometric primitives such as lines, polynomial functions, points and so forth. They are characterized by large scale detail. The primary shortcoming of geometrical model based representation relates to the fact that they can be difficult to infer reliably from sensor data [12].

B. Topological Representation

A topological map is one which captures the connectivity of the environment and has been simplified so that only vital information remains and unnecessary detail has been removed. These maps lack geometric information such as scale, distance and orientation but the relationship between points is maintained. The simplicity of topological maps support much more efficient planning than metric maps [13],[29].

The key to a topological relationship is based on an abstraction of the environment in terms of connectivity between discrete regions or objects, with edges connecting them. In the simplest form, this may involve a complete absence of metric data. A robot employing this representation has no real understanding of the geometric relationship between locations in the environment but the enclosed information is sufficient for the robot to conduct point to point motion. The use of graphs has been exploited in many robotic systems to represent spaces. The following example [10] is representative.

A graph is a kind of abstract data structure that consists of points or nodes connected by links, called lines or edges. Each node corresponds to one of the unique landmarks and each edge corresponds to known paths between them. If the environment consists of networks of corridors and rooms (as found in many indoor environments, such as office buildings or hospitals), it is less complex to specify the topology of important locations and their connection suffice.

Humans represent physical spaces topologically rather than geometrically. For example, when providing the clues needed to lead someone in a building, directions are usually of the form "go down the hall, turn right at the elevator, open the second door on your left," rather than in geometric form. Topological maps are sparse representations of the environment as a collection of visual feature vectors at certain positions. Such representations present some advantages difficult to ignore. First and foremost the computational and memory cost is relatively low. The path planning in metric maps can be computationally very expensive; unlike the lightweight planning nature of graph based structures. Second, they do not require accurate determination of robot's position and therefore are less sensitive to error accumulation, commonly occurring in metric mapping approaches. Topological visual navigation is usually based on key-frame matching to self-localize and navigate to a previously visited location [14, 15].

V. Map-building Phase

A. Terrain Exploration

Our approach considers robots to be like insects, equipped with simple control mechanisms tuned to their environments. Therefore, a model of terrain exploration using a simple two dimensional Brownian random walk was implemented. Such an approach could mimic the navigation behavior of simple animals and microorganisms such as insects. Random walk (also known as Brownian motion) is a process that consists of a sequence of steps, in which the direction and size of each move is determined randomly. The advantage of this approach is minimization of simulation artifacts such as cyclic behavior. During this step the robot collects panoramic snapshots at regular time intervals.

B. Visual Feature Extraction

This collection of panoramic images represents a large amount of raw data and therefore it is necessary to extract some specific features that describe the content of each image. Color histograms are a very appealing graphical representation. Image analysis based on color information is robust for robot map-building and image retrieval problems and, due to their statistical nature, provide a complete rotationally invariant representation when employed with panoramic cameras (figure 1).

Moreover, they are also computationally cheap to implement. Omni-directional vision systems are a special type of vision sensor. Images are obtained by placing a convex mirror a short distance from a camera. These systems provide a 360^{o} view of the robot's environment around the vertical axis.

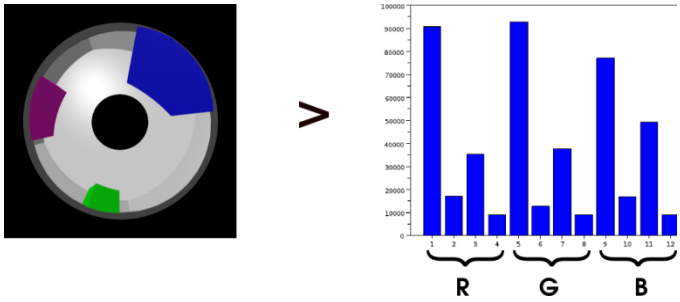

Fig. 1. Omnidirectional snapshot and extracted RGB histograms.

The set of color signatures, extracted during terrain exploration, can be manipulated as a large abstract image database. This is the foundational scheme of a content based image retrieval approach. Self localization can be based on a measure of resemblance between the currently acquired image of the robot and the base of images stored as perceptual signatures representing familiar terrain. Gonzalez and Lacroix [18] suggests a qualitative position refinement technique that localize a rover when it comes back to a previously perceived area, using an image indexing technique on panoramic views based on principal component analysis. The limitation of this procedure is that it cannot perform incrementally, because all learning images are required to compute the subspace.

To measure color histogram similarity, we use the standard Euclidean formula. This distance metric is a comparison between the identical bins in the respective histograms and all bins contribute equally to the distance [19]. The Euclidean distance between two color histograms h and g is given by

$$d_E(h,g) = \sum_{m=0}^{M-1}(h[m] - g[m])^2 \qquad (1)$$

C. Self-Organization of Visual Signatures

In unsupervised learning networks the only data available is the input set. These networks serve two main purposes: topology preservation and vector quantization. Topology preservation means that close input signals are mapped to neurons which are close in the network and conversely, close neurons in the network come from close input signals in the input space, preserving similarities between data as much as possible (figure 2).

There are many reasons why we use a self organizing system for robot mapping, preferred over other mechanisms that have no plasticity properties [20]. The first reason is that less parameters, which describes the robot operation, need to be predetermined. Information given by sensors incorporate noise, leading to erroneous conclusions regarding spatial perception. Information may be contradictory when sensor readings come from different sensors but represents the same robot position. Furthermore, due to the nature of sensors used with respect to the task being performed, extracted information may not be useful. Self-organizing mechanisms make use of all available data without prior assumptions. Data clustering addresses the problem of noise and handles meaningless information.

One of the most robust algorithms is the Growing Neural Gas (GNG) by Fritzke [21]. Growing Neural Gas is a network that can learn the topological relationships from an input set of vectors using a variation of the Hebbian rule. GNG dynamically add or remove nodes and can approximate the input space with higher accuracy compared to a network with predefined structure (figure 2) such as the Kohonen self organizing feature map [22]. The GNG is an adaptive algorithm inspired by the physical properties of uniform gases and the work on self organizing maps. Assuming that a given distribution of points is represented by a container shape, the algorithm will begin to create freely moving particles which will try to expand uniformly to fill the input space. After convergence is reached, the network nodes then represent the shape of the container.

Clustering of static sensor signals has been used before for robot localisation [13],[23]. Different unsupervised neural network architectures have been used to realize topological relationships between input and output space. Baldassari et.al. [24], applied a GNG algorithm for a visual based self-localisation task of a mobile robot in an indoor environment. Images acquired from a camera moving in a pathway, formed an implicit topological representation of the environment. These simulations dictated the effectiveness of the GNG model in recognition speed, classification tasks and in particular topology representation as compared to the popular Kohonen Self Organizing Map (SOM) model. This performance gap, ascribed to the fact that GNG algorithm, that dynamically add and remove nodes, can approximate the input space more accurately than a network with a predefined structure and size - such as a SOM. This is true also since SOM resembles a lossy compression scheme by applying a data projection from a multidimensional space, where perceptual signatures are described, to preferably only a two dimensional space.

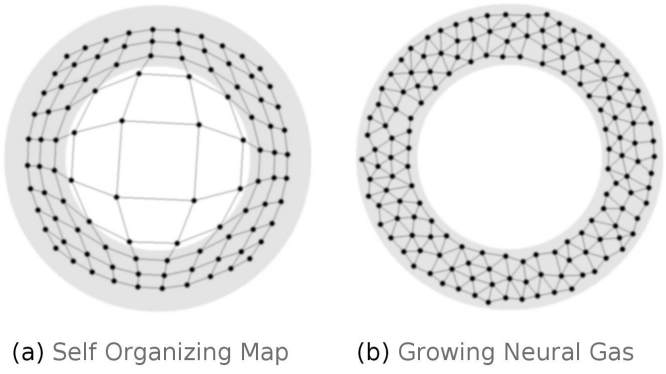

Fig. 2. Topology preservation for SOM and GNG respectively.

VI. The Navigation Phase

A. Path Planning

Prior to navigation, path planning is an important issue as it directs the robot on how to get from an initial position to a goal position. Since the environment is stationary with no other moving obstacles, the process of path planning is straightforward.

Topologically, this problem is equivalent to the shortest path problem of finding a route between two nodes in the graph. Many algorithms have been developed to find a path in a graph. For example, Dijkstra's algorithm [25] computes the optimal path between a single source point to any other point in a graph (figure 3). Since we compute the path once after the mapping phase, a real time algorithm is not necessary.

B. Self-localisation

The robot continuously keeps track of the current location. While the robot moves, collects snapshots and exports corresponding color histograms. Every newly acquired histogram is being compared with every stored histogram in the graph structure. The robot self-localizes when the closest histogram on the topological map is found. Each of the nodes in the graph represents a specific histogram and the closest one indicates the current position of the robot on the map.

C. Visual Navigation

For the robot to conduct point to point navigation, a controller is necessary that will move the robot through a set of intermediate points towards the final position. The proposed robot behavior controller realizes an Elman neural network (Elman NN) and a genetic algorithm (GA). Neural network architectures are particularly well suited for complex pattern classification tasks and genetic algorithms are good optimization procedures because they can explore large and multidimensional spaces to find global solutions. Hence, they are well suited for training neural networks.

The neural controller is composed of a grid of input neurons whose activations are given by the color bins of the corresponding histograms. Two output neurons control the angular torque applied to the left and right wheel of the robot.

A set of neurons with recurrent connections fed from hidden and output neuron layer, help to learn past instances and correlate them with new information. The input neurons of the neural network are activated by sensory data, and the output neurons control the motors of the robot. Within a population, each individual has a different genome describing a different neural network (different weight vectors), thus resulting in specific individual responses to sensory-motor interactions with the environment. These behavioral differences affect the robot's fitness, which is defined, by the number of successive milestones traversed by the robot.

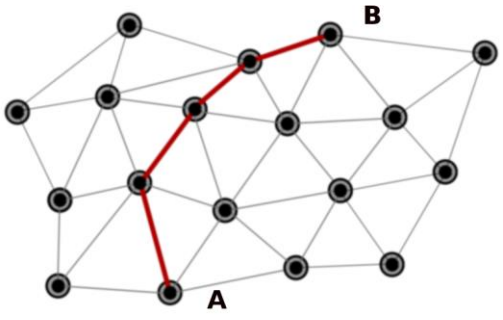

Fig. 3. Disjkstra's graph search algorithm output.

Evolutionary strategies require that a large population of individuals be evaluated over the course of many generations. In the case of evolutionary robotics it has been assumed that it would take far too long to do all of these evaluations in the real world. The main practice is to evaluate in simulation, whether partial or in whole. The aim of this evolutionary strategy is to create a population of agents with different genomes, each defining a set of parameters of the control system of the robot. The genome is this set of parameters whose translation into a phenotype, the actual behavior of the controller, can cause the system to depict biological behaviors. The artificial genome decodes the weight values associated to synaptic connections of an artificial neural network that determines the global visual navigation behavior.

D. Neural Network Controller

The neural network we use (figure 4) is a typical feed-forward architecture with evolvable thresholds and discrete-time, fully-recurrent connections at the output layer [26]. This type of neural network is used to do sequence processing, especially when these sequences are made of indexed data [28]. The processing occurs in steps and it is assumed that neuron outputs are computed instantaneously. A set of twelve input neurons receive information about the color distribution from the images captured from the panoramic camera.

Each neuron covers a band of the color variations in the image that is a bin value is assigned to each input. Each of the RGB color components of the image are divided into four bands. The activation of each neuron is scaled in the interval [0, 1] so that activation 0.5 corresponds to zero torque applied in the wheels. Activation values above and below 0.5 stands for forward and backward rotational speeds, respectively. The two output neurons act also as proprioceptive information about the speed of each wheel. A set of short term memory units stores the values of the output neurons at the previous sensor-motor state and sends them back to the output units through a set of recurrent connections [26]. All other neurons in the hidden layer have recurrent connections to store previous activity.

$$f(x) = 1/(1 + \exp(-x)) \quad (2)$$

Neurons use the sigmoid activation function in the range [0,1], where x is the weighted sum of all inputs (equation 2). For each discrete time interval they encode both the sensorial information and the motor commands passed to the wheels.

E. Evolving Controllers

Algorithms in Evolutionary Robotics (ER) frequently operate on populations of candidate controllers, initially selected from some random initial population of controllers. This population is then repeatedly modified according to a fitness function, a particular type of objective function that is used to indicate the closeness of a given design solution to achieving a set of aims.

Evolutionary Robotics builds upon several aspects of artificial evolution. The Genetics aspect is about what goes into the artificial chromosomes and how these chromosomes are mapped into individuals. Genetic encoding and genotype-phenotype mappings are the key to the evolvability of a system.

In our case the genotype represents the architecture of a controller in a form of a binary string and the phenotype represents the possible solution space. The population of robot controllers is also referred to as genomes.

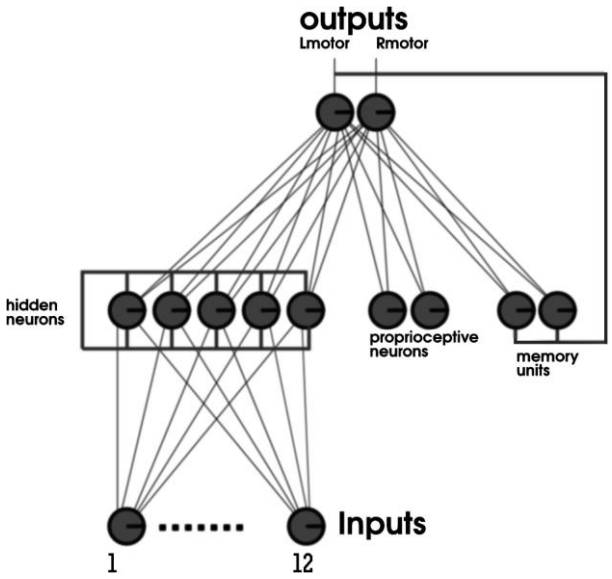

Fig. 4. Discrete-time recurrent neural network

Evolutionary algorithms have been widely used to design cognitive architectures for robots with emergent behaviors (see [16, 17] for an overview). The main strength is their ability to cope well with high complexity problems using only a high-level reward function. Best candidates are rewarded only for their global efficiency because of the impossibility of foreseeing every sub-goal the robot has to solve. If the global objective is very hard then initial performance may be so poor that the evolutionary process is hard to initiate. Another problem is local minima in which the evolutionary process may become trapped. A fitness function must be simplistic yet descriptive enough for targeting specific goals. Designing a fitness function is essential to the successful use of a genetic algorithm. If the fitness function is poorly designed, the algorithm will either converge on an inappropriate solution, or will have difficulties in converging at all.

For a successful incremental evolution process the system requires an accurate knowledge of the problem to be solved so as to lead the evolutionary algorithm to perfect convergence. For graph based robot navigation the global task can be divided into smaller tasks. Both global task and sub-tasks are self-similar, i.e. the goal is to transfer the robot from one point to another. Since in our case the different sub-tasks are in nature exact copies of the main task, by just dividing the path that the robot needs to traverse, the only requirement is to determine when to switch from one sub-task to another. Fitness function is an objective function used as a metric to calculate the distance of each individual from a set of goals.

The success of evolutionary algorithms depends on the fitness function design.

A good function design must guarantee that a collection of solutions exists, differentiating enough, with values that changes neither too rapidly nor too slowly with the given parameters of the optimization problem. The fitness function was designed to select robots for their ability to arrive at the goal zone. The neural network has a set of evolvable connections that are individually encoded in the genome. A population of 100 individuals is randomly initialized and each individual genome is decoded into the synapses of the neural network. The twenty percent of the population with the highest values are used for reproduction and the rest discarded. The new genomes have a crossover value of 0.1 per pair and mutation probability of 0.01. The meaning of crossover is swapping a pair of genetic strings around a randomly chosen point. Mutation consists of toggling the value of a random bit in the genetic sequence. The best two genomes from the previous generation are inserted to the current generation, unaltered, to improve the stability of the process. This strategy is known as elitist selection.

F. The Evolution Process

The fitness function was designed to select the best robots to arrive at the goal node and is described as follows. The fitness value is the percentage of the distance the robot covered between two adjacent nodes in the path. Every time the robot reaches a node in the node sequence, as extracted from the path planning phase, it is rewarded with a value of 1. Since it is extremely difficult for the robot to match the current perceived histogram with the target node, we made the assumption that 90% of the covered distance corresponds to successful goal reaching.

The robot must traverse the nodes in the specific order as dictated from the outcome of the Dijkstra's algorithm. If the robot arrives at a goal node that is not successive in order, the robot is not awarded for this sub-goal. Successful individuals have to arrive at all sub-goal nodes through this specific order. The running fitness value for every agent in the population is the summation of extra value gained for each successive step plus the current percentage of the distance between currently arrived at node and the next one in the sequence.

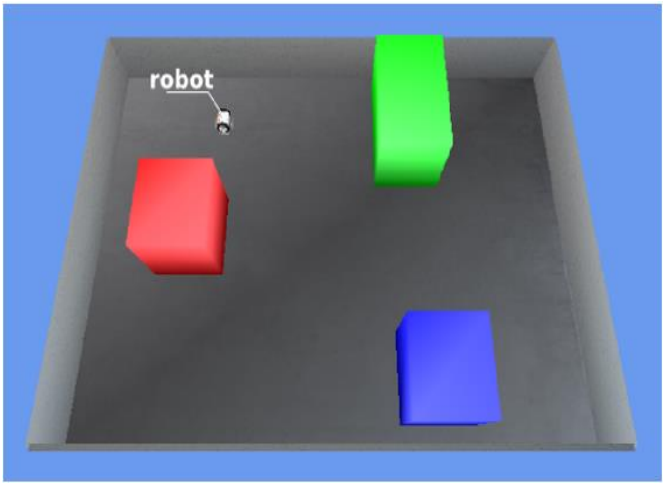

Fig. 5. The simulated environment and the robot used in our experiments

VII. Experimental Setup

A. The Robot

The simulated robot can be seen in figures 5. The omnidirectional camera is widely used in visual based robot navigation and localization, which is due to the large field of view. Images are obtained by placing a convex mirror a short distance from a camera. The main advantage that led us to promote this solution is the large field of view compared to orthographic or standard cameras. The system provides a 360^o view of the robot's environment around the vertical axis when it is mounted on top of the robot. Landmarks are always in the field of view except for occasional occlusion and therefore have increased reliability. This is advantageous when utilizing topological representations as the more information the image contains the more stable it is. Another advantage is the orientation independency when employed with statistical methods such as color histograms.

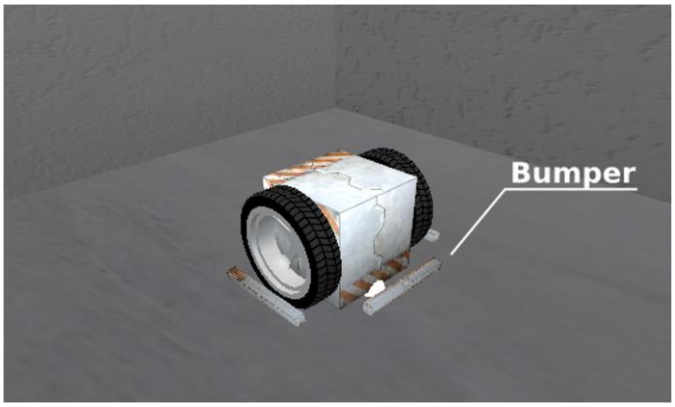

Fig. 6. Simulated differential drive robot. The robot has four bumpers to detect collisions with walls and obstacles.

The robot is cubical in shape with two independent drive wheels attached in the middle of the chassis and two trailing casters, front and rear. This is a typical differential drive setup and the robot can change its direction by varying only the relative rotation speed of its wheels and hence does not require an additional steering mechanism. The robot is equipped with two, one bit, horizontal axis bumper bars. The purpose of the tactile sensors, when a reaction to a collision occurs, is to reposition the next individual to initial conditions and start a new simulation trial.

B. The Environment

For the experiments we used a simple 3D world, a closed rectangular arena with colored obstacles, dark gray walls and no ceiling (figure 6). This environment is not as visually complex as a typical real life environment. The primary goal was to demonstrate the plausibility of evolving agents that could use cognitive maps and behaviors based on visual information which otherwise would be very difficult if not impossible to employ.

Both for the robot and the simulated environment we used the Bullet physics libraries, a freely available software package that models gravity, mass, friction, and collisions. For modeling the environment as well as the view from the omnidirectional camera, we used the XNA graphics framework. Well understood image processing tasks such as color histogram extraction were accomplished using the well known open Computer Vision (openCV) library. To model the reflective surface of the sphere we applied a method of environmental mapping known as Cube Mapping [27]. This is a technique for approximating the appearance of a reflective surface by means of a pre-computed texture image. The image is generated, for every simulation step, by projecting the surroundings of the sphere onto the six faces of a cube. This cubical texture is then wrapped onto the sphere to represent reflection lighting properties.

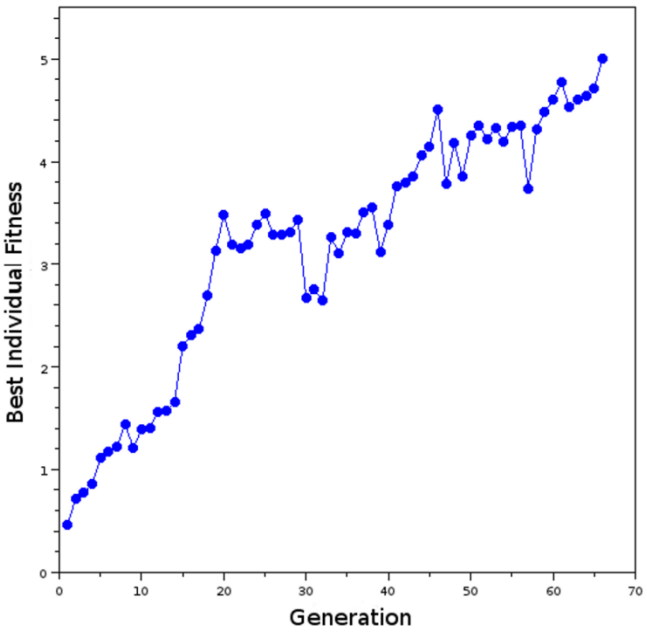

Fig. 7. Best individual fitness value from each generation.

C. Experimental Procedure

Initially a robot is allowed to freely navigate in the environment in order to build a collection of 500 panoramic snapshots of the environment from different perspective views. A GNG algorithm, performing off-line, formed a grid with topological relations between these visual cues. The grid starts with only two nodes and grows until the criterion of 20 nodes is met. Based on this grid, a shortest path is extracted to indicate optimal route from a starting position to a global target position in the arena. A genetic algorithm evolved a neuro-controller to allow a robot to successively follow the six nodes the optimal path consists of. Each individual robot tested for a period of time lasting for 10 seconds or 1000 simulation cycles. Trials were truncated earlier if collisions detected from the bumpers.

VIII. Results

This section shows experimental results of the proposed method. Several sets of experiments were performed with varying parameters relating with the GNG algorithm, the neural network architecture and the genetic algorithm. Something worth mentioning is the fact that the dark shades of the environment gave better results than other colorations. This is simple to explain since black color interprets as absence of color and does not interfere with the three other landmarks, the

discrete nature of which is being enhanced. Figure 7 depicts a record of the best individual score for each generation to evaluate the solution domain. As can be seen, a navigation controller evolved after 66 generations. The robot that used this controller, managed to pass through all the intermediate points until the final objective. The path followed by the robot is shown in Figure 8. The gray and red points correspond to intermediate sub-goals and final goal respectively. The optimal path planning computed with Dijkstra's algorithm between an initial and final position in the graph that was generated by the GNG algorithm.

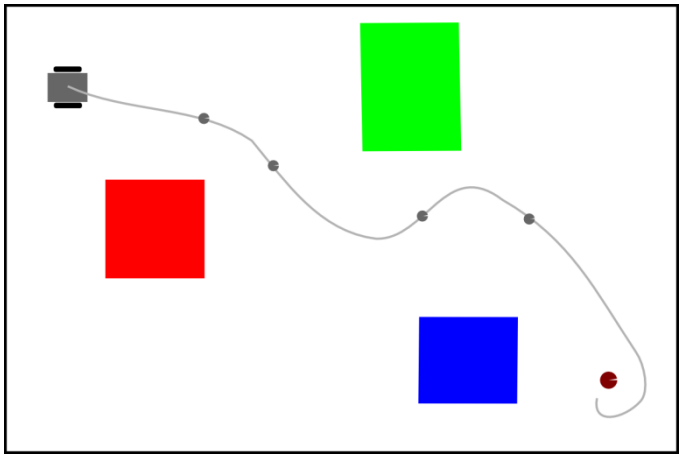

Fig. 8. .The robot successfully followed the sequence of nodes. The small gray dots are the positions that the robot encountered the threshold of 90% of the distance covered between two adjacent nodes. (A successful controller is always awarded with a fitness value of 5). The difference between the actual position and the robot position is due to the error in the calculation of the best matching unit and the 90% accuracy threshold.

IX. Conclusions

This paper explores the advantages of evolutionary sub-goal robot navigation with a cognitive map architecture. All methods used have been tested using a simulated environment. The GNG algorithm has been previously shown to be effective in forming topological maps through an appearance based framework. Evolutionary strategies have also been applied successfully in solving complex problems such as visual navigation. However these algorithms may take some time to converge to an optimal solution. Feature selection is a particularly important step for building robust learning models. Our method is based on global only image properties and may suffer from the problem of perceptual aliasing [30], the fact that different physical locations correspond to similar sensory perceptions.

However the purpose of this study was to demonstrate the efficiency of simple algorithms to solve complex systems. After verification of the aforementioned algorithms using simulations, these need to be evaluated on actual robots and modify as necessary to ensure acceptable real life robot navigation.

Further research might explore alternative visual scene interpretation methods for dealing with more complex navigation scenarios.

Acknowledgment

The authors would like to thank all laboratory members for their valuable discussions through this research.

References

[1] I. Ulrich and I. Nourbakhsh, Appearance-based place recognition for topological localization, vol. 2, no. April. Ieee, 2000, pp. 1023–1029.

[2] S. Se, D. G. Lowe, and J. J. Little, Vision-based global localization and mapping for mobile robots, vol. 21, no. 3. IEEE, 2005, pp. 364–375.

[3] A. Ascani, E. Frontoni, A. Mancini, and P. Zingaretti, “Feature group matching for appearance-based localization,” in IEEERSJ International Conference on Intelligent Robots and Systems, 2008.

[4] R. Sim and G. Dudek, “Comparing image-based localization methods,” in Pattern Recognition, 2003, vol. 18, pp. 1560–1562.

[5] J. J. Leonard and H. F. Durrant-Whyte, Mobile robot localization by tracking geometric beacons, vol. 7, no. 3. IEEE, 1991, pp. 376–382.

[6] [6] B. J. A. Kröse, N. Vlassis, and R. Bunschoten, “Omnidirectional Vision for Appearance-based Robot Localization,” in Int Workshop on Sensor Based Intelligent Robots, 2002.

[7] T. S. Collett and S. P. D. Judd, “Multiple stored views and landmark guidance in ants,” Nature, vol. 392, no. 6677, pp. 710–714, 1998.

[8] B. A. Cartwright and T. S. Collett, “How honey bees use landmarks to guide their return to a food source,” Nature, vol. 295, no. 5850, pp. 560–564, 1982.

[9] D. G. Lowe, “Distinctive Image Features from Scale-Invariant Keypoints,” International Journal of Computer Vision, vol. 60, no. 2, pp. 91–110, 2004.

[10] [10] M. O. Franz, B. Schölkopf, H. A. Mallot, and H. H. Bülthoff, “Learning view graphs for robot navigation,” Autonomous Robots, vol. 5, no. 1, pp. 111–125, 1998.

[11] [11] C. Siagian and L. Itti, Biologically Inspired Mobile Robot Vision Localization, vol. 25, no. 4. IEEE, 2009, pp. 861–873.

[12] H. H. Gonzalez-Banos and J. C. Latombe, “Navigation Strategies for Exploring Indoor Environments,” The International Journal of Robotics Research, vol. 21, no. 10–11, pp. 829–848, 2002.

[13] M. V. Butz, E. Shirinov, and K. L. Reif, “Self-Organizing Sensorimotor Maps Plus Internal Motivations Yield Animal-Like Behavior,” Adaptive Behavior, vol. 18, no. 3–4, pp. 315–337, 2010.

[14] O. Booij, B. Terwijn, Z. Zivkovic, and B. Krose, “Navigation using an appearance based topological map,” Proceedings 2007 IEEE International Conference on Robotics and Automation, no. April, pp. 3927–3932, 2007.

[15] Y. W. Y. Wang, D. C. D. Chen, and C. S. C. Shi, Autonomous Navigation Based on a Novel Topological Map, vol. 1. Ieee, 2009, pp. 254–257.

[16] S. Nolfi, “Evolving robots able to self-localize in the environment: the importance of viewing cognition as the result of processes occurring at different time-scales,” Connection Science, vol. 14, no. 3, pp. 231–244, 2002.

[17] I. Harvey, E. D. Paolo, R. Wood, M. Quinn, and E. Tuci, “Evolutionary Robotics: A New Scientific Tool for Studying Cognition,” Artificial life, vol. 11, no. 1–2, pp. 79–98, 2005.

[18] J. J. Gonzalez-Barbosa and S. Lacroix, Rover localization in natural environments by indexing panoramic images, vol. 2, no. May. Ieee, 2002, pp. 1365–1370.

[19] J. R. Smith and S. Chang, “Tools and techniques for color image retrieval,” Image Rochester NY, vol. 2670, no. 3, pp. 426–437, 1996.

[20] U. Nehmzow, “Map building through self-organisation for robot navigation,” in Advances in Robot Learning 8th European Workshop on Learning Robots EWLR8 Proceedings Lecture Notes in Artificial Intelligence Vol1812 SpringerVerlag Berlin Germany, 2000, vol. 1812, pp. 1–22.

[21] B. Fritzke, “A Growing Neural Gas Network Learns Topologies,” Advances in Neural Information Processing Systems 7, vol. 7, no. 1, pp. 625–632, 1995.

[22] T. Kohonen, “Self-organized formation of topologically correct feature maps,” Biological Cybernetics, vol. 43, no. 1, pp. 59–69, 1982.

[23] S. Yamada, "Recognizing environments from action sequences using self-organizing maps," Applied Soft Computing, vol. 4, no. 1, pp. 35–47, 2004.

[24] P. Baldassarri, P. Puliti, A. Montesanto, and G. Tascini, "Self-Organizing Maps versus Growing Neural Gas in a Robotic Application," in Proceedings of the 7th International Work-Conference on Artificial and Natural Neural Networks: Part II: Artificial Neural Nets Problem Solving Methods, 2003, pp. 201–208.

[25] E. W. Dijkstra, "A note on two problems in connexion with graphs," Numerische Mathematik, vol. 1, no. 1, pp. 269–271, 1959.

[26] D. Floreano, M. Suzuki, and C. Mattiussi, "Active Vision and Receptive Field Development in Evolutionary Robots," Evolutionary Computation, vol. 13, no. 4. pp. 527–544, 2005.

[27] N. Greene, Environment Mapping and Other Applications of World Projections, vol. 6, no. 11. IEEE, 1986, pp. 21–29.

[28] J. L. Elman, "Finding Structure in Time," Cognitive Science, vol. 14, no. 2, pp. 179–211, 1990.

[29] S. Thrun, "Robotic Mapping: A Survey," Science, vol. 298, no. February, pp. 1–35, 2002.

[30] A. Angeli, S. Doncieux, J. A. Meyer, and D. Filliat, Incremental vision-based topological SLAM. Ieee, 2008, pp. 22–26.

Prediction of assets behavior in financial series using machine learning algorithms

Esteves da Silva, Diego
Dept. Computer Engineering
IME – Military Institute of Engineering
Rio de Janeiro, Brazil

Duarte, Julio Cesar
Dept. Computer Engineering
IME – Military Institute of Engineering
Rio de Janeiro, Brazil

***Abstract*—The prediction of financial assets using either classification or regression models, is a challenge that has been growing in the recent years, despite the large number of publications of forecasting models for this task. Basically, the non-linear tendency of the series and the unexpected behavior of assets (compared to forecasts generated in studies of fundamental analysis or technical analysis) make this problem very hard to solve. In this work, we present for this task some modeling techniques using Support Vector Machines (SVM) and a comparative performance analysis against other basic machine learning approaches, such as Logistic Regression and Naive Bayes. We use an evaluation set based on company stocks of the BVM&F, the official stock market in Brazil, the third largest in the world. We show good prediction results, and we conclude that it is not possible to find a single model that generates good results for every asset. We also present how to evaluate such parameters for each model. The generated model can also provide additional information to other approaches, such as regression models**

Keywords—Forecasting; Stock Market; Machine Learning; Financial Series

I. INTRODUCTION

The prediction of financial market assets is an issue that concerns both investors and researchers. In recent years, it has been studied using different machine learning approaches, as show in [12]. Despite the large amount of research, the prediction of the behavior of an asset in the real world, either with classification or regression models, is still a difficult task to accomplish [13].

The main difficulty on making good predictions is due to both the non-linear characteristic of financial time series and the great amount of uncertainty and noise found in financial market data [14], [15], [16]. For this reason, we argue that classical statistical models are not good to make this kind of prediction. This type of time series requires the use of algorithms with a greater ability to generalize, such as Support Vector Machine (SVM) and Artificial Neural Networks (ANN).

This work focuses in solving the asset prediction problem in the financial market, addressing the problem as a classification task and modeling it using supervised techniques such as Support Vector Machine, Logistic Regression and Naïve Bayes together with interday data to generate its classifiers.

The main purpose is to serve as decision model for the investor and can still be used as an entry into new models, particularly regression, in order to reduce its error.

The choice of the Support Vector Machine (SVM) algorithm was made in order to present results comparable and often superior to those achieved by other machine learning algorithms such as Artificial Neural Networks [30],[31].

We also use the Logistic Regression (LR) (with gradient descent method to choose the best parameters) and Naive Bayes algorithms (NB) to serve as a comparison in our study [3]. A baseline (BLS) has been implemented to verify the distance between the probabilities of success of an investor without any market knowledge to the accuracy found with some parameters applied to algorithms. We also use the open source Framework FAMA [6] for development and implementation of algorithms.

Despite good results in recent studies [12], the challenge of finding models with good generalization ability with actual data is still open. We conclude with the results of the experiments that we can find models with good amount of hits if the parameters are set correctly, and verify that, despite the good generalization characteristic proposed in algorithms in machine learning algorithms, it is not possible to apply a sole model for all stock assets.

II. RELATED WORK IN ASSETS' PREDICTIONS

In recent years several techniques for regression and classification financial assets have been explored, from classical statistical methods to more complex algorithms for machine learning, such as Artificial Neural Networks [19],[20], Logistic Regression [17],[18], PLSR [21] and more recently Support Vector Machine [22],[23],[24]. Reference works in the area prove that these soft computing techniques are well accepted for the study and evaluation of financial series.

The main difference between most of these works is the output information, while some of them provide the action to be taken by the user (classification problem), some others focus on the minimum and maximum stock values achieved during the day (regression problem).

Whatever the choice, we still got the same problem: the accuracy's loss in new periods and scenarios.

Our novel contributions are the analysis (interday stock parameters and some others variables in this problem) of how this models (focusing in the classifiers generated by SVM) behave with new data scenarios and the adjustments needed to minimize the loss percentage rate expected between training and tests scenarios. In order to achieve these results, we define a hybrid model using a sliding cross validation environment, where the model is re-trained after a defined period

III. Machine Learning Techniques and Modeling

In this section we detail the machine learning algorithms used in this work, as well, as their important parameters. For the training task, we set our target variable (y) as "+1" if the day's closing value of the asset is grater them the day before's, which means that today, the asset closing value grew when compared to the closing value of the day before, also, if the value of the subtraction (day closing value – day-1 closing value) is negative, then we set the output target variable as "-1", thus creating a binary classification problem.

A. Tendency Keeper (TK)

Tendency Keeper is actually not a machine learning algorithm and it was used as our baseline system (BLS) for comparisons. The TK approach performs next day classification only considering the closing value in the day (cvd) subtracted the closing value of the previous day (cvd-1). If we have a negative value (cvd < cvd-1) then the output value for the next day is classified as the negative class ("-1"), on the other way around, if we have a zero or positive value (cvd >= cvd-1), then the TK sets the positive class to the target variable ("+1").

Here, we expect an accuracy rate close to 50%, similar to a simple guess, which is the probability of success of an investor without any knowledge of the financial market.

We use this one as a lower limit to compare the quality of classifiers.

B. Naïve Bayes (NB)

The Naive Bayes algorithm is a probabilistic model based on Bayes rule. Because of its simplicity, this algorithm is widely used in Machine Learning, for both discrete and continuous *X*. It is a naive approach because it considers the attributes to be conditionally independent, i.e., a given event does not imply another one.

In other words the attributes $X_1, \ldots, X_n$ are all conditionally independent given *Y* and the data has a normal symmetrical distribution. Despite this naive and simplistic premise, it reports good performances in several classification tasks [7].

We can represent Bayes rule as:

$$P(Y = y_i | X = x_k) = \frac{P(X=x_k|Y=y_i)\, P(Y=y_i)}{\sum_j P(X=x_k|Y=y_j)\, P(Y=y_j)} \quad (1)$$

Where:

y_i denotes the target value of the e[th] example

x_k denotes the k[th] attribute value for an example *x*

Our implementation assumes that for each attribute x_k in ith example *x*, we calculate standard-deviation (σ) and the average (μ) for each class, in our study case, "+1" and "-1".

After this we compare the result of each formula (as defined in Equation 1) for each class. The algorithm evaluate the class ("+1" or "-1") using the higher output value of the calculation for each class

$$\frac{1}{(\sigma(C) * \sqrt{2\pi})} * e^{-z} \quad (2)$$

Where z is defined by:

$$\frac{((x_k) - \mu(C))^2}{2 * \sigma(C)^2} \quad (3)$$

C. Logistic Regression

Logistic Regression is a function approximation algorithm that uses training data to directly estimate P(Y|X). It is an approach to learn functions of the form $f: X \rightarrow Y$.

Roughly, it gives the probability of y = 1 as a set of discrete or continuous variables in a vector X. In this implementation we use a gradient descendent function to find the best set of parameters.

As all others algorithms, our output value is labeled as "+1" or "-1". We can denote an example by $\bar{x}$ and the value of k^{th} feature as x_k. It also defines an additional feature, $x_0 = 1$ (bias feature). The probability of an example being a positive value is given by:

$$p\,(y = +1\,|\bar{x}) = g(\textstyle\sum_{k=0}^{n} w_k x_k) \quad (4)$$

$$\text{Where g(z)} = \frac{1}{1+e^{-z}} \quad (5)$$

and w_k, $k \in \{0, \ldots, n\}$ denote the weight for the k^{th} feature. In training we get weight vector (W) defined by the gradient descendent method.

D. Support Vector Machine (SVM)

Support Vector Machine (SVM) is nowadays the most promising machine learning algorithms, is based by statistical learning theory [4], developed by study cases started with [5] and establishes a series of principles to be followed in obtaining classifiers with good generalization.

Basically, the algorithm defines some key points to be the support vectors, at first defined by the biggest distance between the linear classifier and the closest class's examples (labeled as +1 and -1 values). In other words, it defines a margin which is the width that the boundary could be increased by, before achieves a data example. In the experiments sections, we will explain more directly how its variations (kernels and theirs parameters) impacted the prediction result.

We used the library Libsvm [1], with was integrated in FAMA framework to implement our experiments.

Some solutions for solving classifications problems requires that input data must be linearly separated, but we know that is not always possible. To solve this issue, Vapnik proposed a mathematical method to transform low-dimensional data into a high-dimensional projection (using kernel functions), which is easier to separate input data linearly.

The resulting hyperplane is defined maximizing the distance between the "nearest" vectors of different classes. The thinking is that a bigger margin directly implies in the best capacity of generalization. The Figure 1 shows this idea.

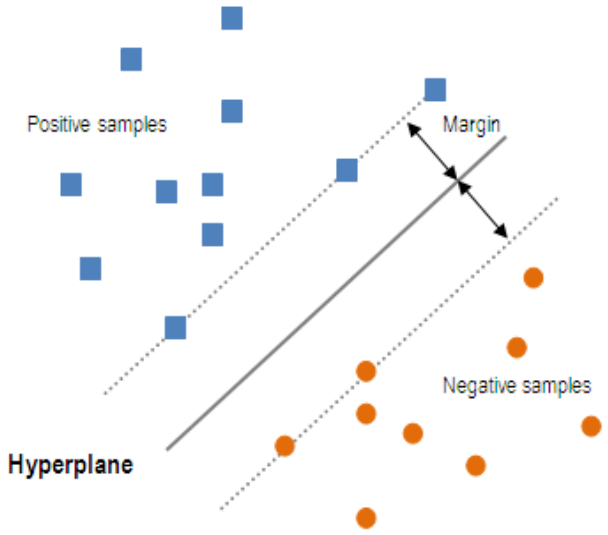

Fig. 1. The simplest kind of SVM: samples and key-points as support vectors (on the dashed line) as maximum margin linear classifier.

The Kernels are functions that help the transformation from low-dimensional feature space into a higher-dimensional feature space, which is a necessary condition for separating the input data values properly.

There are some kernels implementations and we describe the kernels type used into our model analysis. Despite the fact that the LIBSVM library supports several formulations for classification, regression and distribution estimation, we focus our work on the classification models: C-Support Vector Classification [9] and nu-Support Vector Classification [10].

As kernel types, there are many kernels functions, but the common are: linear, polynomial, sigmoid and radial base function.

- Linear: $K(x_i, x_j) = x_i^T x_j$
- Polynomial: $K(x_i, x_j) = (\gamma x_i^T x_j + r)^d, \gamma > 0$
- Sigmoid: $K(x_i, x_j) = \exp(-\gamma | x_i - x_j|^2), \gamma > 0$
- Radial Base Function: $K(x_i, x_j) = tanh(\gamma x_i^T x_j + r)$

where K is called the kernel function and x_i are the training vectors. We test all these in our experiments. The results are showed and detailed in section 4

As we can see, depending on the kernel choice, some parameters (γ, r, d) have to be set.

IV. Experiments and Results

A. Database

We use data from the Bovespa website [8], available through interface files, to create a financial series. The prepossessing task produced a new database contains 107(187-80) records with information between 01-Jan-2006 and 31-Dec-2006-10, since we need to disregard the first 80 values (window's maximum size) to set the discrepancy values into our generated dataset. In the original dataset, we have 187 days, in order to compute the difference of the 80 day before's, we need to discard 80 first days.

The preprocessing task must consider some factors such as: outliers' removal from the sample, attributes' selection and scaling of the values

B. Input Attributes

From our database, we selected the attributes, according to technical analysis, that are most relevant to the final value of an stock [25]: opening price (open), closing price (close), day maximum (max), day minimum (min) and volume (vol). We labeled these values as "base attributes".

Moreover we used the series discrepancy (3, 5, 10, 15, 20, 40, 60 or 80 days). The results show the direct impact in model sensibility when we change the window, overfitting the model when using bigger window values.

A good pattern that was found is the combination between these "base attributes" and the series discrepancy values. We realize that when used together, this combination can be good for accuracy since we have a low discrepancy (most of the time when this value is equal 3 or 5). This pattern was valid only for values less than or equal to 5.

As example, from original database values, we produce the following input structure, using a discrepancy value of 3, showed in Table I.

TABLE I. An simple example with the first six day's values as input matrix for 3 day's discrepancy value.

PETR4								
Open	***Close***	***Min***	***Max***	***Vol (*10^9)***	***d-1***	***d-2***	***d-3***	***y***
39,1	39,4	39,1	39,7	15,98	-0,28	0,69	2,19	+1
39,5	40,8	39,5	40,8	24,15	1,40	-0,28	0,69	+1
40,6	40,9	40,3	41,3	18,07	0,10	1,40	-0,28	+1
44,1	43,7	43,1	44,4	27,51	2,80	0,10	1,40	-1
43,4	42,8	42,5	43,9	23,86	-0,90	2,80	0,10	+1
42,9	43,4	42,9	43,8	38,53	0,60	-0,90	2,80	-1

C. Outliers: split and inplit

We must consider two relevant aspects in financial series: split and inplit. Both are techniques used as strategy aiming asset price increase.

"Split" is a strategy that companies use in order to improve the liquidity of an asset. The Split technique occurs when the

stock price is too expansive, difficulting the financial transaction, often caused by memory investor [12].

"Inplit" is the inverse operation of the "split". The inplit is used to to enhance the liquidity of the asset when their price is far below the market and reducing the volatility of the asset (when the asset's value is too low any variation represents a large variation of percentage).

In this work, we must consider that operations (both split and inplit) as a noise in the financial series, since it generates a large variation in the price of the asset, although they do not cause any impact in the investment portfolio's value

D. Scaling

In machine learning techniques, it is advisable to put all input values into a range of [-1, +1] or [0, +1]. This increase the performance of algorithms (by avoid numerical difficulties during the calculation, for instance kernel functions usually depend on the inner products of feature vectors) and doesn't privilege some (greater) numeric values. Warren S. Sarle [13] explains the importance of scaling in your research.

Obviously, the same scaling method must be used in both training and testing dataset. For example, if the x attribute of training was scaled from [-100, +100] to [-1, +1] and the same attribute in the test data lies in the range [-120, +80] then the result test dataset must be scaled to [-1.20, + 0.8]

After the data preprocessing task, we perform some analysis of the SVM parameters in order to find a model that presents a good performance with new data.

V. EXPERIMENTS

Among the choice of attributes, we analyze the impact of some parameters and their variations into model´s accuracy. These parameters are described in Table II.

TABLE II. ALGORITHMS PARAMETERS FOR MODEL TRAINING.

Parameter	*Observations*
svmtype	0 = c-SVC, 1 = v-SVC
kernel type	0 = Linear, 1 = Polynomial, 2 = RBF, 3 = Sigmoid
degree	Set degree in kernel function (polynomial, RBF and Sigmoid)
gamma	Set gamma value in kernel function (polynomial and sigmoid)
coef0	Set coef0 in kernel function
C	Set c parameter for C-SVC
V	Set v parameter for v-SVC

Furthermore, we analyze some specifics details in modeling task as training period, input attributes and cross validation method compared with our sliding cross validation implementation.

One problem yet to be solved is finding a good training period. Given the characteristics of financial time series, we can not train with a very large (subject to underfitting) or a very small dataset (subject to overfitting) [9]. The next Tables (III, IV and V) shows this behavior. We argue the oldest values are less important for closing value day then closer values. When we work with a bigger training dataset, the output model cannot find a generic good model for prediction.

TABLE III. SVM – ACCURACY OF SVM IN DIFFERENT SIZES OF TRANINNING BASES

Stock	**Period**				
	Window	***5 months***	***10 months***	***15 months***	***20 months***
ALLL11	80	90%	84%	70%	65%
PETR4	80	89%	80%	62%	61%
ELET6	80	92%	82%	71%	65%
CSNA3	80	95%	82%	72%	58%

[a.] (SVM Type = nu-SVC, Kernel Type = Linear, nu parameter value = 0.5)

TABLE IV. NB - ACCURACY OF SVM IN DIFFERENT SIZES OF TRANINNING BASES

Stock	**Period**				
	Window	***5 months***	***10 months***	***15 months***	***20 months***
ALLL11	80	83%	74%	56%	54%
PETR4	80	85%	83%	76%	58%
ELET6	80	84%	73%	60%	48%
CSNA3	80	91%	77%	76%	58%

TABLE V. LR - ACCURACY OF SVM IN DIFFERENT SIZES OF TRANINNING BASES

Stock	**Period**				
	Window	***5 months***	***10 months***	***15 months***	***20 months***
ALLL11	80	55%	49%	49%	48%
PETR4	80	45%	48%	47%	47%
ELET6	80	48%	45%	49%	49%
CSNA3	80	56%	50%	45%	45%

From technical analysis, we used basic values as: opening value, closing value, highest and lower value in the day and also volume. Dow's theory argues that these variables can be used to predict the market movement [26]. We cannot take this statement into our model for all assets. Basically we found a pattern in some assets, when we use a small discrepancy (3, 5) we can see little improvement in accuracy but, when this value grows, in most cases, this improvement is lost. Furthermore, there are some assets where this affirmative is not true, such as ELET6 asset.

In Table VI and Table VII, we show the accuracy of SVM and NB training considering discrepancy values (D) and considering both base attributes plus discrepancy values (BA+D). For ALLL11 and also CSNA3 we cannot see any (real) improvement into hit rate when se use both input groups. For PETR4 in some window size values we have a considered gain. For ELET6 the combination of base attributes and discrepancy values helps in the prediction task for any window size value when we compare SVM results. In Table VIII, we show the results of the cross validation training with 80% of data and testing with 20%. Table IX show the cross-validation results for NB.

TABLE VI. ACCURACY OF SVM MODEL IN TRAINING DATABASE FOR DIFFERENT WINDOW SIZE AND DIFFERENT INPUT PARAMETERS

Window	ALLL11		PETR4		CSNA3		ELET6	
	D	BA+ D	D	BA+ D	D	BA+ D	D	BA+ D
3	54%	53%	54%	56%	58%	47%	54%	61%
5	57%	57%	55%	52%	48%	53%	54%	57%
10	59%	42%	63%	46%	58%	56%	53%	59%
15	58%	60%	61%	50%	66%	62%	58%	69%
20	63%	57%	68%	52%	71%	57%	68%	72%
40	76%	75%	79%	86%	83%	84%	72%	81%
60	85%	83%	86%	84%	87%	87%	88%	89%
80	90%	90%	89%	89%	94%	95%	90%	92%

5 months series length (SVM Type = nu-SVC, Kernel Type = Linear, nu parameter value = 0.5) (SVM Type = nu-SVC, Kernel Type = Linear, nu parameter value = 0.5)

TABLE VII. ACCURACY OF NB MODEL IN TRAINING DATABASE FOR DIFFERENT WINDOW SIZE AND DIFFERENT INPUT PARAMETERS

Window	ALLL11		PETR4		CSNA3		ELET6	
	D	BA+ D	D	BA+ D	D	BA+ D	D	BA+ D
3	63%	62%	55%	64%	57%	59%	54%	65%
5	62%	61%	62%	68%	61%	62%	54%	64%
10	60%	61%	64%	66%	68%	70%	57%	59%
15	66%	66%	69%	67%	74%	72%	65%	64%
20	69%	68%	72%	70%	75%	71%	64%	60%
40	71%	72%	76%	77%	81%	83%	66%	61%
60	77%	77%	82%	80%	86%	85%	78%	76%
80	83%	83%	86%	85%	91%	91%	85%	84%

5 months series length

Bezzera da Silva et. Al. [11] studies the correlation between stocks in Bovespa with market graph by Power Law.

Despite the difference in the research focus, we can see the relation between stocks and if we can cluster these different groups, specifics model rules can be applied to get best model as possible.

Analyzing the variations of kernels, we can see the best values for accuracy by using the Polynomial Kernel and window variable value set to 3 and 5 (for ELET6). This test is carried out with the nu value of 0.5 [2].

TABLE VIII. COMPARING SVM CROSS-VALIDATION (80/20) AND TRAINNING ACCURACY (%)

Window	ALLL11		PETR4		CSNA3		ELET6	
	Train	80/ 20	Train	80/ 20	Train	80/ 20	Train	80/ 20
3	63	64	63	64	54	59	55	64
5	82	68	81	68	80	64	80	59
10	89	64	94	64	94	59	95	59
15	92	64	96	50	95	59	95	59
20	96	64	100	50	97	59	100	59
40	100	64	100	59	100	59	100	59
60	100	64	100	59	100	59	100	59
80	100	68	100	59	100	59	100	59

5 months series length (SVM Type = nu-SVC, Kernel Type = Linear, nu parameter value = 0.5) (SVM Type = nu-SVC, Kernel Type = Linear, nu parameter value = 0.5)

TABLE IX. COMPARING NB CROSS-VALIDATION (80/20) AND TRAINNING ACCURACY (%)

Window	ALLL11		PETR4		CSNA3		ELET6	
	Train	80/ 20	Train	80/ 20	Train	80/ 20	Train	80/ 20
3	63	59	55	64	57	45	54	40
5	62	36	62	68	61	40	54	36
10	60	54	64	64	68	60	57	40
15	66	54	69	50	74	60	65	59
20	69	54	72	68	75	54	64	40
40	71	54	76	59	81	45	66	27
60	77	63	82	63	86	27	78	13
80	83	54	86	59	91	54	85	22

In financial series models, it is important to retrain the model after a certain period in attempt to get the actual tendency. We recognize the importance of historical data, of course, but argue that only a specific time period is really important in order to make a correct prediction. We can prove this affirmative comparing standard cross-validation method with 80% of total data used to train and get the classifier and 20% to test the accuracy of the model and sliding cross-validation method. This one was created using the same parameters used with traditional cross-validation but being retrained before predict next day tendency.

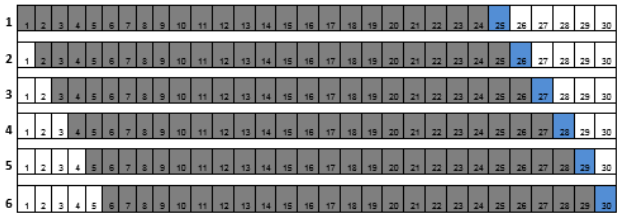

Fig. 2. Sliding Cross-Validation example with 30 days dataset. Train days = 24. Test days = 6

In our tests we have used 80 days to train and predict next day tendency (high or low). With "sliding" validation, we get the average of the output values to calculate model´s accuracy. This parameter is still open in our study and presents best performance with SVM approach.

Table X shows the difference in accuracy between standard cross-validation (C1) and sliding cross-validation (C2) which strongly indicates the need of retraining the model with 80-days prior.

TABLE X. COMPARISON BETWEEN CROSS-VALIDATION AND SLIDING CROSS-VALIDATION METHODS

Window	ALLL11		PETR4		CSNA3		ELET6	
	C1	C2	C1	C2	C1	C2	C1	C2
3	64%	65%	64%	71%	59%	64%	64%	68%
5	68%	71%	68%	71%	64%	65%	59%	68%
10	64%	65%	64%	64%	59%	64%	59%	76%
15	64%	62%	50%	64%	59%	64%	59%	68%
20	64%	65%	50%	64%	59%	64%	59%	68%
40	64%	71%	59%	64%	59%	64%	59%	68%
60	64%	76%	59%	64%	59%	64%	59%	68%
80	68%	65%	59%	64%	59%	64%	59%	68%

As we can see our method sliding cross-validation performs best when compared with cross-validation method. This shows the need to retrain the model after a certain time period, likely looking for the tendency period

VI. CONCLUSION AND FUTURE WORK

As expected, the SVM algorithm had a better accuracy than the other algorithms studied in this work and it also presented good generalization abilities. It can be noticed that the parameter adjustment using kernel functions and the defined margin, especially regarding the implementation, directly impacted the outcome of the model. Despite all difficulties found in the financial time series, such as noise and uncertainties, after adjustment of the data, we obtained good results to serve as a basis for decision making. Another important factor is the period considered for training the model, which does not produce good results in cross validation when it is too small or too large. The approach to validation of the model followed the method of the experiment. The retraining presented with our sliding cross validation method provides the best results compared with cross validation method. It highlighted the need to retrain the model after a certain period.

In attempt to do better predictions, some factors will be considered in future works. The **moving averages** (simple, weighted, exponential and others), are often used in technical analysis as input parameters in the model to indicate an uptrend or downtrend (through lines of support and resistance). It can be a good factor to the tABLEmodel once we have difference in the behavior of the predictor variable in a downward trend and upward trend.

We also can look for the relation between stocks. Recent works use graphs to **group stocks** through its correlation [11]. This grouping can bring benefits to the data analysis, since it is expected that correlated assets by similarity in behavior.

We argue that the last days have more influence on the price´s behavior of the stock and it can be proved that by sliding validation method that considers only 80-days to train and produce a better model. Next steps can consider analyze of the variation of this variable in accuracy results as well as **calculate the input variables by weights**. We also will consider **a hybrid model** created by the analysis of confusion matrix. Finally the prediction target can be reformulated to transform the problem to multiclass. A **sensibility factor** can separate the samples into 3 classes as “high negative variation”, “neutral variation” or “high positive variation” by calculates the variation of price. This can put the focus on more specific situations.

On the other hand, recent works have focused in **semantic observation** [27],[28],[29]. Rules can be extracted from the database and applied to the model in an attempt to find a pattern that minimizes the prediction error.

REFERENCES

[1] Chang, C. C., & Lin, C. J. (2007). LIBSVM: a Library for Support Vector Machines. Available at http://www.csie.ntu.edu.tw/ cjlin/libsvm.

[2] Hsu, C. W., Chang, C. C., & Lin, C. J., (2003). A Practical Guide to Support Vector Classification.Available at http://www.csie.ntu.edu.tw/cjlin/libsvm

[3] Tom M. Mitchell. Machine Learning. McGraw-Hill, New York, 1997.

[4] V. N. Vapnik. The nature of Statistical learning theory. Springer-Verlag, New York, 1995.

[5] V. N. Vapnik and A. Y. Chervonenkis.On the uniform convergence of relative frequencies of events to their probabilities. Theory of Probability and its Applications,16(2):283–305, 1971

[6] FAMA: Framework para Aprendizado de Máquina. Avaliable athttps://code.google.com/p/fama

[7] A. McCallum and K. Nigam, A comparison of event models for Naive

bayes text classi¯cation, In Proc. of the AAAI-98 Workshop on learning for text categorization, pp. 41-48

[8] Bovespa Historical Data Series availably at: http://www.bmfbovespa.com.br/shared/iframe.aspx?idioma=ptbr&url=http://www.mfbovespa.com.br/pt-br/cotacoes historicas/FormSeriesHistoricas.asp

[9] Cortes and V. Vapnik. Support-vector network. Machine Learning, 20:273{297,1995.

[10] Scholkopf, A. Smola, R. C. Williamson, and P. L. Bartlett. New support vector algorithms. Neural Computation, 12:1207{1245, 2000.

[11] Bezerra da Silva, Eduardo, de Lima, Leonardo Silva, Attias, Thiago. “Uma Aplicação da teoria de grafos em redes complexas: estudo de caso do mercado de ações da Bovespa”, Rio de Janeiro, CEFET, 2009.

[12] Atsalakis, G. S.;Valavanis, K. P.. Surveying Stock Market Forecasting Techniques – Part II: Soft Computing Methods. Expert Systems with Applications, 36, 3, 5932-5941, 2009.

[13] Leonardo C. Martinez, Diego N. da Hora, J. R. M Palotti, Gisele L. Pappa, and W. Meira Jr. From na artificial neural network to a stock market day-trading system: A case study on the bm&f bovespa. The 2009 International Joint Conference on Neural Networks, 2009.

[14] Yaser S. Abu-Mostafa and Amir F. Atiya. Introduction to financial forecasting. Appl Intell., 6(3):205-213, 1996.

[15] R. Lawrence. Using Neural Networks to Forecast Stock Market Prices. University Of Manitoba, 1997.

[16] Bruce Vanstone and Gavin Finnie. An empirical methodology for developing stockmarket trading systems using artificial neural networks. Expert Syst. Appl., 36(3):6668-6680, 2009.

[17] Arun U., Gautam B. and Avijan D. Forecasting Stock Performance in Indian Market using Multinomial Logistic Regression.Journal of Business Studies Quartely, 2012.

[18] Dutta, A. et al. (2008).”Classification and Prediction of Stock Performance using Logistic Regression: An Empirical Examination from Indian Stock Market: Redefining Business Horizons”: McMillan Advanced Research Series.p.46-62.

[19] Ajith Abraham, Baikunth Nath and P. K. Mahanti. Hybrid intelligent systems for stock market analysis. In International Conference on Computational Science (2), pages 337-345, 2001.

[20] Pei-Chann Chang, Chen-Hao Liu, Jun-Lin Lin, Chin-Yuan Fan, and Celeste S. P. Ng. A neural network with a case based dynamic window for stock trading prediction. Expert Syst. Appl, 36(3):6889-6898, 2009.

[21] Leandro G. M. Alvim; Ruy L. Milidiú; Cícero N. dos Santos. Daily volume forecasting using high-frequency predictors. In IASTED International Conference on Artificial Intelligence and Applications, AIA 2010, Innsbruck, Austria, 2 2010. IASTED.

[22] Rohit Choudhry and Kumkum Garg. A hybrid machine learning system for stock market forecasting. In WASET -Proceedings of World Academy of Science, Engineering and Technology ISSN: , Commenced: 2005, January, volume 39, Copenhagen, DK, 2005

[23] Wei Huang, Yoshiteru Nakamori, and Shou-YangWang. Forecasting stock market movement direction with support vector machine. Comput. Oper. Res., 32(10):2513–2522, 2005

[24] Ling-Bing Tang, Ling-Xiao Tang, and Huan-Ye Sheng. Forecasting volatility based on wavelet support vector machine. Expert Syst. Appl., 36(2):2901–2909, 2009.

[25] Lemos, Flávio; Cardoso, Flávio; Cardoso, Celso. “Análise Técnica Clássica - Com as Mais Recentes Estratégias da Expo Trader Brasil”. Editora Saraiva, 2010.

[26] Robert Rhea. “The Dow Theory (Fraser Publishing Library)”. Barron's The National Financial Weekly; 8th Printing edition, 1932.

[27] Kumar, B. Rama; Kumar, S. Bangari; Prasad S. Chandragiri. "Financial News Classification Using SVM". International Journal of Scientific and Research Publications, Volume 2, Issue 3, March 2012

[28] Alencar, P. Franco; Ávila, M. Guilherme; "Mineração Web - Predição do comportamento de ativos na Bovespa", Brasília, Universidade de Brasília, 2011.

[29] Lopes, Jefferson P. Thomas; Hiratani, Gabriel Koji Lemos; Barth, Fabricio J.;Rodrigues Jr., Orlando; Pinto, Juliana Maracci. "Mineração de Opiniões aplicada à Análise de Investimentos", São Paulo, Centro Universitário SENAC, 2008.

[30] Joachims, T. (2002). Learning to Classify Text using Support Vector Machines: Methods, Theory, e Algorithms. Kluwer International Series in Engineering and Computer Science. Kluwer Academic Publishers, Norwell, MA

[31] Noble, W. S. (2004). Kernel Methods in Computational Biology, chapter Support vector machine applications in computational biology, pages 71–92. MIT Press, Cambridge, MA